

Valentin Mader

**Aspects of hadronic transitions of
mesons and baryons in the
Dyson-Schwinger approach to QCD**

Diplomarbeit

zur Erlangung des akademischen Titels eines
Magisters
an der Naturwissenschaftlichen Fakultät der
Karl-Franzens-Universität Graz

Betreuer:

Priv.-Doz. Mag. Dr. Andreas Krassnigg
Institut für Physik,
Fachbereich Theoretische Physik

2010

Contents

1	Motivation	1
2	The S-matrix and Green Functions in QCD	2
2.1	S-matrix and Green functions	2
2.1.1	The S-matrix	3
2.1.2	Green functions and LSZ reduction formula	4
2.1.3	Dyson's equations	4
2.2	The path integral formalism	6
2.2.1	The path integral	6
2.2.2	LSZ reduction formula revisited	7
2.2.3	Dyson-Schwinger equations	7
2.3	Bound state equations	9
2.3.1	Bethe-Salpeter equation	10
2.3.2	Covariant Faddeev equation	12
2.4	Intrinsic structure of QCD Green functions	14
3	The triangle diagram and its ingredients	16
3.1	Quarks	17
3.1.1	Color and flavor structure	17
3.1.2	Lorentz and Dirac structure	17
3.1.3	Rainbow truncation	19
3.2	Mesons	20
3.2.1	Flavor and color structure	22
3.2.2	Dirac structure – pseudoscalar meson	22
3.2.3	Dirac structure – vector meson	25
3.3	Baryons	26
3.3.1	Diquarks	26
3.3.2	Quark-diquark amplitudes	29
4	Calculations and results	31
4.1	Invariant amplitude, decay width and phasespace	31
4.2	Interaction model	33
4.3	Mesons: $\rho \rightarrow \pi\pi$	33
4.4	Baryons: $\Delta \rightarrow N\pi$	38
5	Conclusions and Outlook	42

A	The chiral Munczek-Nemirovsky model	43
A.1	Quark Dyson-Schwinger equation	44
A.1.1	Rainbow truncation	44
A.2	Meson Bethe-Salpeter equation	48
A.2.1	Ladder Truncation	49
A.2.2	Pseudoscalar meson	51
A.2.3	Vector meson	53
A.2.4	Diquarks	54
B	Technicalities	56
B.1	Construction of flavor and color matrices	56
B.1.1	Fundamental representations of $SU(2)$	56
B.1.2	Irreducible representation of $SU(2) \otimes SU(2)$	58
B.1.3	Color-singlet representation of $SU(3) \otimes SU(3)$	59
B.2	Kinematics in the triangle diagram	61
B.2.1	General considerations	61
B.2.2	Breit frame	62
B.2.3	$\rho \rightarrow \pi\pi$	64
B.2.4	$\Delta \rightarrow N\pi$	65
B.3	The quark propagator in the complex plane	67
B.4	Taylor expansion	67
B.5	Euclidean spacetime	69

Chapter 1

Motivation

Since Gell-Mann and Zweig invented the concept of quarks as the constituents in hadrons [1–3], quark models have had a huge success in the qualitative as well as quantitative description of the hadron spectrum, in particular since their realization as fundamental fields in a quantum gauge theory, quantum chromodynamics (QCD), it is widely believed that quarks are part of the set of fundamental elementary particles that build our world.

During the decades of hadron phenomenology by means of quarks, many approaches appeared, which range from non-relativistic quantum mechanical constituent quark models, to their relativistic extensions, perturbative QCD, effective field theories, QCD sum rules, Lattice QCD, AdS/QCD and, what is performed in this thesis, coupled DSE/BSE calculations. Next to the masses, decay widths are essential components of the hadron spectrum. Hadronic decay widths are particularly important for the understanding of the behavior of the strong interaction, since they connect the behavior of elementary degrees of freedom of QCD, quarks and gluons, to reactions between observable states, such as mesons and baryons.

In this thesis we want to describe hadronic transitions within the Green functions approach of coupled Dyson-Schwinger–Bethe-Salpeter calculations of QCD, which has been done previously for mesonic transitions [4, 5], and achieved reasonable results. Here we want to revisit this calculations for the $\rho \rightarrow \pi\pi$ -transition and add some insight with regard to model details. Additionally we extend this approach also to the baryon case and provide first exploratory study there. In this way we open a field of important processes, which had up to now not yet been considered in this approach.

An intrinsic feature of the coupled Dyson-Schwinger–Bethe-Salpeter approach is that one extracts gauge independent observables, such as masses and decay widths, from gauge dependent objects, such as Green functions and Bethe-Salpeter amplitudes. The choice of a gauge is always a matter of the question one tries to answer, but also of convenience. In this thesis we choose Landau gauge, since it is manifestly Lorentz covariant by construction and thus allows Lorentz covariant statements. In addition many other hadron studies in the coupled Dyson-Schwinger-Bethe-Salpeter approach in the last decade, were performed in this setup and thus providing a broad and well studied background and basis for this work. We work in the isospin-symmetric limit and in Euclidean momentum space.

Chapter 2

The S-matrix and Green Functions in QCD

In modern theoretical physics a theory is characterized by its Lagrangian or, equivalently, its action. But these quantities alone do not make any physics, yet. As physics is a *natural* science, it is always connected to experiment. So one has to extract information about the behavior of particular mathematical objects in the Lagrangian and translate them to a corresponding behavior of an object in nature. In classical theories, both mechanics and field theories, one extracts information about the movement of a particle, e.g., its equation of motion via the Euler-Lagrange equations, which are a mathematically and physically sophisticated version of Newton's laws, out of the Lagrangian. With the rise of quantum theories and their formulation in terms of the Feynman path integral formalism and Schwinger's variational principle the situation changed and new methods had to be invented. One, that sticks to the spirit of the Euler-Lagrange formalism and provides the equations of motion of the Green functions is the Dyson-Schwinger approach.

In this chapter we want to set up the theoretical framework of the Bethe-Salpeter and Dyson-Schwinger equations and their application to hadron phenomenology. This will enable us to make statements about the behavior of physical objects susceptible to the strong nuclear force.

2.1 S-matrix and Green functions

S-matrix elements and Green functions are the central objects of attention for any theoretical physicist doing phenomenology by means of quantum field theories, since they connect the theoretical formalism to observables. They usually stand at the beginning of every quantum field theory course and the main aspects of this section can be found in any introductory book to quantum field theory. For this reason we will be quite brief, present only the main results and for details refer to, e.g., [6, 7].

2.1.1 The S-matrix

Already in quantum mechanical scattering theory one uses the Heisenberg S-matrix to connect transition probabilities to measurable quantities as, e.g., scattering cross sections or decay widths. Also in quantum field theories all theoretical approaches have to use the instrument of the S-matrix, if they want to connect their theoretical formalism to measurable quantities.

The S-matrix, also called the infinite time evolution operator $U(\infty)$, is the transition operator between asymptotic states, with its matrix elements being defined as transition amplitudes, thus giving transition probabilities, from an initial state i to a final state f ,

$$S_{fi} = \langle f|i \rangle \quad , \quad (2.1)$$

which can be rewritten in terms of j incoming and $n - j$ outgoing particles

$$S[\phi_1 \dots \phi_n] = \langle \phi_{j+1} \dots \phi_n | \phi_1 \dots \phi_j \rangle \quad . \quad (2.2)$$

The S-matrix can be decomposed in an interacting part T , where scattering occurs and a non interacting part, where the ingoing objects remain unaffected,

$$S_{fi} = \delta_{fi} + T_{fi} \quad . \quad (2.3)$$

By extracting momentum conservation we can define the invariant transition matrix element \mathcal{M} between an initial state i and a final state f

$$T_{fi} = (2\pi)^4 \delta^{(4)}(p_f - p_i) \mathcal{M}_{fi} \quad , \quad (2.4)$$

where $p_{i,f}$ are the sets of the momenta of the incoming and outgoing particles.

Experiments in elementary particle physics almost exclusively deal with processes where bulks of particles collide and scatter off each other. Thus, one very important observable is the scattering cross section, which is a measure for the probability of a certain event, i.e. occurring of a particular final state. Having this probability interpretation of both the S-matrix and the scattering cross section, it is possible to find a relation among them and one can express the differential cross-section in terms of the invariant S-matrix element \mathcal{M} ,

$$d\sigma_f = \mathcal{N} \int d\Pi_f |\mathcal{M}_{fi}|^2 \quad , \quad (2.5)$$

with \mathcal{N} being a normalization constant and $\int d\Pi_f$ a phasespace integral over the final states. By considering a decay of one particle into two decay products one can connect the scattering cross section to the Breit-Wigner decay width and fix the normalization constant to

$$\Gamma = \frac{1}{2M} \sum_f \int d\Pi_f |\mathcal{M}_{fi}|^2 \quad , \quad (2.6)$$

with M being the mass of the decaying particle.

2.1.2 Green functions and LSZ reduction formula

In the formalism of second quantization n -point connected Green functions are interpreted as the time ordered vacuum expectation value of n Heisenberg creation and annihilation operators

$$G^{(n)}[\phi_1 \dots \phi_n] := \langle \Omega | T[\phi_1 \dots \phi_n] | \Omega \rangle \quad . \quad (2.7)$$

A connection between Green functions and S-matrix elements in this picture can be given by the Lehmann, Symanzik and Zimmermann (LSZ) reduction formula in second quantization language

$$G^{(n)}[\phi_1 \dots \phi_n] \sim \prod_{i=1}^n D_i S[\phi_1 \dots \phi_n] \quad , \quad (2.8)$$

where D_i are propagators of the respective fields and \sim means that the pole structure on both sides are equivalent [6].

In usual perturbation theory, the calculations of S-matrix elements or Green functions are performed by means of the Feynman theory. To proceed one would now draw all Feynman graphs that represent interactions which contribute to a certain process up to a given order in the structure constant α , calculate them using the Feynman rules, sum them and then finally get the differential cross section calculated up to this order. This suggests that one is able to calculate any cross section of any process up to any precision, provided one has enough time and calculational power to perform these calculations.

However, this expansion in the coupling constant is only valid for $\alpha < 1$. In quantum electrodynamics, where $\alpha^{-1} \approx 137$ this approach works to a very high precision, making QED the up to now most precisely experimentally tested theory in physics. In QCD this kind of perturbation theory is also quite successful in the high energy regime due to asymptotic freedom. One very important part of physics, namely that concerned with the constituents of ordinary matter, made out of light hadrons, such as protons, neutrons and pions, however, is dominated by an energy scale of the order of one GeV and thus cannot be investigated by this otherwise so highly successful tool. To describe QCD in the low-energy domain one has to find a way to calculate S-matrix elements without performing the expansion in the coupling constant.

2.1.3 Dyson's equations

One further manifestation of the strong connection between the S-matrix and Green functions are the Dyson equations. In references [8, 9] Dyson developed two sets of equations for 1-particle or 2-point and vertex or 3-point QED-Green functions. The former can straightforwardly be generalized to all connected n -particle Green functions in quantum field theories by summing up all n -particle irreducible interactions by means of Feynman diagrams. Thus these equations are only valid up to given order in perturbation theory, and can not be addressed as fully non-perturbative. However, similar to the assumption that if a theory is renormalizable up to any order in perturbation theory it is also renormalizable non-perturbatively, the Dyson equations are assumed also to be valid in the non-perturbative regime.



Figure 2.1: The Dyson equation for the three-particle Green function (2.9b)

In the first set of his equations Dyson expressed the Green function in terms of what is nowadays called the T-matrix, for the second he introduces proper n -particle irreducible Green functions, by the implicit definition that these kinds of Green functions can not be written as a sum of two or more parts of which one is again a proper n -particle irreducible Green function.

These equations read in the compact operator notation

$$G^{(n)} = G_0^{(n)} + G_0^{(n)} T^{(n)} G_0^{(n)} \quad (2.9a)$$

$$G^{(n)} = G_0^{(n)} + G_0^{(n)} K^{(n)} G^{(n)} \quad , \quad (2.9b)$$

with $G_0^{(n)} = \prod_i^n D_i$ being the product of n one particle propagators D_i and the n -particle interaction kernel $K^{(n)}$ being the sum over all proper k -particle irreducible interactions with $2k \leq n$,

$$K^{(n)} = K_{irr}^{(n)} + \sum_i K_{irr}^{(n-1)} \otimes D_i^{-1} + \dots \quad .$$

By performing some algebraic manipulations, one can find a Dyson equation for the T-matrix

$$T^{(n)} = K^{(n)} + K^{(n)} G_0^{(n)} T^{(n)} = K^{(n)} + T^{(n)} G_0^{(n)} K^{(n)} \quad , \quad (2.9c)$$

and also some reexpressions of (2.9b) and (2.9c)

$$G^{(n)-1} = G_0^{(n)-1} - K^{(n)} \quad (2.10a)$$

$$T^{(n)-1} = K^{(n)-1} - G_0^{(n)} \quad . \quad (2.10b)$$

All equations (2.9) and (2.10) are equivalent and can be used interchangeably.

The Dyson equations go beyond standard perturbation theory in the sense that after performing a skeleton expansion of the n -particle interaction kernel $K^{(n)}$ in (2.9b) or (2.9c), the equation sums this kernel up infinitely many times, as one can see from the iterative reinsertion of the full Green function into the Dyson equation (2.9b),

$$\begin{aligned} G^{(n)} = & G_0^{(n)} + G_0^{(n)} K^{(n)} G_0^{(n)} + G_0^{(n)} K^{(n)} G_0^{(n)} K^{(n)} G_0^{(n)} \\ & + G_0^{(n)} K^{(n)} G_0^{(n)} K^{(n)} G_0^{(n)} K^{(n)} G_0^{(n)} + \dots \quad (2.11) \end{aligned}$$

Thus terms up to any order are taken into account, but again, due to the finite expansion of the interaction kernel, only a finite subset of all possible interactions will be taken into account.

2.2 The path integral formalism

There are many ways to quantize a classical theory. One approach that is used quite often in contemporary calculations like lattice QCD and Dyson-Schwinger studies, since it allows both perturbative and non-perturbative calculations, is the *path-integral approach* to quantum field theories. It rests on an (functional) integral over all possible field configurations, which contains all information about the theory and is quite similar to the partition function in classical statistical mechanics. Knowing this object in all details is equivalent to having solved the theory.

However, this approach has its own caveats. On the background of a continuous spacetime for example the mathematical existence of the path integral can not be taken to be guaranteed. Also, the Wick-rotation necessary for numerical treatments can become impossible with the unexpected appearance of singularities. Nevertheless the functional integral formalism provides an additional, complementary way to gain new insight into quantum field theories. Especially its relationship to the Euler-Lagrange formalism via the Schwinger-Dyson equations, its strong founding on the action of the theory and its relationship to statistical physics make it highly attractive.

2.2.1 The path integral

As mentioned above, one way to define a quantum field theory is to write down its *generating functional* of the full Green functions, as functional integral over all field configurations weighted by means of their action, which in Euclidean space reads

$$Z[J] = \int \mathcal{D}\phi e^{-S[\phi]+J\phi} \quad , \quad (2.12)$$

where ϕ now stands for any ensemble of possibly interacting fields and J for the corresponding sources. For brevity we suppressed here all dependencies on spacetime coordinates and possible inner quantum numbers, such as spin, flavor and color. The product in the exponential in the above equation has to be understood as a product in all occurring spaces. Thus it implicitly includes integration over spacetime and corresponding sums over matrix indices in spaces with discrete quantum numbers. Explicitly this product reads $J\phi = \sum_{i,c} \int dz J_{ac}^i(z) \phi_{cb}^i(z)$, with i labeling fundamental fields and their sources, respectively, and a, b, c representing sets of matrix indices.

Green functions are now obtained by functional derivatives of the generating functional at zero external sources

$$G^{full}[\phi_1 \dots \phi_n] = \frac{\delta}{\delta J_1} \dots \frac{\delta}{\delta J_n} Z[J] \Big|_{J=0} \quad . \quad (2.13)$$

In general one distinguishes between full, connected and proper one particle irreducible (1PI) Green functions. While the full n -point Green functions take all kinds of interactions between these n points into account (including vacuum bubbles), the connected ones only include these Green functions for which all external points are connected to at least one other. The proper 1PI Green functions consist of all Green functions that can not be divided into two parts.

The functional Integral $Z[J]$ as described in (2.12) is the generating functional for the full Green functions. The generating functional for the connected

Green functions is obtained by

$$W[J] = -\ln Z[J] \quad . \quad (2.14)$$

The generating functional of the proper 1PI Green functions is a Legendre transform of $W[J]$ with respect of the “classical” fields, $\tilde{\phi} = \langle \Omega | \phi | \Omega \rangle$. It reads

$$\Gamma[\tilde{\phi}] = -W[J] + J\tilde{\phi} \quad . \quad (2.15)$$

If it is not mentioned otherwise we will concentrate on the connected Green functions in the following. As already mentioned, these can be related to the vacuum expectation value of time ordered fields,

$$\begin{aligned} \langle \Omega | T[\phi_1 \dots \phi_n] | \Omega \rangle &:= G[\phi_1 \dots \phi_n] \\ &= \frac{\delta}{\delta J_1} \dots \frac{\delta}{\delta J_n} W[J] \Big|_{J=0} = \frac{1}{Z[0]} \frac{\delta}{\delta J_1} \dots \frac{\delta}{\delta J_n} Z[J] \Big|_{J=0} \quad . \end{aligned} \quad (2.16)$$

2.2.2 LSZ reduction formula revisited

As in the second quantization formalism, it is also possible in the path integral approach to find a relation between Green functions and S-matrix elements. It is just the functional integral representation of the LSZ reduction formula, now expressed by means of the generating functionals,

$$S = : \exp \left(\phi_i D_i^{-1} \frac{\delta}{\delta J_i} \right) : Z[J] \Big|_{J=0} \quad (2.17a)$$

$$= Z[0] : \exp \left(\phi_i D_i^{-1} \frac{\delta}{\delta J_i} \right) : W[J] \Big|_{J=0} \quad , \quad (2.17b)$$

with the colon denoting normal ordering and D_i^{-1} being the corresponding inverse propagator of the field ϕ_i . In this form the LSZ formula represents a direct connection between the S-matrix and the generating functionals $Z[J]$ and $W[J]$. This expression can be transformed into a relation between S-matrix elements and Green functions,

$$S_{fi} = \prod_{i=1}^n \phi_i D_i^{-1} G^{full}[\phi_1 \dots \phi_n] \quad (2.18a)$$

$$= Z[0] \prod_{i=1}^n \phi_i D_i^{-1} G[\phi_1 \dots \phi_n] \quad . \quad (2.18b)$$

These equations show a deep relation between the S-matrix elements and Green functions. Not only the pole structures are equivalent as stated in the last section, but, by amputating or attaching external leg factors, the S-matrix elements and the corresponding full Green functions can be transformed into each other, as already indicated in the Dyson equation, all statements that are made about S-matrix elements can be transferred onto Green functions and vice versa.

2.2.3 Dyson-Schwinger equations

Following Section 2.1.3 it is desirable to establish relations between Green functions also in the path integral formalism. Schwinger [10, 11] derived such a set



Figure 2.2: The fermion DSE

of relations. It became clear that the equations derived in this way are the same as stated by Dyson in [9] for 2 and 3-point Green functions, but extend them to all n -point Green functions. Thus these equations are nowadays called the Dyson-Schwinger equations of a quantum field theory.

Following the pathway of the Euler-Lagrange-equations, where the action of a theory is assumed to be extremal and thus is invariant under an infinitely small change of the fields, for the Dyson-Schwinger equations one assumes that the generating functional of the full Green functions is invariant under such a shift in the fields. This can be translated into the condition, that the derivative of the generating functional with respect to a field vanishes [12, 13]

$$0 = \int \mathcal{D}\phi \frac{\delta}{\delta\phi} e^{-S+J\phi} . \quad (2.19)$$

This condition leads to the generating Dyson-Schwinger equations for the connected Green functions,

$$-\frac{\delta S}{\delta\phi_i} \left[\frac{\delta W}{\delta J} + \frac{\delta}{\delta J} \right] + J_i = 0 , \quad (2.20)$$

where the index i specifies one particular field and its source, respectively. Higher n -point functions can now be derived by acting with $n - 1$ functional derivatives with respect to the sources onto Equation (2.20).

For example, the Dyson-Schwinger equation for the fermion propagator S in QED and QCD reads

$$S^{-1} = S_0^{-1} + \int g \tilde{D}_{\mu\nu} \tilde{\gamma}_\mu S \tilde{\Gamma}_\nu . \quad (2.21)$$

where $\tilde{D}_{\mu\nu}$ is the gauge boson propagator, $\tilde{\gamma}_\mu$ the bare fermion-boson vertex and $\tilde{\Gamma}_\nu$ the dressed fermion-boson vertex. In fact it is the Dyson equation (2.10a) for $n = 1$ and the particle being a fermion.

The Dyson-Schwinger equations are the equations of motion for the Green functions. Thus, solving these equations means solving the theory. A complete solution is not possible in general, since the Dyson-Schwinger equations couple different Green functions to each other. As we can read off (2.21) the Dyson-Schwinger equation for the quark propagator in QCD couples to the quark-gluon vertex and the gluon propagator. These again via their respective Dyson-Schwinger equations involve, e.g., the triple gluon vertex and the ghost propagator. This gives a system of infinitely many coupled equations. To solve at least a small subset of these equations means to truncate the infinite tower of equations. A simple demonstration of how this can be achieved will be given in Appendix A. However, if one is only interested in the behavior of the Green

functions in a small momentum regime, e.g. the infrared, one is able to extract information about the scaling behavior without any truncation, thus taking the whole set of DSE's into account [14, 15].

To derive the equations for higher n -point functions and more involved Lagrangians is a tedious task. An algorithmical derivation is implemented in the Mathematica package DoDSE [16].

2.3 Bound state equations

In quantum field theories bound states appear as poles in Green functions. Thus, in the attempt to describe n -particle bound states, one has to investigate the $2n$ -point Green function and investigate its properties at the poles where the total momentum squared of the Green function equates a bound state mass. In Euclidean metric this condition reads $P^2 = -M^2$. The starting point therefore is the generalized Dyson equation as discussed in Section 2.1.3 for the $2n$ -point Green function $G^{(n)}$ Equation (2.9b)

$$G^{(n)} = G_0^{(n)} + G_0^{(n)} K^{(n)} G^{(n)} \quad (2.22)$$

The crucial step now is to assume that at a bound state pole the Green function is dominated by a transition amplitude of the n constituents into a bound state, propagating as bound state and then again split into the constituents. With $\Psi^{(n)} = \langle \Psi | T[\prod_i^n \phi_i] | \Omega \rangle$ denoting this transition amplitude the pole assumption reads,

$$G^{(n)} \xrightarrow{P^2 = -M^2} \Psi^{(n)} \frac{C(P)}{P^2 + M^2} \bar{\Psi}^{(n)} \quad (2.23)$$

where $C(P)$ is a function depending on the spin of the bound state. Plugging the pole assumption into (2.22), and dropping the first term on the right-hand side, since it does not contribute at the pole, yields,

$$\Psi^{(n)} \frac{C(P)}{P^2 + M^2} \bar{\Psi}^{(n)} = G_0^{(n)} K^{(n)} \Psi^{(n)} \frac{C(P)}{P^2 + M^2} \bar{\Psi}^{(n)} \quad , \quad (2.24)$$

which can be simplified to

$$\Psi^{(n)} = G_0^{(n)} K^{(n)} \Psi^{(n)} \quad . \quad (2.25a)$$

One can introduce vertex amplitudes $\Gamma^{(n)} = G_0^{(n)-1} \Psi^{(n)}$, as the transition amplitudes with amputated legs, which yields

$$\Gamma^{(n)} = K^{(n)} G_0^{(n)} \Gamma^{(n)} \quad . \quad (2.25b)$$

Equations (2.25a) and (2.25b) can be used interchangeably depending on the specific problem one deals with, and according to convenience. Note that instead of handling the Dyson equation for the Green functions one could have also started with the Dyson equation for the T-matrix (2.9c) making the pole assumption and then end up with (2.25b) directly.

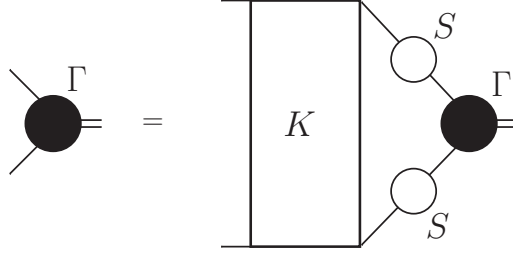


Figure 2.3: The homogenous Bethe-Salpeter equation for the vertex amplitude Γ , Equation (2.30).

Normalization

As any homogenous equation, Equations (2.25), and especially their solutions, are only defined up to a multiplicative scalar factor. Thus one has to find a physically motivated normalization condition, e.g. claiming probability conservation, which is expressed in the condition that the residue at the pole has to be 1. To achieve this one differentiates the inverse Dyson equation Eq.(2.10a) with respect to the total momentum P_μ , using the relation $(A^{-1})' = A^{-1}A'A^{-1}$, [17]

$$\frac{\partial}{\partial P_\mu} G^{(n)-1} = G^{(n)-1} \left(\frac{\partial}{\partial P_\mu} G^{(n)} \right) G^{(n)-1} = \frac{\partial}{\partial P_\mu} \left(G_0^{(n)-1} - K^{(n)} \right) \quad (2.26)$$

$$\frac{\partial}{\partial P_\mu} G^{(n)} = G^{(n)} \frac{\partial}{\partial P_\mu} \left(G_0^{(n)-1} - K^{(n)} \right) G^{(n)} \quad (2.27)$$

and then introduces the pole assumption,

$$\frac{\partial}{\partial P_\mu} \frac{\Psi^{(n)} C(P) \bar{\Psi}^{(n)}}{P^2 + M^2} = \frac{\Psi^{(n)} C(P) \bar{\Psi}^{(n)}}{P^2 + M^2} \frac{\partial}{\partial P_\mu} \left(G_0^{(n)-1} - K^{(n)} \right) \frac{\Psi^{(n)} C(P) \bar{\Psi}^{(n)}}{P^2 + M^2} . \quad (2.28)$$

Now performing the derivative on the lhs and comparing the residues on both sides the normalization condition reads:

$$2P_\mu = \bar{\Psi} \frac{\partial}{\partial P_\mu} \left(G_0^{(n)-1} - K^{(n)} \right) \Psi \quad (2.29a)$$

$$= \bar{\Gamma} \left(\frac{\partial}{\partial P_\mu} G_0^{(n)} - G_0^{(n)} \left(\frac{\partial}{\partial P_\mu} K^{(n)} \right) G_0^{(n)} \right) \Gamma . \quad (2.29b)$$

We now found a set of equations, whose solutions describe general n -particle bound states. The homogenous equations (2.25) and the corresponding normalization conditions (2.29) determine the transition amplitude Ψ and vertex amplitude Γ completely.

2.3.1 Bethe-Salpeter equation

The Bethe-Salpeter equation [17–19] is concerned with two-particle bound states. In fact it is the special case of Equation (2.25) for $n = 2$.

In this case the vertex amplitude has two independent momenta, which can be expressed as the total momentum P and the relative momentum q . In addition it can also depend on inner quantum numbers like spin, flavor or color. Writing down explicitly the dependence on momentum and inner quantum numbers, Equation (2.25) for two fermions ($D_i := S_i$) reads

$$\Gamma_{ab}(P, q) = \int \bar{d}^4 k K(P, q, k)_{ab}^{a'b'} S_{a'c'}(k - \eta P) \Gamma_{c'd'}(P, k) S_{d'b'}(k + \bar{\eta} P), \quad (2.30)$$

where $\bar{d}^4 k$ is short for $\frac{d^4 k}{(2\pi)^4}$, and η and $\bar{\eta}$, with $\eta + \bar{\eta} = 1$, are momentum partitioning parameters. The Latin indices here stand for a collective set of matrix indices for all occurring inner quantum numbers, which are flavor, color and spin in the QCD case. A graphical representation of the Bethe-Salpeter equation is given in Figure 2.3. The interaction kernel K contains all proper two particle irreducible interactions. In Feynman language it can be expressed as an infinite sum of all possible interaction graphs that can appear in the theory. A diagrammatical representation of the first few terms of a skeleton expansion of the meson and diquark BSE-kernel is given in Figure 2.5. Obviously in practical calculations one can not take all processes into account, thus one has to truncate. When solving the Bethe-Salpeter equation explicitly in Appendix A we will perform such a truncation.

Another ingredient needed to solve the Bethe-Salpeter equation are the propagators. Since the Bethe-Salpeter equation itself does not constrain them any further, they have to be seen as external input. One could either use the free fermion propagators, or model dressed propagators by pole sums. An approach that sticks to the ambition of a self-consistent Lorentz covariant set-up is to use the propagators as solutions of their corresponding Dyson-Schwinger equation.

The vertex amplitude Γ for the Bethe-Salpeter equation is called the Bethe-Salpeter amplitude. For the case of mesons, consisting of a quark-antiquark pair, the Bethe-Salpeter amplitude can be interpreted as an effective quark-meson vertex. When performing these kinds of calculations it is helpful to keep such a physical interpretation in mind.

When the interaction kernel does not depend on the total momentum, which is true for the later used ladder truncation of the Bethe-Salpeter equation, the normalization condition, Equation (2.29b), reduces to

$$2P_\mu = \bar{\Gamma} \frac{\partial}{\partial P_\mu} (S_1 \otimes S_2) \Gamma, \quad (2.31)$$

which, multiplied by P_μ , yields

$$2P^2 = \bar{\Gamma} P_\mu \frac{\partial}{\partial P_\mu} (S_1 \otimes S_2) \Gamma, \quad (2.32)$$

which for full momentum and inner quantum number dependence reads

$$2P^2 = P_\mu \frac{\partial}{\partial P_\mu} \text{tr}_{Dcf} \left\{ \int \bar{d}^4 k \bar{\Gamma}(-\tilde{P}, k) S(k_+) \Gamma(\tilde{P}, k) S(k_-) \right\} \Big|_{P^2 = \tilde{P}^2 = -M^2}. \quad (2.33)$$

with $k_\pm = k \pm \frac{1}{2}P$ and where we already wrote the terms within the trace in the right order for the matrix multiplication in Dirac, color and flavor space. A graphical representation of the BSE norm in this sense is shown in Figure 2.4.

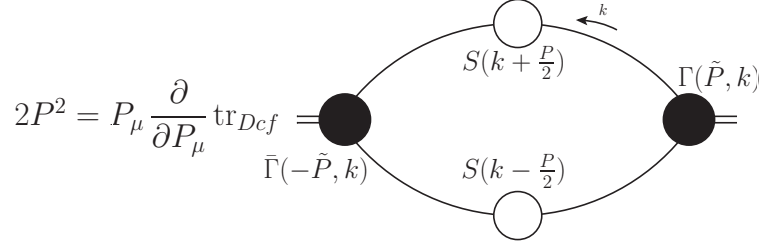


Figure 2.4: The norm of the Bethe-Salpeter equation in ladder truncation, Equation (2.33).

2.3.2 Covariant Faddeev equation

In quark models baryons are interpreted as three-fermion bound states. To treat baryons in the self consistent Dyson-Schwinger-Bethe-Salpeter equation approach¹, one has to consider the case $n = 3$ of Equation (2.25b),

$$\Gamma^{(3)} = K^{(3)} G_0^{(3)} \Gamma^{(3)} \quad , \quad (2.34)$$

with the interaction kernel

$$K^{(3)} = K_{irr}^{(3)} + \sum_{i=1}^3 K_{irr}^{(2)} \otimes S_i^{-1} \quad , \quad (2.35)$$

where i in each case denotes the spectator quark, which does not interact with the other two. The Faddeev assumption states that the 3-particle irreducible interactions can be neglected and one can approximate the kernel by

$$K^{(3)} = \sum_{i=1}^3 K_{irr}^{(2)} \otimes S_i^{-1} := \sum_{i=1}^3 K_i \quad (2.36)$$

where the subscript i denotes the respective spectator quark. To proceed further now, it is helpful to define the Faddeev components Γ_i by inserting (2.36) into (2.34)

$$\Gamma^{(3)} = \sum_{i=1}^3 K_i G_0^{(3)} \Gamma^{(3)} := \sum_{i=1}^3 \Gamma_i \quad (2.37)$$

and also the 2-particle T-matrix in the 3-body problem by using (2.9c)

$$\mathbb{T}_i = K_i + \mathbb{T}_i G_0^{(3)} K_i \quad . \quad (2.38)$$

Multiplying Equation (2.38) with $G_0^{(3)} \Gamma^{(3)}$ from the right yields,

$$\mathbb{T}_i G_0^{(3)} \Gamma^{(3)} = K_i G_0^{(3)} \Gamma^{(3)} + \mathbb{T}_i G_0^{(3)} K_i G_0^{(3)} \Gamma^{(3)} \quad (2.39)$$

$$= (\mathbf{1} + \mathbb{T}_i G_0^{(3)}) \Gamma_i \quad (2.40)$$

$$\Gamma_i = \mathbb{T}_i G_0^{(3)} (\Gamma^{(3)} - \Gamma_i) \quad (2.41)$$

$$\Gamma_i = \mathbb{T}_i G_0^{(3)} (\Gamma_j + \Gamma_k) \quad . \quad (2.42)$$

¹For a more detailed discussion of the following see, e.g., [20]

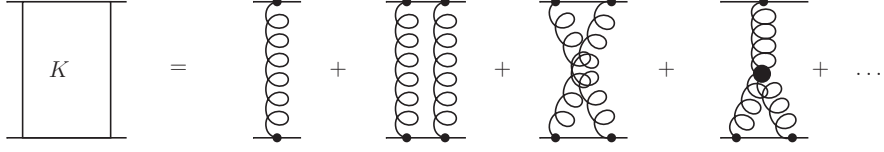


Figure 2.5: The first few terms of a skeleton expansion of the quark-antiquark interaction kernel in the meson BSE and quark-quark interaction in the diquark BSE.

We have now found a set of coupled equations for the Faddeev components that make up the three-particle vertex amplitude according to (2.37). Thus we found equations whose solutions will provide us with descriptions of the 3-particle bound state. The only missing link is the 2-particle T-matrix T_i .

Diquark BSE

Up to now we neglected 3-particle interaction, thereby assuming that the baryon 2-quark correlations give the dominant contributions to the 3-quark bound states. This concept can be made use of by introducing the *diquark* as a correlation of two quarks. This allows us to approximate the 2-particle T-matrix T_i with the pole assumption, as stated at the beginning of this section,

$$T_i \xrightarrow{P^2 = -M_a^2} \chi_i^a D_i^a \bar{\chi}_i^a \otimes S_i^{-1} \quad , \quad (2.43)$$

where a denotes the specific diquark correlation, i.e. its spin, color and flavor structure, $\chi^a = \Gamma_a^{(2)}$ the diquark vertex amplitude, and $D^a = \frac{C_a(P)}{P^2 + M_a^2}$ the diquark propagator. For the case of diquark bound states we can write down the Bethe-Salpeter equation for the diquark a

$$\chi_a = K^{(2)} G_0^{(2)} \chi_a \quad . \quad (2.44)$$

Note that a particular three-body bound state can contain more than one kind of diquark. Thus, to make an ansatz for the whole T_i -matrix we have to sum over all possible diquark correlations such that

$$T_i = \sum_a \chi^a D^a \bar{\chi}^a \otimes S_i^{-1} \quad . \quad (2.45)$$

Quark-diquark BSE

The main advantage of the quark-diquark set-up is that the three body problem is reduced to two two-body problems. We already solved the first one, since in the diquark we have to take into account interactions of two quarks which in QCD is described via gluons. For example we can perform an skeleton expansion for the quark-quark kernel and get a Bethe-Salpeter equation for two quarks as described in the last section.

For the next step, the quark-diquark BSE, the quark-diquark interaction kernel is not known a priori either. We will see in the following that the quark-diquark interaction kernel is not a gluon, but an iterative quark exchange: the

quarks iteratively form diquark bound states with each other, and thus all three quarks are bound together.

To see this we first define the quark-diquark Bethe-Salpeter amplitudes Φ_i by means of the Faddeev components Γ_i ,

$$\Gamma_i = \sum_a \chi^a D^a \Phi_i^a \quad , \quad (2.46)$$

which can be inserted into the Faddeev equation (2.42) and leads to

$$\Phi_i^a = \sum_b \bar{\chi}_i^a S_k \chi_j^b S_j D_j^b \Phi_j^b + \sum_c \bar{\chi}_i^a S_j \chi_k^c S_k D_k^c \Phi_k^c \quad (2.47)$$

which for identical quarks can be simplified, and thus reads in a symbolic notation

$$\Phi^a = \sum_{b,c} \underbrace{\bar{\chi}^a S \chi^b}_{K^{ab}} \underbrace{S D^{bc}}_{G_0} \Phi^c \quad . \quad (2.48)$$

To clarify that we deal with a Bethe-Salpeter equation we specified the BSE interaction kernel K and the free propagators G_0 , and we got the expected result. The three-body problem of the baryon can be reduced to a coupled set of two-body problems. At first one has to solve the Bethe-Salpeter equation for diquarks within a given model and then one can construct a quark-diquark Bethe-Salpeter equation, whose interaction kernel is a quark exchange between the diquark bound states.

2.4 Intrinsic structure of QCD Green functions

QCD features an opulent intrinsic structure, which has to be reflected by its Green Functions and analogously in its S-matrix elements. Every object in QCD carries certain Lorentz, Dirac, flavor and color quantum numbers. So the general structure of one particular QCD Green function depending on a certain set of external parameters s_i is:

$$G(s_i) = \sum_{\mu\alpha a A} F_{\mu\alpha a A}(s_i) \cdot \left[L_\mu(s_i) \otimes D_\alpha(s_i) \otimes f_A(s_i) \otimes c_a(s_i) \right] \quad , \quad (2.49)$$

where $F(s_i)_{\mu\alpha a A}$ are scalar functions that contain only scalar combinations of the external parameters s_i . L, D, f and c stand for particular elements of a particular representation of the underlying symmetry group of Lorentz, Dirac, flavor and color structure, respectively. Since we are usually working with matrix representations they are in general matrix valued objects.

In QCD mainly two kinds of true representations occur, namely fundamental representations (i.e. quarks, anti-quarks) and the adjoint representation (i.e. gluons) of $SU(N)$ groups or combinations thereof, e.g., the flavor space of a diquark is $SU(N_f) \otimes SU(N_f)$.

All elements of a Lie-group can be expressed in terms of linear combinations of the Lie-algebra, which is the tangential space of the group manifold in the $\mathbb{1}$ -element. Both of the above kinds of representations are connected to the algebra of the group, so they do not only feature their intrinsic group structure, but also they inherit the algebraic structure of the group-algebra, which implies linear

space properties. Thus, we can find a basis and with the trace it is even possible to imply a scalar product on these spaces, so we can define orthogonality. In this sense it is possible to expand the group structure L , D , f and c onto a particular chosen basis and then find the corresponding functions F . The aim is now to find a suitable, not necessarily orthonormal, basis in the corresponding group spaces and span the investigated Green function onto them.

Note that, eventhough they are not Green functions in the strict meaning of the term, since they are no vacuum expectation values of fundamental fields and as can be seen in the derivation of the Bethe-Salpeter equation, the Bethe-Salpeter amplitudes are parts of the residue of a 4-point Green function at a bound-state pole. In this sense the BSA's inherit a color, flavor and Dirac structure from their particular parent Green function at a certain pole.

Chapter 3

The triangle diagram and its ingredients

As already mentioned in Section 2 the coupled Bethe-Salpeter-Dyson-Schwinger approach to hadron phenomenology is rich in accessible observables. Calculations of electromagnetic form factors of pseudoscalar mesons substantiated the long-standing hypothesis of vector meson dominance (VMD) in this approach [21, 22]. The VMD-hypothesis states that the hadronic part of the vacuum polarization of the photon is dominated by the ρ^0 -meson, since it is the lightest hadron with the same quantum numbers as the photon. One important consequence is, that the quark-photon vertex should contain a pole at a momentum transfer that corresponds to the ρ^0 -meson mass squared, as could also be found in the Dyson-Schwinger-Bethe-Salpeter formalism in [21]. This motivated the calculation of the $\rho \rightarrow \pi\pi$ transition self-consistently in the same approach, as it was performed in [4, 5]. In this chapter we will set up the calculational structure, and present all ingredients that we need to calculate hadronic transitions.

As we want to describe decays or three-composite-particle interactions, the skeleton for our calculations is represented by the triangle diagram, which in the term shown in Figure 3.1 corresponds to a generalized impulse approximation. The input needed for its treatment are expressions for propagators and

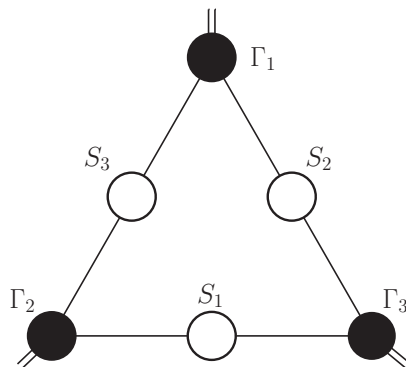


Figure 3.1: Triangle diagram

amplitudes of the participating particles, which are in our case quarks, diquarks, mesons and baryons. This is a well known setup and has been used for calculations of e.g. meson [22–24] and baryon [25–27] electromagnetic form factors, two photon decays of mesons [28–30] and, as we intend to calculate, meson hadronic transitions [4].

The building blocks are (numerical) solutions of the corresponding integral equations: the quark Dyson-Schwinger equation, the Bethe-Salpeter equations for mesons and diquarks as well as the quark-diquark Bethe-Salpeter equation for baryons. They serve as mathematical representations of the underlying physical objects and processes.

3.1 Quarks

One basic quantity in all of our calculations is the dressed quark-propagator, which is the two-point Green function of the quark field.

$$S(p) = G^{(2)}[\psi^\dagger(p), \psi(p)] = \langle \Omega | T[\psi^\dagger(p), \psi(p)] | \Omega \rangle \quad , \quad (3.1)$$

In this section, I would like to present its general structure, different parameterizations and its Dyson-Schwinger equation. Afterwards I present the general strategy how to solve this equation and even solve it for a simple toy model with massless quarks in Appendix A. Even in this simple case, the quark propagator already shows some interesting properties that are generic for non-perturbative QCD calculations.

3.1.1 Color and flavor structure

We will now study the QCD intrinsic structure of the quark propagator as explained in the last section.

A quark will not change its color, when it is propagating in spacetime and only self interactions occur. So the only structure in color space, that has a non vanishing scalar function is just proportional to $\mathbb{1}_c$ in color space. The same is true for its flavor part since the fundamental interaction in QCD is flavor-blind. So by now the quark propagator with specified color and flavor structure looks like:

$$S_{\alpha\beta ABab}(p) = S_{\alpha\beta}(p) \otimes \frac{1}{\sqrt{N_f}} \delta_{AB} \otimes \frac{1}{\sqrt{N_c}} \delta_{ab} \quad , \quad (3.2)$$

where $S_{\alpha\beta}(p)$ still contains the Lorentz and Dirac structure.

3.1.2 Lorentz and Dirac structure

If one is dealing with Dirac fermions one often chooses the Dirac- γ -matrices $\{\gamma_1, \gamma_2, \gamma_3, \gamma_4\}$ to define a simultaneous representation in Dirac and Lorentz space. This can be done since the commutators of components of the Lorentz vector made out of these matrices

$$\gamma_\mu = (\gamma_1, \gamma_2, \gamma_3, \gamma_4) \quad (3.3)$$

are generators of the Lorentz-group

$$S^{\mu\nu} = -\frac{1}{4} [\gamma_\mu, \gamma_\nu] \quad . \quad (3.4)$$

Thus, the construction of a particular basis in Lorentz and Dirac space in the course of this thesis will often be handled simultaneously by use of the Lorentz vector of the Dirac-matrices γ_μ .

The quark propagator depends on the Lorentz vector p_μ but is itself a Lorentz scalar. To find a suitable basis in Dirac and Lorentz space we have to look for Lorentz scalars that can be constructed out of p_μ and γ_μ . There are only three possibilities, the momentum squared $p_\mu p_\mu = p^2$, the scalar product $p_\mu \gamma_\mu = \not{p}$, and the square $\gamma_\mu \gamma_\mu = 4\mathbf{1}_D$. Since the two squares are linearly dependent, we found two linearly independent elements for the combined Dirac-Lorentz basis for the quark propagator $\{\mathbf{1}_D, \not{p}\}$.

The invariant amplitudes depend on scalars that are constructed out of the external parameters. In this case there are four external parameters p_μ which can be combined to one Lorentz scalar p^2 which is then the only variable for the scalar functions.

Now, naming the functions according to their associated physical meaning, vectorial and scalar part, σ_v and σ_s , we have found the full structure of the quark propagator:

$$S(p) = (-i\sigma_v(p^2)\not{p} + \sigma_s(p^2)\mathbf{1}_D) \otimes \frac{1}{\sqrt{N_f}}\mathbf{1}_f \otimes \frac{1}{\sqrt{N_c}}\mathbf{1}_c \quad , \quad (3.5)$$

where the $-i$ in front of the first term stems from the conventions in Euclidean space.

In many calculations one is not interested in the quark propagator but its inverse. Also sometimes it is of interest to point out the difference between dressed and free quark propagator more clearly. Suppressing color and flavor dependence for the moment, one can parameterize the inverse quark propagator as

$$S^{-1}(p) = A(p^2)i\not{p} + B(p^2)\mathbf{1}_D \quad , \quad (3.6)$$

in comparison with the inverse of the free quark propagator $S_0^{-1}(p) = i\not{p} + m\mathbf{1}_D$. Sometimes also a third parameterization is used, which allows a interpretation of the dressing functions in a physical sense:

$$S(p) = \frac{Z(p^2)}{i\not{p} + M(p^2)} \quad . \quad (3.7)$$

Where $M(p^2)$ is referred to as the momentum (and gauge) dependent “quark mass function“ and $Z(p^2)$ as the ”quark wave function renormalization“. All three parameterizations are connected to each other via algebraical manipulations and can be used interchangeably.

$$\sigma_v(p^2) = \frac{A(p^2)}{A^2(p^2)p^2 + B^2(p^2)} \quad \sigma_s(p^2) = \frac{B(p^2)}{A^2(p^2)p^2 + B^2(p^2)} \quad (3.8a)$$

$$A(p^2) = \frac{\sigma_v(p^2)}{\sigma_v^2(p^2)p^2 + \sigma_s^2(p^2)} \quad B(p^2) = \frac{\sigma_s(p^2)}{\sigma_v^2(p^2)p^2 + \sigma_s^2(p^2)} \quad (3.8b)$$

$$Z(p^2) = \frac{1}{A(p^2)} \quad M(p^2) = \frac{B(p^2)}{A(p^2)} \quad (3.8c)$$

As we have seen in Section 2.2, in quantum field theories for every Green function there exists a corresponding equation of motion, its Dyson-Schwinger equation. The quark Dyson-Schwinger equation, synonymously called the “QCD gap



Figure 3.2: The quark DSE in rainbow truncation

equation”, reads

$$S^{-1}(p) = S_0^{-1}(p) + \int \bar{d}^4 k D_{\mu\nu}^{ab}(p-k) \left(g \frac{\lambda^a}{2} \gamma_\mu \right) S(k) g \Gamma_\nu^b(k, p). \quad (3.9)$$

It contains the dressed quark Propagator $S(p)$, depending on the quark-momentum p , and its inverse, the inverse of the free quark propagator $S_0(p)$, the dressed gluon propagator $D_{\mu\nu}^{ab}(p-k)$, the dressed quark-gluon vertex $\Gamma_\nu^b(k, p)$ and the bare quark-gluon vertex $\frac{\lambda^a}{2} \gamma_\mu$ each with coupling g . The λ^a represent the Gell-Mann matrices, as generators of the fundamental representation of $SU(3)_c$. The second term in (3.9) is also called the quark self energy. A diagrammatical representation of the equation was already given in Figure 2.2.

3.1.3 Rainbow truncation

In Appendix A I will present an explicit solution of the quark Dyson-Schwinger equation in a simple model. Here I will only present the main steps.

As already mentioned above, to perform a calculation using the quark Dyson-Schwinger equation one has to know descriptions of the dressed gluon propagator and the dressed quark-gluon vertex. The most easy possibility is to replace the dressed terms by their bare expressions. The mismatch introduced by this truncation is compensated by an effective interaction strength,

$$g^2 D_{\mu\nu}(p-k) \Gamma_\nu^a(k, p) \rightarrow \mathcal{G}((p-k)^2) \frac{T_{\mu\nu}(p-k)}{(p-k)^2} \frac{\lambda^a}{2} \gamma_\nu \quad (3.10)$$

and thus the quark-Dyson Schwinger equation in rainbow truncation reads

$$S^{-1}(p) = S_0^{-1}(p) + \frac{4}{3} \int \bar{d}^4 k \frac{\mathcal{G}((p-k)^2)}{(p-k)^2} T_{\mu\nu}(p-k) \gamma_\mu S(k) \gamma_\nu \quad (3.11)$$

See also Figure 3.2 for a graphical representation.

By using one of the parameterizations for the quark propagator given above one can proceed further and transform Equation (3.11) into a set of two coupled equations, as it will be shown in Appendix A.1.1. When using the parameterization (3.6) for the inverse quark propagator one gets:

$$B(p^2) = m + 4 \int \bar{d}^4 k \frac{\mathcal{G}((p-k)^2)}{(p-k)^2} \frac{B(p^2)}{A^2(p^2) p^2 + B^2(p^2)} \quad (3.12a)$$

$$p^2 A(p^2) = p^2 + \frac{4}{3} \int \bar{d}^4 k \frac{\mathcal{G}((p-k)^2)}{(p-k)^2} \frac{(p^2 - p \cdot k)(p \cdot k - k^2)}{(p-k)^2} \frac{A(p^2)}{A^2(p^2) p^2 + B^2(p^2)}. \quad (3.12b)$$

To achieve an explicit solution of (3.12) one piece is still unknown. The coupling strength \mathcal{G} is unspecified and has to be modeled. On the one hand this can account for truncation artefacts, on the other hand it represents physical input and by introducing reasonable parameters one can attempt to learn something about the nature of the strong interaction. Within the last decades several models have been developed, starting with the first simple model by Munczek and Nemirovsky [31], which even gives analytic solutions in some limits, and which will be under investigation in more detail in Appendix A, going to more sophisticated models, which try to model the strong interaction in a realistic way and match perturbative QCD to one [21, 32] and two loops [33] and have to be solved numerically, to others which are dominated by the mid-momentum regime for the sake of numerical simplicity [34]. After choosing one certain kind of interaction one solves the coupled system of integral equations (3.12) with standard numerical techniques. For the calculations of the decays we consistently used the model by Maris and Tandy [21], which will be introduced in Section 4.2 and in which case all equations have to be solved numerically.

A more detailed derivation of Equations (3.12) and an explicit solution of the quark DSE within the model of Munczek and Nemirovsky will be presented in Appendix A, where, in the chiral limit, these equations can be solved analytically. Note that both as input in the BSE and the triangle diagram the dressing functions of the quark propagator have to be known in a parabolic domain in the complex p^2 -plane. A short introduction and further references regarding this issue can be found in Appendix B.3.

3.2 Mesons

In quark models and QCD phenomenology mesons basically¹ are viewed as quark-antiquark bound states, which makes them the most simple hadrons and interesting objects to be studied. For several decades now, they were intensely studied in terms of any model of hadron phenomenology. Especially the pion attracted lots of interest, as it is seen as *would-be* Goldstone-boson of dynamical chiral symmetry breaking, and at the same time can be regarded as a $q\bar{q}$ bound state, which is, e.g., problematic in a constituent-quark picture.

Two-particle bound states in quantum field theories can be described by means of Bethe-Salpeter amplitudes as solutions of the Bethe Salpeter equation as described in Section 2.3. Following the procedure of the last section at first I will shortly present the Bethe Salpeter equation and then list suitable parameterizations of the Bethe-Salpeter amplitudes in color, flavor and Dirac space. Again, calculational details are shifted to Appendix A, which also includes an explicit solution of the meson Bethe-Salpeter equation for pseudoscalar and vector mesons in the Munczek-Nemirovsky model, where an analytical solution is possible. For more sophisticated models this is not the case and one has to solve the Bethe-Salpeter equation numerically. This is usually done by a simple iteration method, but the use of more elaborated algorithms is of great advantage [36].

¹Contemporary discussions of some mesons as, e.g., diquark-antidiquark boundstates, tetraquarks, meson-molecule states or mixing effects with glue-balls, etc. are not taken into account here. See e.g. [35] and references therein

As derived in Section 2.3 the homogenous Bethe-Salpeter equation reads

$$\Gamma_{\alpha\beta AB ab}(P, q) = \int \bar{d}^4 k K(P, q, k)_{\alpha\beta AB ab}^{\alpha'\beta' A'B' a'b'} [S(k - \eta P) \Gamma(P, k) S(k + \bar{\eta} P)]_{\alpha'\beta' A'B' a'b'} \quad (3.13)$$

with its solution the Bethe-Salpeter amplitude $\Gamma_{ab AB \alpha\beta}(P, q)$ and an interaction kernel $K(P, q, k)$ not further specified up to now. The indices label the Dirac (Greek), flavor (capital Latin) and color (lowercase Latin) indices of the quark and the anti-quark.

The terms $S(p)$ in the Bethe-Salpeter equation are quark propagators, which we take as solution of their Dyson-Schwinger equation. In order to make the calculations as self-consistent as possible we will have to specify the BSE kernel according to the effective interaction in the gap equation, as well as the rainbow truncation used there. This truncation will be explicitly performed in Appendix A.2.1. Here we only quote the ladder truncated interaction kernel,

$$K(P, q, k) \rightarrow -\frac{4}{3} \mathcal{G}((q - k)^2) \gamma_\mu \frac{T_{\mu\nu}(p - k)}{(p - k)^2} \gamma_\nu \quad (3.14)$$

which give the meson Bethe-Salpeter equation in ladder truncation

$$\Gamma_{\alpha\beta}(P, q) = -\frac{4}{3} \int \bar{d}^4 k \frac{\mathcal{G}((q - k)^2)}{(q - k)^2} T_{\mu\nu}(q - k) \gamma_\mu S(k - \frac{P}{2}) \Gamma(P, k) S(k + \frac{P}{2}) \gamma_\nu \quad (3.15)$$

As mentioned above, coupled Bethe-Salpeter–Dyson-Schwinger equation studies require the quark propagator to be calculated in the complex plane. This can be directly extracted from (3.13). Recall the arguments of the quark propagator dressing functions $\sigma_{v,s}(p^2)$, which yields in the Bethe-Salpeter amplitude

$$(k - \eta P)^2 = k^2 + \eta^2 P^2 - 2\eta k \cdot P = k^2 - \eta^2 M^2 - 2i\eta k_4 M \quad (3.16a)$$

$$(k + \bar{\eta} P)^2 = k^2 + \bar{\eta}^2 P^2 + 2\bar{\eta} k \cdot P = k^2 + \bar{\eta}^2 M^2 - 2i\bar{\eta} k_4 M \quad (3.16b)$$

where we assumed to work in the rest frame of the bound-state and thus $P_\mu = (\vec{0}, iM)$ with M being the bound-state mass. One sees that the domain in the complex plane in which both quark propagators have to be known is smallest for equal momentum partitioning $\eta = \bar{\eta} = \frac{1}{2}$, which we will use from now on. We also can read off (3.16) that the domain increases with the mass of the bound state. Due to possible singularities in the quark dressing functions $\sigma_{v,s}(p^2)$, this is among the biggest technical restrictions onto the prospects of this approach to hadron phenomenology until methods are developed to deal with such singularities [37].

Bethe-Salpeter amplitudes inherit a color, flavor and Dirac structure from their parent Green function. In practical calculations, when doing phenomenology, one chooses a certain channel by imposing particular quantum numbers, especially in flavor and Dirac space, onto the Bethe Salpeter amplitude. This is done via taking a subset of a chosen basis in these spaces.

3.2.1 Flavor and color structure

In the isospin-symmetric limit we have to find representations of the combination of one quark and one anti-quark, being in the fundamental and the conjugate fundamental representation of $SU(2)$ flavor. In Appendix B.1 we give a detailed discussion about the construction of the $SU(2) \otimes SU(2)$ multiplets in the different representations and the corresponding Clebsch-Gordan coefficients, so here we only state the results for the isovector triplet r^{+0-} and isoscalar singlet r^s

$$r^+ = |u\bar{d}\rangle = \frac{1}{2}(\sigma_1 + i\sigma_2) \quad (3.17a)$$

$$r^0 = \frac{1}{\sqrt{2}}(|u\bar{u}\rangle - |d\bar{d}\rangle) = -\frac{1}{\sqrt{2}}\sigma_3 \quad (3.17b)$$

$$r^- = -|d\bar{u}\rangle = -\frac{1}{2}(\sigma_1 - i\sigma_2) \quad (3.17c)$$

$$r^s = |u\bar{u}\rangle + |d\bar{d}\rangle = \frac{1}{\sqrt{2}}\mathbb{1} \quad (3.17d)$$

which are normalized to $\text{tr}_f \left\{ (r^I)^\dagger r^J \right\} = \delta^{IJ}$.

As mesons are measured in experiments for them the confinement hypothesis implies that their color structure is the one of a color singlet, which is derived in Appendix B.1 and for a quark-antiquark system is just proportional to $\mathbb{1}_c$. We are already able now to explicitly write down the color and flavor part of the meson Bethe-Salpeter amplitude

$$\Gamma_{\alpha\beta AB ab}^I = \Gamma_{\alpha\beta} \otimes r_{AB}^I \otimes \frac{1}{\sqrt{3}}\delta_{a\bar{b}} \quad (3.18)$$

Since we work in the isospin-symmetric limit, all three isovector states will be degenerate in mass. So in explicit calculations of the mass we can just choose one particular I_3 projection. It is convenient to choose the $I_3 = 0$ component, which we will do in the following. For calculations of flavor coefficients in the triangle diagram in Chapter 4 one has to take all possibilities into account.

3.2.2 Dirac structure – pseudoscalar meson

The spin of a particle dictates its behavior under continuous Lorentz transformations. For mesons, being bosons, we only have integer-valued spins, so they behave like Lorentz scalar, vector, or higher spin objects. The discrete Lorentz transformations specify the particles further, in terms of being even or odd under parity, and charge parity in case of equal mass constituents. The particular mesons we want to investigate dictate the particular behavior under Lorentz-transformations, which has to reflect in the corresponding Bethe-Salpeter amplitude. So the guiding principle to the Dirac-structure of the different Bethe-Salpeter amplitudes are the quantum numbers of the particular mesons we want to describe. As we will be concerned with pseudoscalar and vector mesons only, we will stick to the cases $J = 0, 1$. For further details, discussion and expansion to higher spins, see [21, 32, 38–40].

In a Bethe-Salpeter amplitude we have, like in general in any two-body state, two independent momenta, the total momentum P_μ and the relative momentum between the constituents q_μ . Like in the case of the quark propagator we

can combine them with the Dirac matrices γ_μ to give us the appropriate behavior under Lorentz transformations. We will now first construct a basis for a scalar Bethe-Salpeter amplitude from which we then can easily switch to the pseudoscalar or pion Bethe-Salpeter amplitude.

The three vectors above can be combined to six Lorentz scalars, which are just their squares $P^2 = -M^2$, q^2 , $\gamma_\mu \gamma_\mu = 4 \mathbf{1}_D$ and scalar products $i \not{P}$, $i \not{q}$ and $P \cdot q$. All vector squares and the scalar product $P \cdot q$ are, in Dirac space, proportional to $\mathbf{1}_D$, so they are linearly dependent, but linearly independent to the other two. Looking for other basis vectors, we find the commutator $-\frac{1}{2} [\not{q}, \not{P}]$, which is linearly independent to the other three basis vectors found so far and completes the set of possible basis states, since any other combination of P_μ , q_μ and γ_μ can be shown to be proportional to the ones already found. Note that all basis functions are, as all scalar products of two Lorentz vectors, even under parity transformation, thus we found a basis for scalar-meson Bethe-Salpeter amplitudes

$$\begin{aligned} \tau_1^{(s)} &= \mathbf{1} & \tau_3^{(s)} &= i \not{q} \\ \tau_2^{(s)} &= i \not{P} & \tau_4^{(s)} &= -\frac{1}{2} [\not{q}, \not{P}] \end{aligned} \quad , \quad (3.19)$$

which we could use to start an investigation of scalar mesons. But, since we want to expand this approach also to other kinds of mesons some further investigations are needed.

One meson that is of interest in hadron phenomenology in general and in this thesis in particular is the pion. The pion is not a scalar, but a *pseudo*-scalar particle. That means that it is not an even parity eigenstate like a scalar but an odd one. To achieve this different behavior one multiplies a factor $\pm i \gamma_5$, which is odd under parity transformation, to every basis vector from the left. Thus a basis for a general pseudoscalar meson reads

$$\begin{aligned} \tau_1^{(ps)} &= i \gamma_5 \mathbf{1} & \tau_3^{(ps)} &= \gamma_5 \not{q} \\ \tau_2^{(ps)} &= \gamma_5 \not{P} & \tau_4^{(ps)} &= -\frac{i}{2} \gamma_5 [\not{q}, \not{P}] \end{aligned} \quad (3.20)$$

For C-Parity eigenstates like the π^0 , it is convenient to choose a basis where all basis elements behave in the same manner under C-Parity. A C-Parity transformation flips all internal quantum numbers, including the relative momentum inside the Bethe-Salpeter amplitude q , but not the total momentum P . So the scalar product $q \cdot P$ is odd under C-Parity transformations and it can be explicitly pulled out of every invariant amplitude F and attached to the basis vector. While τ_1 , τ_2 and τ_4 in the basis (3.20) are even under C-Parity, τ_3 is not, thus we write explicitly a factor of $P \cdot q$ in front of τ_3 and we get our basis for the pion Bethe-Salpeter amplitude:

$$\begin{aligned} \tau_1^{(\pi)} &= i \gamma_5 \mathbf{1} & \tau_3^{(\pi)} &= P \cdot q \gamma_5 \not{q} \\ \tau_2^{(\pi)} &= \gamma_5 \not{P} & \tau_4^{(\pi)} &= -\frac{i}{2} \gamma_5 [\not{q}, \not{P}] \end{aligned} \quad (3.21)$$

Now we have constructed a basis which perfectly fits the quantum numbers of the π^0 -state $J^{PC} = 0^{-+}$. Since all the basis functions are even under C-Parity, all amplitudes F must be so, too. If the investigated state is not a

C-parity eigenstate the behavior of the basis will not play such an important role. Now finally we can write down a basis for the internal structure of the Bethe-Salpeter amplitude for a general π -meson of isospin projection I

$$\Gamma^{(\pi)}(P, q) = \sum_i F_{iI}(P, q) \tau_i^{(\pi)} \otimes r^I \otimes \frac{1}{\sqrt{3}} \delta_{a\bar{b}} \quad (3.22)$$

The invariant amplitudes $F_i(P, q)$ are Lorentz scalars, and so can only depend on the three Lorentz-scalar combinations that can be constructed from P and q , namely, P^2 , q^2 , and $P \cdot q$. The latter is often replaced by the cosine $z = P \cdot q / \sqrt{P^2 q^2}$ with $-1 \leq z \leq 1$.

$$\Gamma^{(\pi)}(P, q) = \sum_i F_i(P^2, q^2, z) \tau_i^{(\pi)} \otimes r^I \otimes \frac{1}{\sqrt{3}} \delta_{a\bar{b}} \quad (3.23)$$

As P is the total momentum, it will be fixed at the bound state poles by the on-shell condition $P^2 = -M^2$. We can use this on-shell condition to differentiate between the particular states, e.g. ground state with $P^2 = -M_0^2$, first excitation with $P^2 = -M_1^2$, etc. Thus at these poles, as a necessary condition for solutions of the homogenous BSE, P^2 is just a discrete parameter and we can write for solutions of the homogenous Bethe-Salpeter equation

$$\Gamma^{(\pi)}(P, q) = \sum_i F_i^{P^2=-M^2}(q^2, z) \tau_i^{(\pi)} \otimes r^I \otimes \frac{1}{\sqrt{3}} \delta_{a\bar{b}} \quad (3.24)$$

Chebyshev expansion

One efficient tool to reduce numerical effort is to expand the dependence of the invariant amplitudes $F_i^{P^2=-M^2}(q^2, z)$ in z onto Chebyshev polynomials of second kind $U(z)$. Since they converge for complex values in the unit circle, i.e. for a real variable in the interval $[-1, 1]$, they are suitable for the expansion of a cosine. In Bethe-Salpeter studies of ground state mesons with equal mass constituents one does not need to take many of them into account.

When performing this expansion a Bethe-Salpeter amplitude reads

$$\Gamma(P, q) = \sum_{i,j} {}^j f_i^{P^2=-M^2}(q^2) U_j(z) \tau_i \otimes r^A \otimes \frac{1}{\sqrt{3}} \delta_{ab} \quad (3.25)$$

where we suppressed the reference to pseudoscalar mesons since this expansion is quite general and can be performed for any kind of Bethe-Salpeter amplitude. For clarification we want to fix here the nomenclature of the different building blocks of a Bethe-Salpeter amplitude.

$\Gamma(P, q)$	Bethe-Salpeter amplitude with total momentum P and relative momentum q
τ_i	Lorentz (basis) covariants
$F_i(P^2, q^2, z), F_i^{P^2=-M^2}(q^2, z)$	Lorentz (invariant) amplitudes depending on P^2 and q^2 and z
$U_j(z)$	Chebyshev-Polynomials of second kind depending on the cosine z
${}^j f_i(P^2, q^2), {}^j f_i^{P^2=-M^2}(q^2)$	Chebyshev moments depending on P^2 and q^2

3.2.3 Dirac structure – vector meson

Following the route above, in principle we are able to construct a Bethe-Salpeter amplitude for any meson. The next step will be a vector meson Bethe-Salpeter amplitude. Since the color and flavor structure is the same as for the pseudoscalar the only difference is the Dirac structure.

A vector meson has its name from the behavior under Lorentz-transformations, which corresponds to angular momentum $J = 1$. Still having the same building blocks as above, P_μ , q_μ and γ_μ , we have to construct Dirac elements that behave like a Lorentz vector. As they are already Lorentz vectors, the only thing we have to do is to multiply them with any Lorentz scalar that we can construct out of them. But these are exactly (3.19), so we are immediately able to write down a first basis for the vector-BSA

$$\begin{aligned}
 \tau_{\mu 1} &= \gamma_\mu & \tau_{\mu 5} &= q_\mu \mathbf{1} & \tau_{\mu 9} &= P_\mu \mathbf{1} \\
 \tau_{\mu 2} &= i \gamma_\mu \not{P} & \tau_{\mu 6} &= i q_\mu \not{P} & \tau_{\mu 10} &= i P_\mu \not{P} \\
 \tau_{\mu 3} &= i \gamma_\mu \not{q} & \tau_{\mu 7} &= i q_\mu \not{q} & \tau_{\mu 11} &= i P_\mu \not{q} \\
 \tau_{\mu 4} &= -\frac{1}{2} \gamma_\mu [\not{q}, \not{P}] & \tau_{\mu 8} &= -\frac{1}{2} q_\mu [\not{q}, \not{P}] & \tau_{\mu 12} &= -\frac{1}{2} P_\mu [\not{q}, \not{P}]
 \end{aligned} \tag{3.26}$$

Any Bethe-Salpeter amplitude is a Lorentz scalar. The basis we have constructed so far behaves like a Lorentz vector, which implies that we need another Lorentz vector to create a Lorentz-scalar. Spin polarizations will help us here.

For a massive $J = 1$ particle there exist three spin-polarizations that are all transverse to its total momentum. So for any polarization λ of a $J = 1$ particle moving with total momentum P_μ there exists a normalized vector $\varepsilon_\mu^\lambda(P)$ with

$$\varepsilon_\mu^\lambda(P) P_\mu = 0 \quad . \tag{3.27}$$

These polarizations are complete, which means that the normalized sum over all polarizations gives the transversal projection operator $T_{\mu\nu}$

$$\frac{1}{n_\lambda} \sum_\lambda \varepsilon_\mu^{\lambda\dagger}(P) \varepsilon_\nu^\lambda(P) := T_{\mu\nu}(P) = \delta_{\mu\nu} - \frac{P_\mu P_\nu}{P^2} \quad , \tag{3.28}$$

with n_λ being the number of polarizations, which in this case is $n_\lambda = 3$, and we choose them as orthogonal,

$$\varepsilon_\mu^\lambda \varepsilon_\mu^{\lambda'} \propto \delta^{\lambda\lambda'} \quad . \tag{3.29}$$

For a vector meson at rest, thus having a total momentum of $P_\mu = (0, 0, 0, iM)$ one choice for the $\varepsilon_\mu^\lambda(P)$ can be $\varepsilon_\mu^1(P) = (1, 0, 0, 0)$, $\varepsilon_\mu^2(P) = (0, 1, 0, 0)$ and $\varepsilon_\mu^3(P) = (0, 0, 1, 0)$.

If we now contract the basis in (3.26) with a certain ε_μ^λ and sum over all λ , all the longitudinal parts vanish. Since we will do this only at the very end of the calculations, we still keep the Lorentz index now, but only keep that part of (3.26) that survives the contraction in the end. With the ρ -meson in mind we additionally specify the behavior under discrete Lorentz transformations and

end up with a basis for vector Bethe-Salpeter amplitudes

$$\begin{aligned}
 \tau_{\mu 1} &= \gamma_{\mu}^T & \tau_{\mu 5} &= i q_{\mu}^T \mathbf{1} \\
 \tau_{\mu 2} &= i \gamma_{\mu}^T \not{P} & \tau_{\mu 6} &= q_{\mu}^T \not{P} \\
 \tau_{\mu 3} &= i [\gamma_{\mu}^T, \not{q}] & \tau_{\mu 7} &= q_{\mu}^T \not{q} \\
 \tau_{\mu 4} &= \frac{1}{2} \gamma_{\mu}^T [\not{q}, \not{P}] - q_{\mu}^T \not{P} & \tau_{\mu 8} &= i q_{\mu}^T [\not{q}, \not{P}]
 \end{aligned} \tag{3.30}$$

where the index T connotes the transversal part $k_{\mu}^T = T_{\mu\nu}(P) k_{\nu}$ for any Lorentz vector k .

After constructing a basis we can, similar to (3.23), write down the general structure for a vector Bethe-Salpeter amplitude

$$\Gamma_{\mu}(P, q) = \sum_i F_i^{P^2 = -M^2}(q^2, z) \tau_{\mu i} \otimes r^I \otimes \frac{1}{\sqrt{3}} \delta_{a\bar{b}} \quad . \tag{3.31}$$

3.3 Baryons

In this thesis baryons are treated as bound states of quarks and diquarks. This concept it introduced by means of the three particle bound state equation in Section 2.3.2. By introducing the Fadeev approximation we were able to turn the three particle equation into a set of coupled two-particle problems

$$\Phi^a = \sum_{b,c} \bar{\Gamma}^a S \Gamma^b S D^{bc} \Phi^c \quad , \tag{3.32}$$

where S denotes a quark and D a diquark propagator, Φ^a denotes the quark-diquark amplitudes and Γ^a the diquark Bethe-Salpeter amplitudes with spectator quark a , respectively. The binding mechanism that binds a baryon in the quark-diquark picture, is given by the iterative union of two quarks into a diquark bound state.

3.3.1 Diquarks

Diquarks are two-quark correlations that can be used to describe baryons by reducing the three-body problem to two two-body problems as described in Chapter 2. In rainbow-ladder truncation of the DSE/BSE system they appear as timelike poles in the quark-quark scattering matrix, so the homogenous Bethe-Salpeter equation can be employed. In this sense they are quite similar to mesons and we can apply the techniques developed above. We only have to find the corresponding color, flavor and Dirac structure for the Bethe-Salpeter amplitude and then solve the diquark-BSE.

Here we only present the structure that has been used in our calculations. A detailed investigation of the structure of diquarks can be found in Appendices A.3 and A.4 of [20] and Section 3.2 of [41] and references therein.

While mesons are quark-antiquark correlations, diquarks are quark-quark correlations. In Feynman diagrammatical language this can be interpreted as flipping one external leg. Thus the main structure is the same but some inner quantum numbers and the behavior under discrete Lorentz transformations can

change compared to the meson case. This is achieved by adding charge conjugation matrices to the corresponding Bethe-Salpeter amplitude and turning around the momentum in one quark propagator. Thus we immediately can write down the diquark Bethe-Salpeter equation in ladder truncation [42, 43]

$$\Gamma_{\alpha\beta}(P, q) C = -\frac{2}{3} \int d^4k \frac{\mathcal{G}((q-k)^2)}{(q-k)^2} T_{\mu\nu}(q-k) \gamma_\mu S(-k + \frac{P}{2}) (\Gamma(P, k) C) S(k + \frac{P}{2}) \gamma_\nu \quad . \quad (3.33)$$

where the only difference from the meson Bethe-Salpeter equation (3.15) is the Charge conjugation matrix C at the Bethe-Salpeter amplitudes, one quark momentum and the different color factor, which reduces the coupling about a factor 2, but stays in the attractive channel. This shows that in ladder approximation diquarks are a valid bound-state concept. A calculation of the color factor is performed in Appendix A.2.

In deducing diquark Bethe-Salpeter amplitudes from the meson case one guiding line is the Pauli principle, which implies that diquarks have to be anti-symmetric under quark exchange, in particular regarding the relative momentum in the diquark and all inner quantum numbers. The Pauli principle implies for diquark Bethe-Salpeter amplitudes

$$\Gamma_{ab AB \alpha\beta}(P, q) = -\Gamma_{ba BA \beta\alpha}(P, -q) \quad . \quad (3.34)$$

Color structure

Diquarks are colored objects. Therefore the color structure of the diquark amplitude is not as simple as in the meson case. Baryons are color singlets built out of three colored quarks in the fundamental representation. Thus in color space we have to find representations of the multiplet $3 \otimes 3 \otimes 3$.

In a group theoretical language this product can be calculated as, see [44],

$$3 \otimes 3 \otimes 3 = (\bar{3} \oplus 6) \otimes 3 = \underbrace{1 \oplus 8}_{\bar{3} \otimes 3} \oplus \underbrace{8 \oplus 10}_{6 \otimes 3} \quad . \quad (3.35)$$

Thus the only possibility to form a color singlet baryon from three fundamentally charged quarks, is to build a color anti-triplet diquark out of two of them. We see that diquarks are antisymmetric color antitriplet states, which can be expressed by means of the normalized Levi-Civita tensor $\frac{1}{\sqrt{6}}\epsilon_{abc}$.

Flavor and Lorentz-Dirac structure

Since the full Bethe-Salpeter amplitude of a diquark has to be anti-symmetric and the color part is already anti-symmetric, the product of flavor and Dirac part has to be symmetric. Since in the two-flavor case, flavor and Lorentz-Dirac structure are representations of $SU(2) \otimes SU(2)$ which can be decomposed into the multiplet structure $2 \otimes 2 = 1_a \oplus 3_s$ with the singlet being anti-symmetric and the triplet being symmetric, it follows that in this case we have diquarks that are either both in the singlet representation, so Lorentz-scalar isoscalar states, or both in the triplet representation, so Lorentz-axialvector isovector. According

to Appendix B.1 the isoscalar and isovector matrices for the diquarks read

$$\mathbf{s}^s = \frac{1}{\sqrt{2}}(ud - du) = \frac{1}{\sqrt{2}}i\sigma_2 \quad (3.36a)$$

$$\mathbf{s}^+ = uu = \frac{1}{2}(\mathbf{1} + \sigma_3) \quad (3.36b)$$

$$\mathbf{s}^0 = \frac{1}{\sqrt{2}}(ud + du) = \frac{1}{\sqrt{2}}\sigma_1 \quad (3.36c)$$

$$\mathbf{s}^- = dd = \frac{1}{2}(\sigma_1 - \sigma_3) \quad (3.36d)$$

The Lorentz-Dirac structure can be derived by what has been accomplished in the last section, where we already found the Dirac structure for pseudoscalar and vector mesons. The exchange of an antiquark in the meson with a quark for the diquark also changes the behavior of the corresponding Bethe-Salpeter amplitude under parity transformations. A J^+ meson becomes a J^- diquark and vice versa. Thus the scalar diquark corresponds to the pseudoscalar meson and the axial vector diquark corresponds to the vector meson. For these we already found a basis in Dirac space. We span the scalar diquark on basis (3.21) and the axialvector diquark on basis (3.30).

Now, that we found a suitable basis for the scalar and axialvector diquark in color, flavor and Dirac space, we can span the Bethe-Salpeter amplitude onto it and get

$$\Gamma^{(sd)}(P, q) = \sum_i F_i(P^2, q^2, z) \left\{ \tau_i^{(ps)} C \right\} \otimes \mathbf{s}^I \otimes \frac{1}{\sqrt{6}}\epsilon_{abc} \quad (3.37)$$

$$\Gamma_\mu^{(avd)}(P, q) = \sum_i F_i(P^2, q^2, z) \left\{ \tau_{\mu i} C \right\} \otimes \mathbf{s}^I \otimes \frac{1}{\sqrt{6}}\epsilon_{abc} \quad , \quad (3.38)$$

where C is a charge conjugation matrix and the mass squared M^2 is still a parameter, since the diquark is not necessarily fixed on its mass shell.

Diquark propagator

For our calculations of baryon decays via the triangle diagram we need to know the propagator of the diquarks. By imposing the pole condition onto the inverse Dyson equation (2.10a)

$$G^{-1} = G_0^{-1} - K \quad (3.39)$$

$$(\chi D \bar{\chi})^{-1} = G_0^{-1} - K \quad (3.40)$$

we get a defining Dyson equation for the diquark propagator

$$D^{-1} = \bar{\chi} G_0^{-1} \chi - \bar{\chi} K \chi = \bar{\Gamma} G_0 \Gamma - \bar{\Gamma} G_0 K G_0 \Gamma \quad , \quad (3.41)$$

where χ are the diquark Bethe-Salpeter wave functions and Γ the diquark Bethe-Salpeter amplitudes as solutions of the diquark BSE. This equation provides us the diquark propagator. A detailed discussion about the solution process of this equation and the off-shell behavior of the diquark propagator can be found in [20].

3.3.2 Quark-diquark amplitudes

Now all ingredients of Equation (3.32) are known. Only the quark-diquark amplitudes are not specified yet. For them one also has to find a certain color, flavor and Dirac structure and span them onto the chosen basis.

Color and flavor structure

Being color singlets the color structure of baryons is the same as in the meson case, namely $\propto \delta^{a\bar{b}}$. The flavor structure is somewhat more subtle, since now we have to combine three quarks,

$$2 \otimes 2 \otimes 2 = (1 \oplus 3) \otimes 2 = \underbrace{2}_{1 \otimes 2} \oplus \underbrace{2 \oplus 4}_{3 \otimes 2} , \quad (3.42)$$

we get two flavor doublets and one flavor quartet. The quartet can clearly be identified with the Delta baryon, thus it only contains isovector diquarks. For the Nucleon is a flavor doublet and thus the situation is not so clear. Indeed it is a mixture of the two doublets above and contains isoscalar and isovector components.

The flavor structure of the individual Nucleon and Delta isospin projections are now calculated via the corresponding Clebsch-Gordan coefficients and the diquark flavor representations (3.36). With the basis $u = \begin{pmatrix} 1 \\ 0 \end{pmatrix}$ and $d = \begin{pmatrix} 0 \\ 1 \end{pmatrix}$, for the individual nucleon isospin projections we get the following Clebsch-Gordan representations [20],

$$p = \left(u \left| \sqrt{\frac{2}{3}} d, -\sqrt{\frac{1}{3}} u, 0 \right. \right), \quad n = \left(d \left| 0, \sqrt{\frac{1}{3}} d, -\sqrt{\frac{2}{3}} u \right. \right) , \quad (3.43)$$

which has to be understood in such a way that the first component has to be tensorial multiplied with the scalar diquark basis matrix, and the other three are multiplied with the axial vector basis matrices. For example the flavor part of the proton Bethe-Salpeter amplitude reads

$$p_f = u \times s^s + \sqrt{\frac{2}{3}} d \times s^+ - \sqrt{\frac{1}{3}} u \times s^0 . \quad (3.44)$$

The corresponding Clebsch-Gordan coefficients for the Delta baryon read

$$\begin{aligned} \Delta^{++} &= \left(u, 0, 0 \right) & \Delta^+ &= \left(\sqrt{\frac{1}{3}} d, \sqrt{\frac{2}{3}} u, 0 \right) \\ \Delta^0 &= \left(0, \sqrt{\frac{2}{3}} d, \sqrt{\frac{1}{3}} u \right) & \Delta^- &= \left(0, 0, d \right) \end{aligned} , \quad (3.45)$$

where there now is no scalar diquark projection.

Dirac structure

In the last section we found a strong correspondence between the flavor and the Dirac structure of diquarks. The isoscalar diquark has to be also a scalar in Dirac space and the isovector diquark corresponds to an axial vector. For the nucleon, being a mixture of isoscalar and isovector diquarks, we get the

following basis for the quark-diquark amplitude $\Gamma(P, q)$ with P being the total momentum and q the relative momentum between quark and diquark [26],

$$\begin{aligned}
 \tau_1^{(Ns)} &= \mathbf{1} & \tau_2^{(Ns)} &= -i \hat{q}^T \\
 \tau_{\mu 1}^{(N\text{av})} &= \gamma_\mu^T & \tau_{\mu 2}^{(N\text{av})} &= i \left(\gamma_\mu^T \hat{q}^T - \hat{q}_\mu^T \right) \\
 \tau_{\mu 3}^{(N\text{av})} &= i \hat{q}_\mu^T \mathbf{1} & \tau_{\mu 4}^{(N\text{av})} &= q_\mu^T \hat{q}_T - \frac{(\hat{q}^T)^2}{3} \gamma_\mu^T \not{P} \\
 \tau_{\mu 5}^{(N\text{av})} &= \hat{P}_\mu \mathbf{1} & \tau_{\mu 6}^{(N\text{av})} &= i \hat{P}_\mu \hat{q}^T \quad ,
 \end{aligned} \tag{3.46}$$

where the hat means normalized vectors and the superscript T denotes the transversal projection with respect to the total nucleon momentum. We normalized before we performed the transversal projection, $\hat{k}_\mu^T = T_{\mu\nu}(P) \left(\frac{k_\nu}{k^2} \right)$.

The corresponding basis for the Delta baryon reads [20],

$$\begin{aligned}
 \tau_{\mu\nu 1}^{(\Delta)} &= \delta_{\mu\nu} \mathbf{1} & \tau_{\mu\nu 2}^{(\Delta)} &= \frac{1}{\sqrt{5}} (2 \gamma_\mu^T p_\nu - 3 \delta_{\mu\nu} \not{p}) \\
 \tau_{\mu\nu 3}^{(\Delta)} &= -\sqrt{3} \hat{P}_\mu p_\nu \not{p} & \tau_{\mu\nu 4}^{(\Delta)} &= -\sqrt{3} \hat{P}_\mu p_\nu \mathbf{1} \\
 \tau_{\mu\nu 5}^{(\Delta)} &= -\gamma_\mu^T p_\nu \not{p} & \tau_{\mu\nu 6}^{(\Delta)} &= -\gamma_\mu^T p_\nu \\
 \tau_{\mu\nu 7}^{(\Delta)} &= \gamma_\mu^T p_\nu \not{p} - \delta_{\mu\nu} \mathbf{1} - 3 p_\mu p_\nu \mathbf{1} & \tau_{\mu\nu 8}^{(\Delta)} &= \frac{1}{\sqrt{5}} (\delta_{\mu\nu} \not{p} + \gamma_\mu^T p_\nu + 5 p_\mu p_\nu \not{p}) \quad ,
 \end{aligned} \tag{3.47}$$

where there appears an additional Lorentz index since the Delta amplitude is contracted with a Rarita-Schwinger spinor, and $p_\mu = i \frac{T_{\mu\nu} q_\nu}{(T_{\mu\nu} q_\nu)^2}$.

The Bethe-Salpeter amplitudes for the Nucleon and Delta-baryon without flavor and color part read

$$\Gamma^{(Ns)}(P, q) = \sum_{k=1}^2 F_k^{(Ns)}(q^2, z) \tau_k^{Ns} \Lambda_+(P) \tag{3.48a}$$

$$\Gamma_\mu^{(N\text{av})}(P, q) = \sum_{k=1}^6 F_k^{(N\text{av})}(q^2, z) \tau_{\mu k}^{N\text{av}} \Lambda_+(P) \tag{3.48b}$$

$$\Gamma_{\mu\nu}^{(\Delta)}(P, q) = \sum_{k=1}^8 F_k^{(\Delta)}(q^2, z) \tau_{\mu\rho k}^\Delta \mathbb{P}_{\rho\nu}(P) \quad , \tag{3.48c}$$

with the positive energy projector

$$\Lambda_+(P) = \frac{1}{2} \left(\mathbf{1}_D + \frac{\not{P}}{iM} \right) \tag{3.49}$$

and the Rarita-Schwinger projector

$$\mathbb{P}_{\rho\nu}(P) = \Lambda_+(P) \left(T_{\rho\nu} - \frac{1}{3} \gamma_\rho^T \gamma_\nu^T \right) \tag{3.50}$$

where the transversality is to be taken with respect to the Δ -total-momentum P_μ and μ, ν and ρ are Lorentz-indices.

Chapter 4

Calculations and results

The aim of this thesis is to calculate hadronic transitions between asymptotic states, which, in quantum field theories, are described via the S-Matrix formalism as introduced in Section 2.1. After having set up all the building blocks and with the solutions of all equations already obtained elsewhere [20, 39, 45] we can go ahead and perform calculations in the triangle diagram. In the first section we will be concerned with the invariant amplitude connected to the triangle diagram and how to calculate decay widths and coupling constants from it. Then we will introduce a certain interaction model which was used when solving the Dyson-Schwinger and Bethe-Salpeter equations and then finally present the results of these calculations.

For mesons we calculated the $\rho \rightarrow \pi\pi$ transition, which has already been under investigation in the same approach [4, 5], but also in constituent quark models [46–49], Lattice QCD [50–55] and chiral perturbation theory [56, 57]. For the baryonic case, we studied the $\Delta \rightarrow N\pi$ transition which has been under investigation, e.g., in relativistic constituent quark models [58, 59], QCD sum rules [60–62] and also Lattice QCD [63].

For better readability we shifted the investigation of kinematical issues within the triangle diagram to Appendix B.2, and we will just use what is described there. In fact it turns out, that we need to know the propagators and Bethe-Salpeter amplitudes in a certain region in the complex plain. For the propagators, this problem already appears when solving the Bethe-Salpeter equation, which is well known and under control. We give a short review about the corresponding ideas in Appendix B.3. For the Bethe-Salpeter amplitudes this problem I solved via a Taylor expansion as described in Appendix B.4.

4.1 Invariant amplitude, decay width and phasespace

In impulse approximation the investigated transitions can be represented by the triangle diagram as presented in Figure 3.1 and correspond to a transition matrix element

$$\mathcal{M} = \text{tr}_{Dfc} \left\{ \int \bar{d}^4k \Gamma_2 S_3 \Gamma_1 S_2 \Gamma_3 S_1 \right\} \quad (4.1)$$

where the Γ_i are descriptions of the participating particles, in our case Bethe-Salpeter amplitudes for mesons and baryons, and the S_i are quark and/or di-quark propagators, respectively.

In experiments concerning decays one very important term is the decay width, which is directly connected to the lifetime of a particle. In terms of a matrix element in quantum field theories the scattering width, see Equation (2.6), reads

$$\Gamma = \frac{1}{2M} \sum_f \int d\Pi_f |\mathcal{M}_{fi}|^2 \quad , \quad (4.2)$$

with M being the mass of the decaying particle and $\int d\Pi_f$ being a phase-space integral. Following [6, p.107] and Appendix D of [5] we want to calculate this phase-space integral now.

For a process of one particle with mass M and momentum p_1 decaying into two particles with masses $M_{2,3}$ and momenta $p_{2,3}$, all momenta defined as incoming, the invariant phase-space integral reads

$$\int d\Pi_f = \int d^3\vec{p}_2 \int d^3\vec{p}_3 \frac{(2\pi)^4 \delta^{(4)}(p_1 + p_2 + p_3)}{(-2i)\sqrt{M_2^2 + \vec{p}_2^2} (-2i)\sqrt{M_3^2 + \vec{p}_3^2}} \quad , \quad (4.3)$$

where we split the 4-vectors p_i into their spacelike and timelike components $p = (\vec{p}, ip_4)$. Note that one only integrates over the spacelike parts. Integration over \vec{p}_3 only eliminates δ -functions and yields

$$= - \int d^3\vec{p}_2 \frac{2\pi}{4\sqrt{M_2^2 + \vec{p}_2^2} \sqrt{M_3^2 + \vec{p}_2^2}} \delta\left(M_1 - \sqrt{M_2^2 + \vec{p}_2^2} - \sqrt{M_3^2 + \vec{p}_2^2}\right) \quad . \quad (4.4)$$

Now one uses the relation $\delta(f(x)) = \frac{\delta(x-\xi)}{|f'(\xi)|}$ with ξ being the roots of f

$$= -\frac{1}{4} \int \frac{d^2\Omega}{(2\pi)^2} \int d\left(\sqrt{\vec{p}_2^2}\right) \frac{\sqrt{\vec{p}_2^2}}{\sqrt{M_2^2 + \vec{p}_2^2} + \sqrt{M_3^2 + \vec{p}_2^2}} \delta(\sqrt{\vec{p}_2^2} - \xi) \quad , \quad (4.5)$$

and ends up with

$$\int d\Pi_f = -\frac{\xi}{4\pi M_1} \quad , \quad (4.6)$$

where we used in the last step that the denominator exactly equals M_1 due to momentum conservation. The roots ξ are given by the condition

$$\xi = \frac{\sqrt{(M_1 + M_2 + M_3)(M_1 + M_2 - M_3)(M_1 - M_2 + M_3)(M_1 - M_2 - M_3)}}{2M_1} \quad , \quad (4.7)$$

and, if the two decay products have the same mass $M_2 = M_3$, ξ simplifies to $\xi = \frac{1}{2}\sqrt{M_1^2 - 4M_2^2}$ and we finally get

$$\int d\Pi_f = -\frac{1}{8\pi} \sqrt{1 - \frac{4M_2^2}{M_1^2}} \quad . \quad (4.8)$$

4.2 Interaction model

As already mentioned in Chapter 3 several interaction models for the coupled system of quark-DSE and meson-BSE in rainbow-ladder truncation are used in the literature. For the triangle calculations we consistently used solutions that were obtained for the model by Maris and Tandy [21],

$$\frac{\mathcal{G}(q^2)}{q^2} = \frac{4\pi^2}{\omega^6} D q^2 e^{(q^2/\omega^2)} + 4\pi \frac{\gamma_m \pi}{\left(\frac{1}{2} \ln \left[\tau + \left(1 + \frac{q^2}{\Lambda_{QCD}}\right)^2 \right] \right)} F(q^2) \quad (4.9)$$

with $F(q^2) = [1 - \exp(-\frac{q^2}{4m_t^2})]/q^2$, $m_t = 0.5\text{GeV}$, $\tau = e^2 - 1$, $\Lambda_{QCD} = 0.234\text{ GeV}$ and $\gamma_m = \frac{12}{33-2N_f}$ and $N_f = 4$. While all these parameters are used to connect ansatz (4.9) to one-loop-order perturbative QCD the two remaining model parameters $\{D, \omega\}$ together with the current quark mass at a certain renormalization point in the quark propagator can be used to fit hadron observables, such as masses or leptonic decay constants. For this particular ansatz, one finds that in a certain parameter range ground state properties remain constant, if one fixes $D \cdot \omega = \text{const}$ [21]. Together with one particular current quark mass this defines a one-parameter model. For the interaction the parameter ω is chosen in the range of

$$\omega \in [0.3, 0.5] \quad (4.10)$$

$$D \cdot \omega = 0.372 \text{ GeV}^3 \quad , \quad (4.11)$$

and we vary the current quark mass from the chiral limit up to the strange quark mass.

Since the model does not describe all π - and ρ -meson observables equally well at the same time for a particular choice of the current quark mass, one has to choose one observable to fix this parameter, e.g. the meson masses. Here we want to highlight two parameter sets, in which, for $\omega = 0.4$, we reproduce the pion and rho-meson mass respectively. In the following we will call them repeatedly **A** for the case where the parameters are fitted to the pion mass and **B** for the rho-meson mass, see also Table 4.1. Comparing our results to lattice studies, one can refer to set-up **A** as the *physical point* or the whole range between **A** and **B** as the *physical region* of our calculations.

4.3 Mesons: $\rho \rightarrow \pi\pi$

According to Equation (4.1), the general matrix element for the $\rho\pi\pi$ -transition reads

$$\mathcal{M}_{\rho\pi\pi} = \text{tr}_{Dcf} \left\{ \int d^4k \bar{\Gamma}^\pi S \Gamma^\rho S \bar{\Gamma}^\pi S \right\} \quad (4.12)$$

where the S are quark propagators as solutions of the quark-DSE and the Γ_i are Bethe-Salpeter amplitudes. Since we work in the isosymmetric limit and neglect any kind of electro-magnetic interaction, the π - and ρ -triplet states are degenerate. The only difference is their flavor content, i.e. their isospin projections.

When calculating the flavor trace, we have to take into account, that an outgoing π^+ corresponds to an incoming π^- and vice versa. As derived in

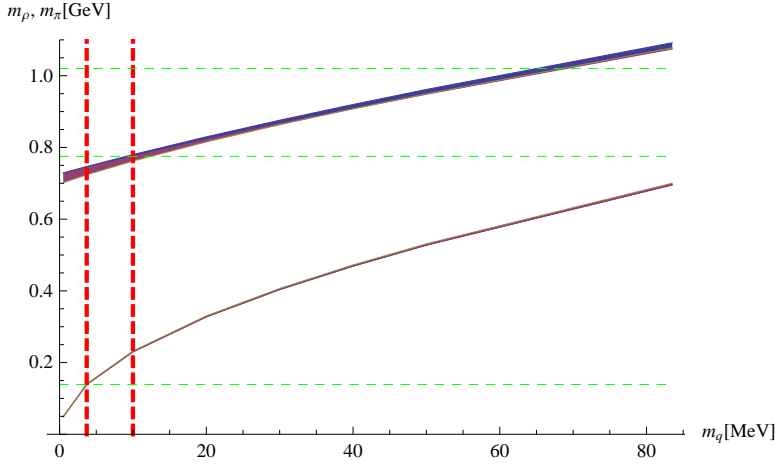


Figure 4.1: The ρ and π -meson masses over the quark mass parameter. As our model preserves a generalized GMOR-relation [64], for small quark masses the pion mass goes proportional to $\sqrt{m_q}$. The bands represent the dependencies on the ω -parameter. The red (vertical) lines correspond to the parameter sets **A** and **B**, the green (horizontal) lines to the experimental values of π -, ρ -, and ϕ -meson, respectively.

Appendix B.1 $(r^+)^\dagger = -r^-$ and $(r^0)^\dagger = r^0$. Exemplary, for the $\rho^0 \rightarrow \pi^+\pi^-$ process the flavor trace yields

$$\begin{aligned}
 \text{tr}_f \{r^0 r^- r^+ - r^0 r^+ r^-\} &= \text{tr}_f \{r^0 [r^+, r^-]\} \\
 &= \frac{1}{4\sqrt{2}} \text{tr}_f \{\sigma_3 [\sigma_1 + i\sigma_2, \sigma_1 - i\sigma_2]\} = \frac{1}{4\sqrt{2}} \text{tr}_f \{\sigma_3 2i [\sigma_2, \sigma_1]\} \\
 &= \frac{1}{4\sqrt{2}} \text{tr}_f \{\sigma_3 4\sigma_3\} = \frac{1}{\sqrt{2}} \text{tr}_f \{\mathbf{1}_f\} = \sqrt{2} \quad . \quad (4.13)
 \end{aligned}$$

The relative minus sign in the first line of (4.13) stems from the fact that the triangle diagram contains a fermion loop and we have to sum over all final states, which in this case means going clockwise and counter-clockwise through the diagram. The flavor factors of the other decays yield the same as (4.13) since, e.g., in the $\rho^+ \rightarrow \pi^0\pi^+$ transition the outgoing π^+ corresponds to a r^- matrix such that one gets $\text{tr}_f \{r^+ r^0 r^- - r^+ r^- r^0\}$, which is the same as (4.13) due to the cyclic property of the trace. The same is true for $\rho^- \rightarrow \pi^0\pi^-$, and thus for every possible $\rho\pi\pi$ -transition we get the same flavor factor. Furthermore, since this is the only difference between the three transitions, all have the same form factors, coupling constants and decay widths. From now on we will not refer to one certain isospin projection but only be concerned with the $\rho\pi\pi$ -transition in general, since there is no way to distinguish between the three cases in our calculations.

With $(\delta^{a\bar{b}})^\dagger = \delta^{b\bar{a}}$, the color part of Equation 4.12 gives

$$\text{tr}_c \left\{ \delta_\pi^{c\bar{d}} \delta_\rho^{ac} \delta_\rho^{a\bar{b}} \delta_\pi^{f\bar{b}} \delta_\pi^{e\bar{f}} \delta_\pi^{d\bar{e}} \right\} = \text{tr}_c \{ \mathbf{1}_c \} = 3 \quad . \quad (4.14)$$

So we find for the matrix element of the $\rho \rightarrow \pi\pi$ -transition with already

traced out color and flavor part

$$\mathcal{M}_{\rho\pi\pi} = 3\sqrt{2} \operatorname{tr}_D \left\{ \int d^4k \bar{\Gamma}^\pi S \Gamma^\rho S \bar{\Gamma}^\pi S \right\} . \quad (4.15)$$

The Lorentz-Dirac part of the calculation is somewhat more involved. The ρ -meson is a massive vector-meson and thus appears in three polarization states which have to be summed over. We can perform this summation at the very end of our calculation by pulling out the polarization vectors of the matrix element

$$\mathcal{M}_{\rho\pi\pi} = \frac{1}{\sqrt{n_\lambda}} \sum_\lambda \mathcal{M}_{\rho\pi\pi}^\lambda = \frac{1}{\sqrt{n_\lambda}} \sum_\lambda \varepsilon_\mu^\lambda \Lambda_\mu^{\rho\pi\pi} \quad (4.16)$$

where n_λ is the number of polarizations, in case of a vector $n_\lambda = 3$ and we defined the vertex amplitude

$$\Lambda_\mu^{\rho\pi\pi} = 3\sqrt{2} \operatorname{tr}_D \left\{ \int d^4k \bar{\Gamma}^\pi S \Gamma_\mu^\rho S \bar{\Gamma}^\pi S \right\} , \quad (4.17)$$

which is the central term in our calculations of the $\rho\pi\pi$ -transition. Usually transition matrix elements are parameterized in terms of form factors as parameterizations of the corresponding currents. The Lorentz-vector Λ_μ can have two linearly independent structures

$$\Lambda_\mu^{\rho\pi\pi} = F(P^2, Q^2, P \cdot Q) 2Q_\mu + G(P^2, Q^2, P \cdot Q) P_\mu \quad (4.18)$$

with the two linearly independent momenta P_μ and Q_μ defined in Equation (B.35). However, as we already mentioned when constructing the Dirac-basis of the vector meson, all longitudinal parts of the vector meson, which give exactly the longitudinal parts of the vertex amplitude, vanish when summing over all polarizations. Thus the term proportional to P_μ vanishes as

$$\begin{aligned} |\mathcal{M}|^2 &= \sum_\lambda |\mathcal{M}^\lambda|^2 = \frac{1}{n_\lambda} \sum_\lambda \varepsilon_\mu^\lambda(P) \Lambda_\mu^{\rho\pi\pi} \varepsilon_\nu^{\lambda*}(P) \Lambda_\nu^{\rho\pi\pi*} \\ &= \frac{1}{n_\lambda} T_{\mu\nu}(P) \Lambda_\mu^{\rho\pi\pi} \Lambda_\nu^{\rho\pi\pi*} = \frac{1}{n_\lambda} (\Lambda_\mu^T)^2 , \end{aligned} \quad (4.19)$$

and we end up with only one formfactor defined by

$$F(P^2, Q^2, P \cdot Q) = \frac{Q_\mu \Lambda_\mu^{\rho\pi\pi}}{2Q^2} . \quad (4.20)$$

The corresponding coupling strength is defined as the form factor, when all external legs go on-shell,

$$g_{\rho\pi\pi} = i F(P^2, Q^2, P \cdot Q) \Big|_{P_i^2 = -M_i^2} . \quad (4.21)$$

The corresponding decay width is calculated via Formula (4.2) with the phase space factor calculated in Equation (4.8). In terms of the effective coupling strength we end up with the hadronic decay width of the ρ -meson decaying into two pions

$$\begin{aligned} \Gamma_{\rho\pi\pi} &= \frac{1}{2M_\rho} \frac{1}{8\pi} \sqrt{1 - \frac{4M_\pi^2}{M_\rho^2}} \frac{1}{3} |2 Q^T g_{\rho\pi\pi}|^2 \\ &= \frac{1}{12\pi M_\rho} \sqrt{1 - \frac{4M_\pi^2}{M_\rho^2}} \kappa^2 |g_{\rho\pi\pi}|^2 , \end{aligned} \quad (4.22)$$

Set	fitted to	M_π	M_ρ	f_π	f_ρ	g	Γ
A	M_π	139	742	131	207	5.19	106
B	M_ρ	230	774	136	213	5.32	76
	Exp.	139.57	775	130	216	5.98	149

Table 4.1: Results and some characteristic values for the two parameter sets **A** and **B** as described in the text. The leptonic decay constants f_i are usually used as check for, e.g., PCAC relations. The experimental values are taken from [65]. All quantities, beside the dimensionless effective coupling strength g , are given in MeV.

with κ being defined in Equation B.34.

The Dirac matrix multiplication and trace in (4.17) have to be understood in such a way that for every $\mu \in \{1, 2, 3, 4\}$ one has to perform these calculations individually and then gets the components of the Lorentz vector Λ_μ . Explicitly it is done via taking the trace first in every component and then integrate over the resulting expressions.

Now we have everything at hand. We know how to calculate the pion Bethe-Salpeter amplitudes for complex momenta, and we know how to calculate the expression Λ_μ and extract the form factor from it. We performed this calculation with solutions of the homogeneous Bethe-Salpeter equation, which already implies the on-shell condition.

The results for the effective coupling strength $g_{\rho\pi\pi}$ and the decay width of the ρ meson Γ_ρ are presented in Figures 4.2 and 4.3, respectively, and for the two parameter sets **A** and **B** explicitly given in Table 4.1. We see a slowly linear growth of the coupling strength with increasing quark mass, and for the physical region, between the parameter sets **A** and **B**, we are roughly 10 to 15% below the experimental value. With increasing pion mass squared the decay width is decreasing fast and at value of around 0.22 GeV^2 the channel closes and decays are not allowed anymore. This strong dependency of the decay width, which goes along with only a weak dependency of the coupling constant is due to the kinematical phase-space factor (4.8), which goes into the decay width, but not the effective coupling constant. The ratio of pion and rho masses increases, and thus the phasespace becomes smaller and vanishes. Since these masses are model dependent quantities the decay width is much more dependent on model details than the effective coupling strength g .

Overall we can state, that we could reproduce experimental values of the coupling strength and decay width in the $\rho\pi\pi$ -system in our approach to a reasonable but not perfect accuracy. The main reason is that in this effective model the ρ -meson is treated as a bound-state, but not a resonance. Explicit inclusion of decays in the interaction kernel of the Bethe-Salpeter equation are expected to cure this deficiency. Naturally, also non-resonant corrections to the rainbow-ladder truncation will improve the result.

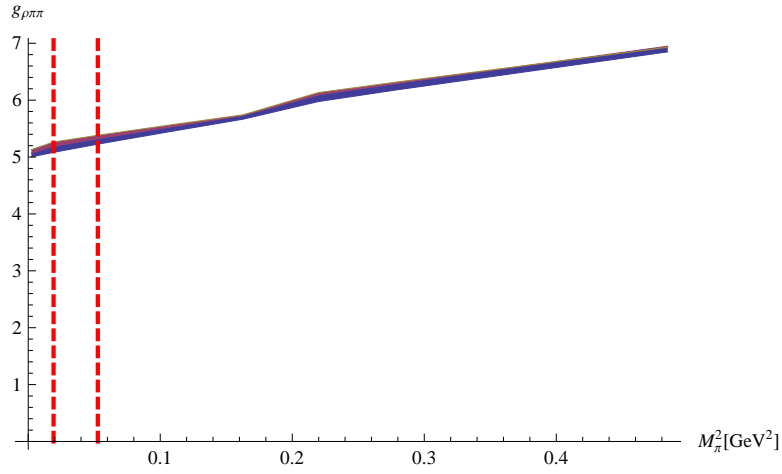


Figure 4.2: The development of the coupling constant g versus the pion mass squared. The bands denote the dependence on the ω -Parameter.

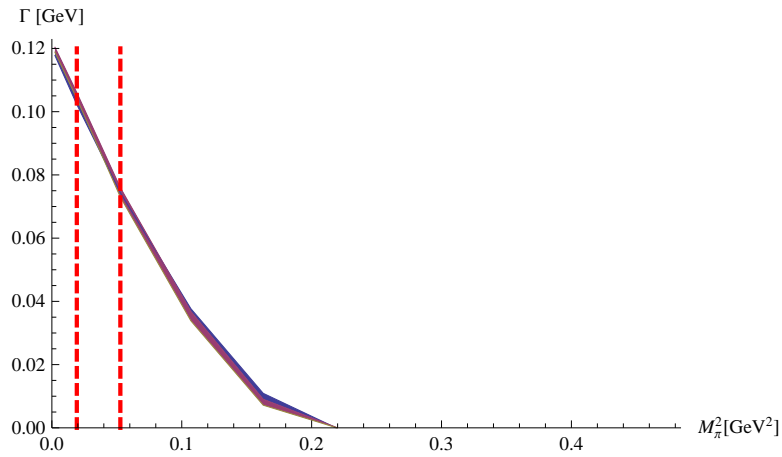


Figure 4.3: The decay width Γ versus the pion mass squared. The bands denote the dependence on the ω -Parameter.

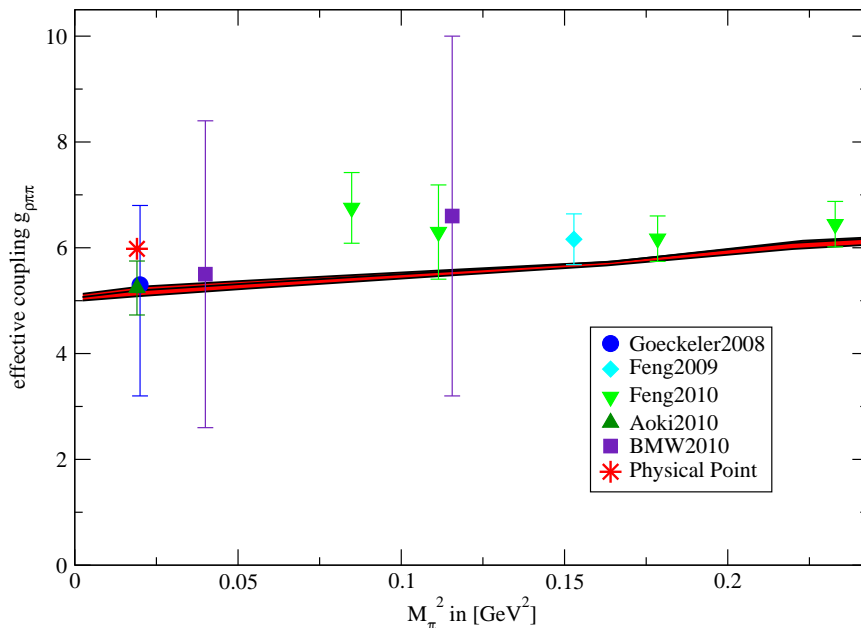


Figure 4.4: Comparison between our results for the effective coupling constant $g_{\rho\pi\pi}$ and different lattice results. Note, that for better readability we shifted the result of the Goeckeler group slightly to the right of the physical point, since they only state one value for the coupling valid for the whole quark mass range.

In recent years lattice simulations of QCD reached lower and lower pion masses towards the physical point. With the pion mass, the ratio $\frac{M_\rho}{M_\pi}$ decreases such that it became possible for these studies to investigate the $\rho\pi\pi$ -transition via the simulation of $\pi\pi$ -scattering processes and extracting corresponding the phase-shift. In Figure 4.4 we compare our results for the effective coupling $g_{\rho\pi\pi}$ with lattice results of different groups: The symbols denote data from references [51] (circles), [52] (diamonds), [53] (triangle down), [54] (triangle up) and [55] (squares). We find reasonable agreement with most of the lattice data and are mostly within the errors provided.

4.4 Baryons: $\Delta \rightarrow N\pi$

For the baryons we investigated the $\Delta N\pi$ -transition which is represented by the matrixelement

$$\mathcal{M}_{\Delta N\pi} = \text{tr}_{Dcf} \left\{ \int \bar{d}^A k \bar{\Gamma}^N D \Gamma^\Delta S \bar{\Gamma}^\pi S \right\} . \quad (4.23)$$

The color trace of Equation (4.23) is the same as the color trace in the $\rho\pi\pi$ -system, Equation (4.14),

$$\text{tr}_c \{ \delta_N^{\bar{c}d} \delta^{\bar{a}c} \delta_\Delta^{\bar{a}b} \delta^{fb} \delta_\pi^{\bar{e}f} \delta^{d\bar{e}} \} = 3 . \quad (4.24)$$

In flavor space there are six different transition, where each flavor factor is calculated via the Clebsch-Gordan composition of the baryons according to

transition	$\Delta^{++} \rightarrow p\pi^+$	$\Delta^+ \rightarrow p\pi^0$	$\Delta^+ \rightarrow n\pi^+$
flavor factor	$\sqrt{\frac{2}{3}}$	$\frac{2}{3}$	$\frac{\sqrt{2}}{3}$
transition	$\Delta^0 \rightarrow n\pi^0$	$\Delta^0 \rightarrow p\pi^-$	$\Delta^- \rightarrow n\pi^-$
flavor factor	$\frac{2}{3}$	$\frac{\sqrt{2}}{3}$	$\sqrt{\frac{2}{3}}$

Table 4.2: The individual transitions in the $\Delta N\pi$ -system and their corresponding flavor factors.

Equations (3.43) and (3.45), with the flavor matrices of the diquarks (3.36). We will present here one calculation explicitly, the other ones are calculated accordingly and given in Table 4.2. The flavor factor for the $\Delta^+ \rightarrow p\pi^0$ decay reads

$$\begin{aligned}
& \text{tr}_f \left\{ \left(\sqrt{\frac{1}{3}} d \times s^+ + \sqrt{\frac{2}{3}} u \times s^0 \right) (r^0)^\dagger \left(\sqrt{\frac{2}{3}} d \times s^+ - \sqrt{\frac{1}{3}} u \times s^0 \right)^\dagger \right\} \\
&= \text{tr}_f \left\{ \left(\sqrt{\frac{1}{3}} d \times s^+ + \sqrt{\frac{2}{3}} u \times s^0 \right) r^0 \left(\sqrt{\frac{2}{3}} \bar{d} \times s^{+\dagger} - \sqrt{\frac{1}{3}} \bar{u} \times s^{0\dagger} \right) \right\} \\
&= \text{tr}_f \left\{ \left(\sqrt{\frac{1}{3}} d \times s^+ \right) r^0 \left(\sqrt{\frac{2}{3}} \bar{d} \times s^{+\dagger} \right) - \left(\sqrt{\frac{2}{3}} u \times s^0 \right) r^0 \left(\sqrt{\frac{1}{3}} \bar{u} \times s^{0\dagger} \right) \right\} \\
&= \frac{\sqrt{2}}{3} \text{tr}_f \{ d r^0 \bar{d} - u r^0 \bar{u} \} = \frac{\sqrt{2}}{3} \left(\frac{1}{\sqrt{2}} + \frac{1}{\sqrt{2}} \right) = \frac{2}{3} \quad (4.25)
\end{aligned}$$

From Table 4.2 we get that the flavor factor for the invariant amplitude of the Δ^{++} and Δ^- are the same. For the other two charge eigenstates one has to sum over all final states as

$$c_f = \sqrt{\left| \frac{2}{3} \right|^2 + \left| \frac{\sqrt{2}}{3} \right|^2} = \sqrt{\frac{4}{9} + \frac{2}{9}} = \sqrt{\frac{2}{3}} \quad . \quad (4.26)$$

Thus for all four charge eigenstates of the Δ we get the same flavor factor for the decay matrix element \mathcal{M} and thus, as for the $\rho\pi\pi$ -transitions, the same effective coupling strength and decay width.

The invariant transition element with specified color and flavor factors becomes

$$\mathcal{M}_{\Delta N\pi} = 3\sqrt{\frac{2}{3}} \text{tr}_D \left\{ \int d^4k \bar{\Gamma}^N D \Gamma^\Delta S \bar{\Gamma}^\pi S \right\} \quad . \quad (4.27)$$

This allows the definition of a vertex amplitude analogous to the mesonic case, where we have to take the fermionic nature of the baryons into account via the appropriate spinor constructions. This is done via the positive energy and Rarita-Schwinger projectors as defined in Section 3.3. Since in the $\Delta N\pi$ -system there are again two linearly independent external momenta, e.g., P_μ and Q_μ as defined in Equation (B.42), the situation is completely analogous to Equation (4.18) and the vertex amplitude becomes

$$\Lambda_\mu^{\Delta N\pi} = F(P^2, Q^2, P \cdot Q) 2 Q_\nu \Lambda_+^N \mathbb{P}_{\nu\mu}^\Delta \quad , \quad (4.28)$$

where the form factor F defines an effective coupling strength if all particles are on-shell [61, 63], which can be parameterized as,

$$\Lambda_\mu^{\Delta N\pi} = \frac{g_{\Delta N\pi}}{2\sqrt{M_N M_\Delta}} 2 Q_\nu \Lambda_+^N \mathbb{P}_{\nu\mu}^\Delta . \quad (4.29)$$

The matrix element for one specific spin configuration and the vertex amplitude are connected via projections onto the particular nucleon Dirac-spinor, denoted by $\sqrt{2M_N}u^s$, and Δ -baryon Rarita-Schwinger spinor, denoted by $\sqrt{2M_\Delta}u_\mu^{s'}$,

$$\mathcal{M}_{\Delta N\pi}^{ss'} = 2\sqrt{M_N M_\Delta} \bar{u}^s \Lambda_\mu^{\Delta N\pi} u_\mu^{s'} \quad (4.30)$$

One then gets via inserting Equation (4.29) into (4.30)

$$\begin{aligned} \mathcal{M}_{\Delta N\pi}^{ss'} &= 2\sqrt{M_N M_\Delta} \bar{u}^s \Lambda_\mu^{\Delta N\pi} u_\mu^{s'} = 2 g_{\Delta N\pi} Q_\nu \bar{u}^s \Lambda_+^N \mathbb{P}_{\nu\mu}^\Delta u_\mu^{s'} \\ &= 2 g_{\Delta N\pi} Q_\nu \bar{u}^s u_\nu^{s'} , \end{aligned} \quad (4.31)$$

and, connecting Equations (4.30) and (4.27),

$$\Lambda_\mu^{\Delta N\pi} = 3\sqrt{\frac{2}{3}} \int d^4k \bar{\Gamma}_\sigma^N D_{\sigma\rho} \Gamma_{\rho\mu}^\Delta S \bar{\Gamma}^\pi S , \quad (4.32)$$

with the Bethe-Salpeter amplitudes of the nucleon and Delta defined in Equation (3.48). Summing over all possible spin combinations yields

$$|\mathcal{M}_{\Delta N\pi}|^2 = \sum_{ss'} |\mathcal{M}_{\Delta N\pi}^{ss'}|^2 = 4 g_{\Delta N\pi}^2 Q_\mu Q_\nu^* \sum_{ss'} \bar{u}^s u_\nu^{s'} \bar{u}_\mu^{s'} u^s \quad (4.33)$$

$$\begin{aligned} &= 4 g_{\Delta N\pi}^2 Q_\mu Q_\nu^* \sum_s \bar{u}^s \mathbb{P}_{\nu\mu}^\Delta u^s \\ &= 4 g_{\Delta N\pi}^2 \sum_s \bar{u}^s \Lambda_+^\Delta \left(|Q_T|^2 - \frac{1}{3} |\mathcal{Q}_T|^2 \right) u^s \end{aligned} \quad (4.34)$$

$$= 4 g_{\Delta N\pi}^2 \frac{2\kappa^2}{3} \sum_s \bar{u}^s \Lambda_+^\Delta u^s = \frac{8\lambda\kappa^2}{3} g_{\Delta N\pi}^2 , \quad (4.35)$$

where we defined the parameter λ as

$$\begin{aligned} \lambda &= \sum_s \bar{u}^s \Lambda_+^\Delta u^s = \text{tr}_D \{ \Lambda_+^\Delta \Lambda_+^N \} = \frac{1}{4} \text{tr}_D \left\{ \left(\mathbf{1} + \frac{\not{P}_\Delta}{iM_\Delta} \right) \left(\mathbf{1} + \frac{\not{P}_N}{iM_N} \right) \right\} \\ &= \frac{1}{4} \text{tr}_D \left\{ \mathbf{1} + \frac{\kappa}{iM_N} \gamma_4 \gamma_3 + \frac{\sqrt{M_N^2 + \kappa^2}}{M_N} \gamma_4 \gamma_4 \right\} = 1 + \frac{\sqrt{M_N^2 + \kappa^2}}{M_N} . \end{aligned} \quad (4.36)$$

With these definitions we get for the effective coupling strength in the $\Delta N\pi$ -system and the strong decay width of the Δ -baryon

$$g_{\Delta N\pi} = \frac{3\sqrt{M_N M_\Delta}}{2\lambda\kappa^2} \text{tr}_D \{ Q_\mu \Lambda_\mu^{\Delta N\pi} \} \quad (4.37a)$$

$$\begin{aligned} \Gamma_{\Delta N\pi} &= \frac{1}{2M_\Delta} \frac{\xi(M_\Delta, M_N, M_\pi)}{4\pi M_\Delta} \frac{8\lambda\kappa^2}{3} g_{\Delta N\pi}^2 \\ &= \frac{\xi(M_\Delta, M_N, M_\pi)}{3\pi M_\Delta^2} \lambda\kappa^2 g_{\Delta N\pi}^2 , \end{aligned} \quad (4.37b)$$

with $\xi(M_1, M_2, M_3)$ defined in Equation (4.7).

A numerical treatment of the coupling and the decay width of the Δ -baryon is not straight-forward. The main reason is that the Chebyshev moments of the Nucleon Bethe-Salpeter amplitude have to be known in a sizable ($\sim M_\Delta$) region of the complex relative-momentum-squared plane (analogous to the quark-propagator case), which is done here for the first time. In particular, the Taylor expansion is very sensitive to the numerical accuracy of the Chebyshev moments close to zero relative momentum squared. To avoid these difficulties, we use only Chebyshev moments up to first order and by this approximation introduce a systematical error which we estimate to be smaller than 10%.

As results for the coupling and decay width of the Δ -baryon we get for our calculations after this numerical simplification

$$g_{\Delta N\pi} = 5.5 \qquad g_{\Delta N\pi}^{exp} = 8.4 \qquad (4.38)$$

$$\Gamma_{\Delta N\pi} = 82 \text{ MeV} \qquad \Gamma_{\Delta N\pi}^{exp} = 118 \text{ MeV} \quad , \qquad (4.39)$$

i.e., roughly 2/3 of the experimental values of the coupling strength and also of the decay width are reproduced, which is a very reasonable result.

To understand the quality of this result as well as the discrepancy with respect to the experimental value, several factors need to be taken into account. First of all, the truncation has several consequences: the structure of the interaction is simple via the rainbow-ladder truncation employed throughout, but consistent in that the axial vector as well as vector WTIs are satisfied in this setup, leading to a generally excellent description of pion properties. The next important point is the diquark approximation for baryons: while its results for the nucleon mass have been recently compared successfully to the corresponding results in a three-quark setup [66], one cannot necessarily expect negligible effects of this approximation for matrix elements like the transition studied here. In particular, the impulse approximation with the pion only coupling to the single quark in the quark-diquark baryon may have a sizable effect compared to an analogous three-quark calculation. Last but not least, the inclusion of explicit pion degrees of freedom as well as nonresonant corrections to rainbow-ladder truncation are expected to have an effect as well.

At the same time it should be stressed, however, that our result is a prediction of the model in the sense that all parameters were fixed already to pion observables and no adjustments or additional parameters were introduced at the baryon level. It is also noteworthy that mesons and baryons are treated on the same footing here, a feature certainly contributing to the success of the approach.

Chapter 5

Conclusions and Outlook

In this thesis we calculated hadronic decays within the Dyson-Schwinger–Bethe-Salpeter approach to hadron phenomenology. In particular we studied the $\rho \rightarrow \pi\pi$ transition in the mesonic and the $\Delta \rightarrow N\pi$ transition in the baryonic sectors, respectively. For the mesonic case we re-investigated earlier studies and found interesting results beyond those already known. In particular we demonstrated that our value of the coupling constant, as a function of the pion mass, agrees reasonably with contemporary studies of this transition in lattice QCD as well as experiment, and we have provided an estimate of the model-parameter dependence in our result.

For the baryonic case we could provide the first exploratory study of a hadronic transition among baryons in the DSE-BSE approach to QCD, in a model setup and truncation that is determined by meson phenomenology and the AVWTI only. In this way we provide a prediction of a quark-core setup for the strong Δ baryon decay width. The numerical result provides about 65% of the experimental value for the coupling, which is perfectly reasonable in this context: Corrections like the inclusion of higher Chebyshev moments in the nucleon amplitude, the contributions from explicit pion degrees of freedom as well as non-resonant contributions to the Nucleon and Δ amplitudes are expected to be non-negligible. Furthermore the treatment of the baryons as three-quark instead of quark-diquark states is expected to further change the result, since the diquark contribution to the decay is not taken into account here.

In both the meson and baryon cases a treatment of the involved hadrons as resonances is needed to provide a reliable picture of hadronic transition processes in QCD. With further algorithmic and numerical improvements, such an approach seems feasible in the near future. More immediate applications for the methods used in this work are the $NN\pi$ coupling and the related Goldberger-Treiman relation, the $\Delta N\gamma$ transition as well as, more generally, the corresponding form factors.

Appendix A

The chiral Munczek-Nemirovsky model

In this appendix I want to present the explicit solutions of the quark Dyson-Schwinger equation in rainbow truncation and the Bethe-Salpeter equation in ladder truncation for pseudoscalar and vector mesons by means of a simple interaction with massless quarks. This model was first introduced by Munczek and Nemirovsky [31] with massive quarks and can be seen as a starting point of the analysis of the hadron spectrum within the coupled Dyson-Schwinger-Bethe-Salpeter approach. By construction the integral equations are transformed into algebraic equations. Thus this model can be seen as a simple toy model, which can be used to demonstrate the main steps which have to be performed when solving the coupled system of equations, but circumvents all the technical issues that appear when solving Integral equations numerically.

The form of interaction we want to use in this appendix reads [31]

$$\frac{\mathcal{G}(q^2)}{q^2} = 8\pi^4 D\delta^{(4)}(q) \quad , \quad (\text{A.1})$$

where $\mathcal{G}(q^2)$ is the effective coupling in the quark DSE and meson BSE, which mimics the combined effect of the dressing of the gluon propagator and quark-gluon vertex, q^2 is the gluon momentum squared and D is the coupling strength. The main structure of this construction is the Dirac- δ , which on the one hand simplifies the solution process a lot, since it turns the integral equations into algebraic ones, but on the other hand in several aspects over simplifies the equations, such that it will give rise to several model artefacts we will come across during the solution process.

A.1 Quark Dyson-Schwinger equation

In Section 3.1 the Dyson-Schwinger equation of the quark propagator was introduced,

$$S^{-1}(p) = S_0^{-1}(p) + \int \bar{d}^4k D_{\mu\nu}^{ab}(p-k) \left(g \frac{\lambda^a}{2} \gamma_\mu \right) S(k) g \Gamma_\nu^b(k, p) \quad . \quad (\text{A.2})$$

To solve this equation one needs to know the dressed gluon propagator and the dressed quark-gluon vertex. These are Green functions, too, and thus obey their own Dyson-Schwinger equations which are again coupled to other Green functions and thus their Dyson-Schwinger equations and so on. At a certain point one has to truncate this infinite system of equations and make ansätze for those Green functions, whose Dyson-Schwinger equation is not taken into account.

Since here we are only interested in the quark propagator and do not want to dive into a more detailed investigation of QCD's Dyson-Schwinger equations, for our purpose it is sufficient to only stick to the quark-DSE (A.2) and make ansätze for the gluon propagator and the quark gluon vertex.

A.1.1 Rainbow truncation

In Landau gauge the gluon propagator takes a quite simple form [12],

$$D_{\mu\nu}^{ab}(p) = \frac{Z(p^2)}{p^2} T_{\mu\nu}(p) \delta^{ab} \quad , \quad (\text{A.3})$$

where $T_{\mu\nu}$ is the transversal projector and $Z(p^2)$ the gluon renormalization function.

The quark-gluon vertex has a more delicate role. On the one hand it consists of twelve linearly independent Lorentz covariants, and on the other hand, as the conjoining part between matter and glue sector, it plays a central role in chiral symmetry breaking and the connection between gluon and quark confinement [67]. Nevertheless, since we want to perform phenomenological calculations and are not interested in the details of the respective structures of the QCD Green functions, we stick to the most simple approximation of the quark-gluon vertex. In our calculation we approximate the Lorenz part of the quark-gluon vertex by γ_μ and get

$$g \Gamma_\nu^b(k, p) \simeq g F(k^2, p^2, k \cdot p) \frac{\lambda^b}{2} \gamma_\mu \quad , \quad (\text{A.4})$$

where the λ^b are the Gell-Mann matrices and $F(k^2, p^2, k \cdot p)$ is the quark-gluon vertex dressing function.

Up to now we specified the color and Lorentz structure for the gluon propagator and the quark gluon vertex but the two dressing functions $Z(p^2)$ and $F(k^2, p^2, k \cdot p)$ are still unknown and have to be modeled, too. This is usually done via a so called effective coupling $\mathcal{G}(k, p)$, which models the combined effect of the gluon renormalization function and the quark-gluon vertex dressing function, and also the mismatch that is done by throwing away all other Lorentz structures of the quark gluon vertex than γ_μ .

Now we have everything at hand and can perform the following truncation of the quark Dyson-Schwinger equation (A.2)

$$g^2 D_{\mu\nu}^{ab}(p-k) \Gamma_\nu^b(k,p) \rightarrow \frac{\mathcal{G}((p-k)^2)}{(p-k)^2} T_{\mu\nu}(p-k) \delta^{ab} \frac{\lambda^b}{2} \gamma_\nu \quad (\text{A.5})$$

and we get

$$S^{-1}(p) = S_0^{-1}(p) + \int d^4k \frac{\mathcal{G}((p-k)^2)}{(p-k)^2} T_{\mu\nu} \left(\frac{\lambda^a}{2} \gamma_\mu \right) S(k) \left(\frac{\lambda^a}{2} \gamma_\nu \right) \quad (\text{A.6})$$

This is the so called rainbow truncation of the quarks DSE as already introduced in Section 3.1.

To proceed further in the solution of the quark DSE, we insert the parameterizations of the quark propagator (3.5) and its inverse (3.6) into the truncated equation (A.6),

$$\begin{aligned} (A(p^2)i\not{p} + B(p^2)) \otimes \frac{\mathbf{1}_f}{\sqrt{2}} \otimes \frac{\mathbf{1}_c}{\sqrt{3}} &= (i\not{p} + m) \otimes \frac{\mathbf{1}_f}{\sqrt{2}} \otimes \frac{\mathbf{1}_c}{\sqrt{3}} \\ &+ \int d^4k \frac{\mathcal{G}((p-k)^2)}{(p-k)^2} T_{\mu\nu}(p-k) \left(\frac{\lambda^a}{2} \gamma_\mu \right) \\ &\quad (-\sigma_v(k^2) i\not{k} + \sigma_s(k^2)) \otimes \frac{\mathbf{1}_f}{\sqrt{2}} \otimes \frac{\mathbf{1}_c}{\sqrt{3}} \left(\frac{\lambda^a}{2} \gamma_\nu \right) \quad (\text{A.7}) \end{aligned}$$

In flavor and color space one now has to take projections, which become quite simple, since on the lhs only one basis state occurs. In flavor space we just pull out the $\frac{1}{\sqrt{2}}\mathbf{1}_f$ on the rhs and thus get

$$\text{tr}_f \left\{ \frac{\mathbf{1}_f^\dagger}{\sqrt{2}} \frac{\mathbf{1}_f}{\sqrt{2}} \right\} = 1 \quad (\text{A.8})$$

on both sides. In color space at first we have to perform some simplifications in the self-energy term

$$\frac{\lambda^a}{2} \frac{\mathbf{1}_c}{\sqrt{3}} \frac{\lambda^a}{2} = \frac{\lambda^a \lambda^a}{4} \frac{1}{\sqrt{3}} = \frac{4}{3} \frac{1}{\sqrt{3}} \mathbf{1}_c \quad (\text{A.9})$$

and then pulling out the $\frac{1}{\sqrt{3}}\mathbf{1}_c$ factor we get on both sides of Equation (A.7)

$$\text{tr}_c \left\{ \frac{\mathbf{1}_c^\dagger}{\sqrt{3}} \frac{\mathbf{1}_c}{\sqrt{3}} \right\} = 1 \quad (\text{A.10})$$

Thus, after performing the traces in flavor and color space the rainbow truncated quark DSE becomes

$$\begin{aligned} A(p^2)i\not{p} + B(p^2) &= i\not{p} + m \\ &+ \frac{4}{3} \int d^4k \frac{\mathcal{G}((p-k)^2)}{(p-k)^2} T_{\mu\nu}(p-k) \gamma_\mu (-\sigma_v(k^2) i\not{k} + \sigma_s(k^2)) \gamma_\nu \quad (\text{A.11}) \end{aligned}$$

with the factor of $\frac{4}{3}$ in front of the integral stemming from the color trace (A.9). To proceed further we reduce the second and third line of (A.11) to

$$\begin{aligned} & \left(\delta_{\mu\nu} - \frac{(p-k)_\mu(p-k)_\nu}{(p-k)^2} \right) \gamma_\mu (-i\sigma_v(k^2)\not{k} + \sigma_s(k^2)) \gamma_\nu \\ &= \sigma_v(k^2) i \left(\not{k} + \frac{(p \cdot k - k^2)(\not{p} - \not{k})}{(p-k)^2} \right) + 3\sigma_s(k^2) \quad , \quad (\text{A.12}) \end{aligned}$$

and simplify further to

$$\begin{aligned} A(p^2)i\not{p} + B(p^2) &= i\not{p} + m + \frac{4}{3} \int d^4k \frac{\mathcal{G}((p-k)^2)}{(p-k)^2} \\ &\times \left(\sigma_v(k^2) i \left(\not{k} + \frac{(p \cdot k - k^2)(\not{p} - \not{k})}{(p-k)^2} \right) + 3\sigma_s(k^2) \right) \quad (\text{A.13}) \end{aligned}$$

On both sides there are parts that are, in Dirac space, proportional to the basis elements $\mathbb{1}_D$ and $i\not{p}$. If we project onto them we get two coupled equations:

$$B(p^2) = m + 4 \int d^4k \frac{\mathcal{G}((p-k)^2)}{(p-k)^2} \sigma_s(k^2) \quad (\text{A.14a})$$

$$p^2 A(p^2) = p^2 + \frac{4}{3} \int d^4k \frac{\mathcal{G}((p-k)^2)}{(p-k)^2} \frac{(p^2 - p \cdot k)(p \cdot k - k^2)}{(p-k)^2} \sigma_v(k^2) \quad (\text{A.14b})$$

Whether to calculate the functions for the propagator, σ_v and σ_s , or its inverse, A and B , is a matter of convenience since they are directly connected via equations (3.8). Here we will calculate the inverse propagator by inserting (3.8b) into (A.14) and then calculate the σ -functions via (3.8a).

The next step is to specify the effective interaction $\mathcal{G}(q^2)$. In this appendix we want to use the model introduced by Munczek and Nemirovsky as introduced in Equation (A.1), which will allow us a simple reduction of the coupled system of equations (A.14).

Inserting (A.1) into (A.14) yields

$$B(p^2) = m + 2D \int d^4k \delta^{(4)}(p-k) \frac{B(k^2)}{k^2 A^2(k^2) + B^2(k^2)} \quad (\text{A.15a})$$

$$p^2 A(p^2) = p^2 + \frac{2}{3} D \int d^4k \delta^{(4)}(p-k) \frac{(p^2 - p \cdot k)(p \cdot k - k^2)}{(p-k)^2} \frac{A(k^2)}{k^2 A^2(k^2) + B^2(k^2)} \quad (\text{A.15b})$$

With the relation $\delta^{(4)}(q) = \frac{1}{\pi^2 q^2} \delta(q^2)$ this can be simplified further to

$$0 = B^3(p^2) - m B^2(p^2) + (p^2 A^2(p^2) - 2D)B(p^2) - m p^2 A(p^2) \quad (\text{A.16a})$$

$$0 = p^2 A^3(p^2) - p^2 A^2(p^2) + (B^2(p^2) - D)A(p^2) - B^2(p^2) \quad , \quad (\text{A.16b})$$

and finally in the chiral limit we end up with

$$0 = B^3(p^2) + (p^2 A^2(p^2) - 2D)B(p^2) \quad (\text{A.17a})$$

$$0 = p^2 A^3(p^2) - p^2 A^2(p^2) + (B^2(p^2) - D)A(p^2) - B^2(p^2) \quad . \quad (\text{A.17b})$$

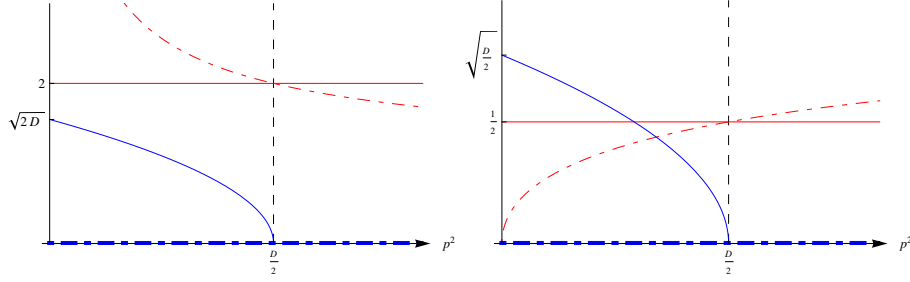


Figure A.1: *Left panel:* Solutions $A(p^2)$ (red) and $B(p^2)$ (blue) as given in (A.19) the dotted lines correspond to solution (A.19a) the solid to (A.19b). Note that the two A-functions cross and $B_{(2)}$ becomes valid at exactly the same point $\frac{D}{2}$. *Right Panel:* The quark mass function $M(p^2)$ (blue) and the quark wave function renormalization $Z(p^2)$ (red) as obtained from (A.20)

These are the equations we want to solve. As we see the Dirac- δ in the interaction transformed the integral equations (A.14) into the algebraic equations (A.17), which are of third order.

Due to the chiral limit (A.17a) has a vanishing solution $B(p^2) = 0$. This leads to a vanishing solution for $A(p^2) = 0$ and for $A(p^2) \neq 0$ one can turn (A.17b) into a quadratic equation which can be solved using standard formulas. For $B(p^2) \neq 0$ one can turn (A.17a) into a quadratic equation and insert the solutions into (A.17b). The solutions for the rainbow-truncated quark Dyson-Schwinger equation in the Munczek-Nemirovsky model with massless quarks are:

$$\begin{aligned} B_{(1)}(p^2) &= 0 \\ A_{(1,1)} &= 0 \end{aligned} \quad (\text{A.18a})$$

$$A_{(1,2/3)}(p^2) = \frac{1}{2} \left(1 \pm \sqrt{1 + \frac{4D}{p^2}} \right) \quad (\text{A.18b})$$

$$\begin{aligned} B_{(2,3)}(p^2) &= \pm \sqrt{2D - p^2 A^2(p^2)} \\ A_{(2,3)}(p^2) &= 2 \quad . \end{aligned} \quad (\text{A.18c})$$

The dressing functions $A(p^2)$ and $B(p^2)$ do not have any direct physical interpretation, but the two secondary terms $Z(p^2) = \frac{1}{A(p^2)}$, the quark wave function, and $M(p^2) = \frac{B(p^2)}{A(p^2)}$, the quark mass function. The physical conditions for $Z(p^2)$ and $M(p^2)$ to be real and non-negative imply the same for $A(p^2)$ and $B(p^2)$. Thus by physical reasons we choose only a subset from (A.18) (additionally dropping $A(p^2) = B(p^2) = 0$):

$$A_{(1)}(p^2) = \frac{1}{2} \left(1 + \sqrt{1 + \frac{4D}{p^2}} \right) \quad B_{(1)}(p^2) = 0 \quad (\text{A.19a})$$

$$A_{(2)}(p^2) = 2 \quad B_{(2)}(p^2) = \sqrt{2D - 4p^2} \quad . \quad (\text{A.19b})$$

Note that solution (A.19b) is only valid in the range of momentum $p^2 < D/2$.

The terms $\sigma_v(p^2)$, $\sigma_s(p^2)$, $Z(p^2)$ and $M(p^2)$ can be deduced from the solutions of $A(p^2)$ and $B(p^2)$ by the relations (3.8).

$$\sigma_{v(1)}(p^2) = \frac{2}{p^2 + p^2 \sqrt{1 + \frac{4D}{p^2}}} \quad \sigma_{s(1)}(p^2) = 0 \quad (\text{A.20a})$$

$$Z_{(1)}(p^2) = \frac{2}{1 + \sqrt{1 + \frac{4D}{p^2}}} \quad M_{(1)}(p^2) = 0 \quad (\text{A.20b})$$

$$\sigma_{v(2)}(p^2) = \frac{1}{D} \quad \sigma_{s(2)}(p^2) = \frac{\sqrt{2D - 4p^2}}{2D} \quad (\text{A.20c})$$

$$Z_{(2)}(p^2) = \frac{1}{2} \quad M_{(2)}(p^2) = \frac{1}{2} \sqrt{2D - 4p^2} \quad (\text{A.20d})$$

The solutions (A.19) for $A(p^2)$ and $B(p^2)$ are shown in Figure A.1 together with the deduced results for the quark wave and mass functions $Z(p^2)$ and $M(p^2)$ from (A.20). Even in this simple model we can already see, at least qualitatively, one striking feature of non-perturbative low energy QCD calculations. The crossing of the two possible solutions and the emergence of a new possible solution at a certain value of p^2 respectively, indicate a transition. In fact, what can be seen here is the dynamical mass generation of QCD due to chiral symmetry breaking. At high energies we have the massless quark we started with, i.e. $M(p^2) = 0$, but below a certain momentum scale, defined by the coupling strength D , namely $\frac{p^2}{D} \leq \frac{1}{2}$ dynamical mass generation is apparent and $M(p^2) \neq 0$. Thus we observe dynamical broken chiral symmetry. The ‘‘physically realized’’ solution is defined piecewise as (A.19a) for $p^2 > \frac{1}{2}D$ and (A.19a) for $p^2 \leq \frac{1}{2}D$. The chiral-quark propagator as the solution of its Dyson-Schwinger equation in rainbow truncation and the Munczek-Nemirovsky interaction model then reads:

$$S_{MN}(p) = \begin{cases} -\frac{1}{D} i \not{p} + \frac{\sqrt{2D - 4p^2}}{2D} & ; p^2 \leq \frac{D}{2} \\ \frac{-2}{\left(1 + \sqrt{1 + \frac{4D}{p^2}}\right) p^2} i \not{p} & ; p^2 > \frac{D}{2} \end{cases} \quad (\text{A.21})$$

A.2 Meson Bethe-Salpeter equation

In the approach to hadron phenomenology we want to use in this thesis mesons are described by Bethe-Salpeter amplitudes as solutions of the quark-antiquark Bethe-Salpeter equation as introduced in Section 2.3 and 3.2. As presented in Equation (3.13) the Bethe-Salpeter equation for mesons reads,

$$\Gamma_{\alpha\beta AB ab}(P, q) = \int \tilde{d}^4 k K(P, q, k)_{\alpha\beta AB ab}^{\alpha'\beta' A'B' a'b'} [S(k - \eta P) \Gamma(P, k) S(k + \bar{\eta} P)]_{\alpha'\beta' A'B' a'b'} \quad (\text{A.22})$$

where $\Gamma_{\alpha\beta AB ab}(P, q)$ are total and relative momentum dependent Bethe-Salpeter amplitudes with their inner quantum numbers spin (Greek letters), flavor (uppercase Latin letters) and color (lowercase Latin letters), $S(q)$ are quark prop-

agators and $K(P, q, k)_{\alpha\beta AB ab}^{\alpha'\beta' A'B' a'b'}$ is the interaction kernel. The quark propagators are taken as a solution from the quark DSE as presented above, the Bethe-Salpeter amplitudes Γ are the solutions of the equation, thus the only part missing is the interaction kernel K . In the derivation of the Dyson equation in Section 2.1.3 the n -particle interaction kernel $K^{(n)}$ got introduced. For the case $n = 2$, $K^{(2)}$ represents all proper 2-particle irreducible interactions, these can be represented by Feynman diagrams that cannot be divided into parts by cutting any amount of fermion lines, and one of them is still a proper 2-particle irreducible interaction.

A.2.1 Ladder Truncation

As in the case of Dyson-Schwinger equations the interaction kernel is a infinite set that has to be truncated. The most simple, so to say 0th order, of the skeleton expansion of the interaction Kernel $K^{(2)}$ is a one-gluon exchange between the two quarks. For the sake of consistency with the rainbow truncated quark DSE one chooses the two occurring quark-gluon vertices and the gluon propagator as bare, dressed by the effective coupling strength $\mathcal{G}(q)$. This truncation of the BSE is called the ladder truncation, and in connection with the rainbow truncation of the quark DSE this coupled system of equations is called the *rainbow-ladder truncation* of the coupled Dyson-Schwinger-Bethe-Salpeter equations.

Thus, taking the whole Dirac, flavor and color structure into account the interaction kernel $K^{(2)}$ of the quark-antiquark Bethe-Salpeter equation in ladder truncation reads¹:

$$K(P, q, k)_{\alpha\beta AB ab}^{\alpha'\beta' A'B' a'b'} \rightarrow -\mathcal{G}((q-k)^2) \frac{[\lambda^i]_a^{\alpha'}}{2} [\gamma_\mu]_\alpha^{\alpha'} \frac{T_{\mu\nu}(p-k)}{(p-k)^2} \delta^{ij} \frac{[\lambda^j]_b^{b'}}{2} [\gamma_\nu]_\beta^{\beta'} \delta_A^{A'} \delta_B^{B'} \quad (\text{A.23})$$

As mentioned at the beginning of the section, we also want to preserve the pion's nature as would-be Goldstone boson in the chiral limit. The guiding line to achieve this is given by the axial-vector Ward-Takahashi identity (AVWTI) as relation between the quark self energy and the quark-antiquark scattering kernel. And indeed it can be shown that the quark self energy in rainbow truncation and the Bethe-Salpeter equation in ladder truncation satisfy the AVWTI, [21, 32, 64]. In this sense we can expect that in a calculation with massless quarks there will be a massless pseudoscalar state.

With this in mind, we can write down the ladder truncated Bethe-Salpeter equation

$$\Gamma_{\alpha\beta}(P, q) = -\frac{4}{3} \int d^4k \frac{\mathcal{G}((q-k)^2)}{(q-k)^2} T_{\mu\nu}(q-k) [\gamma_\mu]_\alpha^\gamma \left[S(k - \frac{P}{2}) \Gamma(P, k) S(k + \frac{P}{2}) \right]_{\gamma\delta} [\gamma_\nu]_\beta^\delta \quad (\text{A.24})$$

¹Note that there does not exist a definite sign convention. If one defines the quark self-energy in the quark DSE with an additional minus sign, this has to be attached by hand. Important is that we are here in an attractive channel.

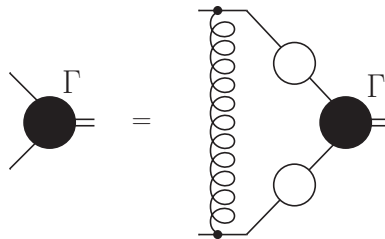


Figure A.2: Bethe-Salpeter equation in ladder truncation

Where we already performed the projections in color,

$$\begin{aligned} \text{tr}_c \left\{ \left(\frac{1}{\sqrt{3}} \delta_{ab} \right)^\dagger \frac{\lambda_{aa'}^i}{2} \delta^{ij} \frac{\lambda_{bb'}^j}{2} \frac{1}{\sqrt{3}} \delta_{a'b'} \right\} &= \frac{1}{12} \delta_{ab} \lambda_{aa'}^i \lambda_{bb'}^i \delta_{a'b'} \\ &= \frac{1}{12} \lambda_{aa'}^i \lambda_{aa'}^i = \frac{4}{3} \quad , \quad (\text{A.25}) \end{aligned}$$

and flavor space,

$$\text{tr}_f \left\{ r_{AB}^I \delta_A^{A'} \delta_B^{B'} r_{A'B'}^I \right\} = \text{tr}_f \left\{ r_{AB}^I r_{AB}^I \right\} = 1 \quad . \quad (\text{A.26})$$

This is a quite general result and the usual starting point for rainbow-ladder truncated Bethe-Salpeter studies. Now we proceed further with our toy model calculations and insert the interaction (A.1) into (A.24),

$$\Gamma(P, q) = -\frac{4}{3} \int d^4 k \frac{D}{2} \delta(q - k) T_{\mu\nu}(q - k) \quad (\text{A.27})$$

$$\begin{aligned} &\gamma_\mu S(k - \frac{P}{2}) \Gamma(P, k) S(k + \frac{P}{2}) \gamma_\nu \\ &= -\int d^4 k \frac{D}{2} \delta(q - k) \delta_{\mu\nu} \gamma_\mu S(k - \frac{P}{2}) \Gamma(P, k) S(k + \frac{P}{2}) \gamma_\nu \quad (\text{A.28}) \end{aligned}$$

$$\Gamma(P, q) = -\frac{D}{2} \gamma_\mu S(q - \frac{P}{2}) \Gamma(P, q) S(q + \frac{P}{2}) \gamma_\mu \quad (\text{A.29})$$

where we used the general relation

$$\int d^4 l \delta^4(l) \frac{(p \cdot l)(q \cdot l)}{l^2} f(p, q, l) = \frac{1}{4} \int d^4 l \delta^4(l) (p \cdot q) f(p, q, l) \quad . \quad (\text{A.30})$$

Equation (A.29) has a somewhat subtle structure, which is due to the simple model we used. The point like interaction is already integrated out, but still (A.29) has solutions for every relative momentum q . Usually, as it was also done in the original paper [31], one chooses $q = 0$. Several arguments for this choice can be found and we will present one physically motivated here.

The effective interaction in the Munczek-Nemirovsky model (A.1) is a point-like interaction in momentum space with its peak exactly at $q^2 = 0$. This implies that the gluon, exchanged between the two quarks, does not transport momentum, thus it will not change the momentum of the quarks. As a consequence any solution with non-vanishing relative momentum q , would remain with this

property forever and the quarks will just drift apart. Since the concept of a bound state principally implies a finite spacial extension, two forever with constant speed dispersing particles clearly can not form a bound state². To describe bound states, only the solution $q = 0$ will give us physically meaningful results.

Thus, from the infinitely many possible solutions of Eq. (A.29), we choose the one with $q = 0$ for physical reasons and get

$$\Gamma(P, 0) = -\frac{D}{2} \gamma_\mu S\left(-\frac{P}{2}\right) \Gamma(P, 0) S\left(\frac{P}{2}\right) \gamma_\mu \quad . \quad (\text{A.31})$$

A.2.2 Pseudoscalar meson

To proceed further we have to specify which kind of mesons we want to calculate. Therefore the Bethe-Salpeter amplitude $\Gamma(P, q)$ is spanned on a set of basis vectors in flavor, color and Dirac-space as deduced in Section 3.2.2. In equations (A.25) and (A.26) we already used the fact that mesons as measurable quantities are color singlets and also that we work in the isospin symmetric two-flavor case, thus only the Lorentz and Dirac parts remain. Following the derivation of Equation (3.21), in Dirac space one basis for a pseudoscalar meson is

$$\begin{aligned} \tau_1^{(\pi)} &= i \gamma_5 \mathbb{1} & \tau_3^{(\pi)} &= P \cdot q \gamma_5 \not{q} \\ \tau_2^{(\pi)} &= \gamma_5 \not{P} & \tau_4^{(\pi)} &= -\frac{i}{2} \gamma_5 [\not{q}, \not{P}] \end{aligned} \quad . \quad (\text{A.32})$$

Following above discussion we choose $q = 0$ which is a model artefact and simplifies the solution of our equation enormously, since the structures of the Bethe-Salpeter amplitude proportional to q vanish and only $\tau_1^{(\pi)}$ and $\tau_2^{(\pi)}$ survive in (A.32). Furthermore their coefficients become constant. With this simplifications we get

$$F_1 i \gamma_5 + F_2 \gamma_5 \not{P} = -\frac{D}{2} \gamma_\mu \left(i \frac{\not{P}}{2} \sigma_v \left(\frac{P^2}{4} \right) + \sigma_s \left(\frac{P^2}{4} \right) \right) \quad (\text{A.33})$$

$$\begin{aligned} &\times (F_1 i \gamma_5 + F_2 \gamma_5 \not{P}) \left(-i \frac{\not{P}}{2} \sigma_v \left(\frac{P^2}{4} \right) + \sigma_s \left(\frac{P^2}{4} \right) \right) \gamma_\mu \\ &= 2D \left(s^2 F_1 - i F_2 \sigma_s \left(\frac{P^2}{4} \right) \sigma_v \left(\frac{P^2}{4} \right) P^2 \right) \gamma_5 \\ &\quad + D \left(s^2 F_2 - i \sigma_v \left(\frac{P^2}{4} \right) \sigma_s \left(\frac{P^2}{4} \right) F_1 \right) \gamma_5 \not{P} \end{aligned} \quad (\text{A.34})$$

with $s^2 = -\frac{P^2}{4} \sigma_v^2 \left(\frac{P^2}{4} \right) + \sigma_s^2 \left(\frac{P^2}{4} \right)$.

If we project onto the Dirac basis we get a linear system of two equations

$$\begin{pmatrix} F_1 \\ F_2 \end{pmatrix} = \begin{pmatrix} 2D s^2 & -i \sigma_s \left(\frac{P^2}{4} \right) \sigma_v \left(\frac{P^2}{4} \right) P^2 \\ i D \sigma_v \left(\frac{P^2}{4} \right) \sigma_s \left(\frac{P^2}{4} \right) & -D s^2 \end{pmatrix} \begin{pmatrix} F_1 \\ F_2 \end{pmatrix} \quad . \quad (\text{A.35})$$

²One can imagine an analogous situation in classical mechanics, where force is change of momentum in time. If one takes two particles with initial momenta, and this momenta does not change, then one would say that there is no mutual force actioning between this two particles. In this sense one could even say that this interaction model used here does not lead to a force in the Newtonian sense.

This is a homogenous system of equations $\vec{F} = K\vec{F}$, which is a very general feature in the solution process of the homogenous Bethe-Salpeter equation. In numerical studies a high-dimensional system of equations of this kind appears. In these studies, the system is solved via considering it as an Eigenvalue-equation $\lambda(P^2)\vec{F} = K\vec{F}$ which is only true for $\lambda(P^2) = 1$. Thus, the problem reduces to calculate the first few Eigenvalues of the matrix K , as functions of P^2 [36]. Applying the condition $\lambda(P^2) = 1$ gives with the on-shell condition $P^2 = -M^2$ the mass of the bound state. The different Eigenvalues are then interpreted as different excitations, with the same quantum numbers.

Nevertheless, since the matrix in (A.35) is only two dimensional we can take a more traditional path. The homogeneous system $\vec{F} = K\vec{F}$ has a non-trivial solution, if the homogenous system $0 = (K - I)\vec{F}$ has one. Therefore the sufficient condition $\det [K - I] = 0$ leads to

$$0 = -\frac{D^2}{8} \left(\sigma_v^2 \left(\frac{P^2}{4} \right) P^2 + 4\sigma_s^2 \left(\frac{P^2}{4} \right) \right)^2 + \frac{D}{4} \left(\sigma_v^2 \left(\frac{P^2}{4} \right) P^2 - 4\sigma_s^2 \left(\frac{P^2}{4} \right) \right) + 1. \quad (\text{A.36})$$

Now we are very close to a solution of the Bethe-Salpeter equation. The last step is to include the functions σ_v and σ_s as they are calculated from our solutions of the quark Dyson-Schwinger equation above and stated in (A.20). The quark propagator (A.21) is only piecewise defined, due to the simple interaction model we use and the chiral limit. Since we work in Euclidean space for a bound state the on-shell condition $P^2 = -M^2$ requires to evaluate the quark propagator dressing function at negative p^2 . In (A.21) we did not make any explicit assumptions about this domain, and so we will just extrapolate from the positive half axis.

The solution process is now straightforward. If we plug (A.20c) into (A.36), we get

$$0 = -\frac{D^2}{8} \left(\frac{2}{D} \right)^2 + \frac{D}{4} \left(2 \frac{P^2 - D}{D^2} \right) + 1 \quad (\text{A.37})$$

$$0 = \frac{P^2}{2D} \quad , \quad (\text{A.38})$$

which can only be true if $P^2 = 0$

Now let's take a step back and again get some overview about what we have done. At first we implied several conditions, needed to describe a particular meson, on the Bethe-Salpeter amplitude. In this case we implied the color, flavor and Dirac quantum numbers for a pseudoskalar meson whose constituents have the same mass, which corresponds directly to the pion. Afterwards we plugged its Bethe-Salpeter amplitude into the Bethe-Salpeter equation, which we truncated in a setup that is consistent with the truncation of the quark Dyson-Schwinger equation whose solution we took as an input into the BSE. We found one valid bound state which has $P^2 = -M^2 = 0$. So we found a massless pseudoscalar bound state out of two fermions with dynamically generated mass. This is exactly what one would expect from [68] and we recover the Pion as Nambu-Goldstone boson of chiral symmetry even in this simple model calculation.

To specify the solution further and to really calculate the π -Bethe-Salpeter amplitude we have to solve (A.35) for the case $P^2 = 0$ which leads to the simple

equations

$$F_1 = 2D \sigma_s^2(0) F_1 = F_1 \equiv c \quad (\text{A.39a})$$

$$F_2 = i D \sigma_v(0) \sigma_s(0) F_1 - D \sigma_s^2(0) F_2 = \frac{i \sqrt{2}}{3\sqrt{D}} c \quad , \quad (\text{A.39b})$$

and we end up with the unnormalized Bethe Salpeter amplitude for the pion in the Munczek-Nemirovsky model with massless quarks

$$\Gamma^{(\pi)}(P, 0) = c_{(\pi)} i \gamma_5 + \frac{i \sqrt{2}}{3\sqrt{D}} c_{(\pi)} \not{P} \quad . \quad (\text{A.40})$$

Normalization

The last step in the explicit solution of the Bethe-Salpeter equation would be to specify the last free parameter $c_{(\pi)}$ by the normalization condition derived in Section 2.3. But again, due to the simple model structure and the chiral limit an awkward situation arises.

If we plug Eq.(A.40) into the normalization condition for the BSE (2.33), we just get the result $0 = 0$. The canonical normalization condition thus is not wrong or invalid, but, in this simple model, it does not give us any new information about the Bethe-Salpeter amplitudes. One now could think of different kinds of normalizations, e.g. normalization of the vector (F_1, F_2) together with a normalization of the basis elements, but, since we will not use the solutions in further calculations we can stop at this point.

A.2.3 Vector meson

As for the pseudoscalar BSA we can also find an explicit analytic solution for the vector BSA in the Munczek-Nemirovsky model in the chiral limit. Choosing the same color and flavor structure as for the pseudoscalar meson or pion, the corresponding vector meson would be the rho-meson.

Pulling out the polarization factors of the vector meson amplitude $\Gamma^v(P, q) = \frac{1}{\sqrt{n_\lambda}} \varepsilon_\mu^\lambda \Gamma_\mu$, Equation (A.31) becomes

$$\Gamma_\mu(P, 0) = -\frac{D}{2} \gamma_\nu S\left(-\frac{P}{2}\right) \Gamma_\mu(P, 0) S\left(\frac{P}{2}\right) \gamma_\nu \quad , \quad (\text{A.41})$$

and thus from the basis of the vector meson BSA (3.30) only two covariants survive, which gives us the equation

$$F_1 \gamma_\mu^T + F_2 \gamma_\mu^T \not{P} = -4D \left(s^2 F_1 - i F_2 P^2 \sigma_s \left(\frac{P^2}{4} \right) \sigma_v \left(\frac{P^2}{4} \right) \right) \gamma_\mu^T \quad , \quad (\text{A.42})$$

where the second covariant on the right hand side vanishes due to

$$\begin{aligned} \gamma_\nu \gamma_\mu^T \gamma_\rho \gamma_\nu P_\rho &= \gamma_\nu \gamma_\nu \gamma_\mu^T \gamma_\rho P_\rho - 2\gamma_\nu \delta_{\mu\nu}^T \gamma_\rho P_\rho + 2\gamma_\nu \gamma_\mu^T \delta_{\nu\rho} P_\rho \\ &= 2\gamma_\mu^T \gamma_\rho P_\rho + 2\gamma_\rho \gamma_\mu^T P_\rho = 4\gamma_\rho^T P_\rho = 0 \quad . \end{aligned} \quad (\text{A.43})$$

Thus we have $F_2 = 0$ and come to the equation

$$F_1 = -4D \left(-\frac{P^2}{4} \sigma_v^2 \left(\frac{P^2}{4} \right) + \sigma_s^2 \left(\frac{P^2}{4} \right) \right) F_1 \quad , \quad (\text{A.44})$$

which again for $p^2 \leq \frac{D}{2}$ can only be solved for

$$P^2 = -4D \longrightarrow M = 2\sqrt{D} \quad . \quad (\text{A.45})$$

Note that (A.44) is true for any constant F_1 as long as (A.45) is fulfilled. Thus the Bethe-Salpeter equation gives us a condition for the mass of the vector meson bound state. In fact the mass of the bound state comes out as a byproduct of the solution process of the BSE. This is a quite general feature of BSE-studies and one reason why this equation is so popular in many areas of theoretical physics. In solving this equation to get descriptions of a certain bound-state, the mass, one of the most important observables, of the bound state just drops out.

Now at the very end of our calculation we have to contract the solution with the polarizations and sum over them and we get the unnormalized solution of the Bethe-Salpeter equation for the vector meson in the Munczek-Nemirovsky model in the chiral limit

$$\Gamma_\mu^{(\rho)}(P, 0) = c_v \gamma_\mu^T \quad , \quad (\text{A.46})$$

which has to be contracted with the polarizations ϵ_μ^λ to give the vector meson Bethe-Salpeter amplitude

$$\Gamma^{(\rho)}(P, 0) = \frac{1}{\sqrt{n_\lambda}} \sum_\lambda \epsilon_\mu^\lambda \Gamma_\mu^{(\rho)}(P, 0) \quad . \quad (\text{A.47})$$

A.2.4 Diquarks

The main difference between diquark and meson studies in the rainbow ladder truncated DSE/BSE studies is the color factor in the Bethe-Salpeter equation. Thus we will not go further into details of a study of diquarks within the Munczek-Nemirovsky model, because everything what was said about the mesons can qualitatively be transported to the diquark case. Our starting point now is the ladder truncated Bethe-Salpeter equation (A.24)

$$\begin{aligned} \Gamma_{\alpha\beta}(P, q) = c_c c_f \int d^4k \frac{\mathcal{G}((q-k)^2)}{(q-k)^2} T_{\mu\nu}(q-k) \\ [\gamma_\mu]_\alpha^\gamma \left[S(k - \frac{P}{2}) \Gamma(P, k) S(k + \frac{P}{2}) \right]_{\gamma\delta} [\gamma_\nu]_\beta^\delta \quad . \quad (\text{A.48}) \end{aligned}$$

with a color and flavor factors c_c, c_f . The flavor trace is simple, since all flavor matrices are properly normalized,

$$c_f = \text{tr}_f \left\{ s_{AB}^I \delta_A^{A'} \delta_B^{B'} s_{A'B'}^I \right\} = \text{tr}_f \left\{ s_{AB}^I s_{AB}^I \right\} = 1 \quad . \quad (\text{A.49})$$

The color trace gives,

$$\begin{aligned} c_c = \text{tr}_c \left\{ \left(\frac{1}{\sqrt{6}} \epsilon_{abc} \right)^\dagger \frac{\lambda_{aa'}^i}{2} \delta^{ij} \frac{\lambda_{bb'}^j}{2} \frac{1}{\sqrt{6}} \epsilon_{a'b'c} \right\} \\ = \frac{1}{24} (\delta_{aa'} \delta_{bb'} - \delta_{ab'} \delta_{ba'}) \lambda_{aa'}^i \lambda_{bb'}^i = \frac{1}{24} (\lambda_{aa}^i \lambda_{bb}^i - \lambda_{ab}^i \lambda_{ba}^i) \\ = \frac{1}{24} (0 - 16) = -\frac{2}{3} \quad , \quad (\text{A.50}) \end{aligned}$$

which exactly leads to an attractive diquark channel, but the coupling strength is only half of what it is in the meson case.

Appendix B

Technicalities

B.1 Construction of flavor and color matrices

B.1.1 Fundamental representations of $SU(2)$

Throughout this thesis we work with 2 quark flavors that have the same mass. Thus symmetry in iso-spin space is not explicitly broken, a situation that usually is called the iso-symmetric limit.

In this case the up and down quark form a doublet under $SU(2)$, which is exactly the spin group of, e.g., an electron, in a fundamental representation. Also their anti-quarks form a doublet under $SU(2)$ in a fundamental representation. However, these two representations are not identical. While the quarks transform according to what usual is called *the fundamental representation*, in the following denoted by 2 , the anti-quarks transform according to *the conjugate complex fundamental representation*¹[44], denoted by $\bar{2}$.

We will now impose several transformation properties onto the $\begin{pmatrix} u \\ d \end{pmatrix}$ doublet and the $\begin{pmatrix} \bar{u} \\ \bar{d} \end{pmatrix}$ anti-doublet. These can be seen as phenomenological input, or also just as definitions for up and down (anti-)quark. From these general transformation properties we will find the generators of the representations.

The projection of the up quark onto an arbitrary chosen 3-axis in isospin-space usually is defined as isospin $+\frac{1}{2}$, while the down quark has $-\frac{1}{2}$. Like in usual quantum mechanics, we can also define ladder operators, that rise and lower the isospin. Thus we choose the following *definitions*:

$$\tau_3 u = +\frac{1}{2} \qquad \tau_3 d = -\frac{1}{2} \qquad (\text{B.1a})$$

$$\tau_+ u = 0 \qquad \tau_+ d = u \qquad (\text{B.1b})$$

$$\tau_- u = d \qquad \tau_- d = 0 \quad , \qquad (\text{B.1c})$$

from which we can read off the matrix representations

$$\tau_+ = \begin{pmatrix} 0 & 1 \\ 0 & 0 \end{pmatrix} \qquad \tau_- = \begin{pmatrix} 0 & 0 \\ 1 & 0 \end{pmatrix} \qquad \tau_3 = \begin{pmatrix} \frac{1}{2} & 0 \\ 0 & -\frac{1}{2} \end{pmatrix} \quad . \qquad (\text{B.2})$$

¹Indeed there are even 4 fundamental representations of the general linear group [69, p. 264]

With the identification $\tau_{\pm} = \tau_1 \pm i\tau_2$ one recognizes in (B.2) the Pauli matrices σ_i as (twice the) generators of the 2 representation,

$$\tau_1 = \frac{1}{2} \begin{pmatrix} 0 & 1 \\ 1 & 0 \end{pmatrix} = \frac{\sigma_1}{2}, \quad \tau_2 = \frac{1}{2} \begin{pmatrix} 0 & -i \\ i & 0 \end{pmatrix} = \frac{\sigma_2}{2}, \quad \tau_3 = \frac{1}{2} \begin{pmatrix} 1 & 0 \\ 0 & -1 \end{pmatrix} = \frac{\sigma_3}{2}. \quad (\text{B.3})$$

We can apply the same procedure to the anti-doublet. If we define the anti quarks as follows,

$$\bar{\tau}_3 \bar{u} = -\frac{1}{2} \qquad \bar{\tau}_3 \bar{d} = +\frac{1}{2} \quad (\text{B.4a})$$

$$\bar{\tau}_+ \bar{u} = -\bar{d} \qquad \bar{\tau}_+ \bar{d} = 0 \quad (\text{B.4b})$$

$$\bar{\tau}_- \bar{u} = 0 \qquad \bar{\tau}_- \bar{d} = -\bar{u} \quad (\text{B.4c})$$

we find the ladder operators of the conjugate complex fundamental representation $\bar{2}$,

$$\bar{\tau}_+ = \begin{pmatrix} 0 & 0 \\ -1 & 0 \end{pmatrix} \qquad \bar{\tau}_- = \begin{pmatrix} 0 & -1 \\ 0 & 0 \end{pmatrix}, \quad (\text{B.5a})$$

and its generators,

$$\bar{\tau}_1 = \frac{1}{2} \begin{pmatrix} 0 & -1 \\ -1 & 0 \end{pmatrix} \qquad \bar{\tau}_2 = \frac{1}{2} \begin{pmatrix} 0 & -i \\ i & 0 \end{pmatrix} \qquad \bar{\tau}_3 = \frac{1}{2} \begin{pmatrix} -1 & 0 \\ 0 & 1 \end{pmatrix}. \quad (\text{B.5b})$$

So, starting from transformation properties of the doublet, we could find matrix representations of the fundamental representation 2 and its complex conjugate $\bar{2}$. One could also go the other way round in postulating the existence of the complex conjugate representation, and then find that the generators of both representations are connected via

$$\bar{\tau}_i = -\tau_i^* \quad (\text{B.6})$$

as it was done for $SU(3)$ in [44]. Here we took this path since it is more reasonable for what follows. Note that the generators are normalized according to $\text{tr} \left\{ \tau_i^\dagger \tau_i \right\} = 1$.

In the theory of angular momentum in quantum mechanics, as described, e.g., in [70], one can identify eigenstates of rotation operators uniquely by the quadratic Casimir operator, J^2 , and the 3-axis projection, J_3 , by their eigenvalues

$$\vec{J}^2 |j, m\rangle = j(j+1) |j, m\rangle \qquad J_z |j, m\rangle = m |j, m\rangle; \quad -j \leq m \leq j \quad (\text{B.7})$$

For both cases above we can recover the quadratic Casimir of $SU(2)$

$$\sum_i \tau_i^2 = \sum_i \bar{\tau}_i^2 = \frac{1}{4} \sum_i \sigma_i^2 = \frac{3}{4} \mathbf{1}, \quad (\text{B.8})$$

which corresponds to the value $j = 1/2$.

B.1.2 Irreducible representation of $SU(2) \otimes SU(2)$

A central issue in this thesis are two-body problems. On the quark level these are mesons and diquarks. While both require to find irreducible representations of the product group $SU(2) \otimes SU(2)$, the cases have one subtle difference. While diquarks are built out of two quarks, such that we need to combine doublets from the same representation $\mathbf{2}$, mesons are built of a quark and an antiquark, such that we have to combine the two representations $\mathbf{2}$ and $\bar{\mathbf{2}}$. This will lead to quite different matrix representations of the product group.

In a general group theoretical notation one can write

$$\mathbf{2} \otimes \mathbf{2} = \mathbf{1}_a \oplus \mathbf{3}_s \quad , \quad (\text{B.9})$$

which is also valid for $\mathbf{2} \otimes \bar{\mathbf{2}}$. This means that the irreducible representations of the product group will be an anti-symmetric singlet and a symmetric triplet state.

Clebsch-Gordan coefficients

In quantum mechanics, finding an irreducible representation of a product group is reduced to the recursive calculation of Clebsch-Gordan coefficients. For diquarks $SU(2) \otimes SU(2)$ is just the same as one would combine two spin- $\frac{1}{2}$ electrons, since both quarks (as both electrons) correspond to the $\mathbf{2}$ -doublet and this calculation is demonstrated in many introductory books to quantum mechanics, like, e.g., [70]. The idea is that one implements a basis transformation from the separate basis of the two $\mathbf{2}$ representations (left hand side of Equation (B.9)) to a basis of the two irreducible representations (right hand side of Equation (B.9)) $|j_1, m_1, j_2, m_2\rangle \rightarrow |j, m\rangle$,

$$\begin{aligned} |j, m\rangle &= \sum_{m_1, m_2} |j_1, m_1, j_2, m_2\rangle \langle j_1, m_1, j_2, m_2 | j, m\rangle \\ &= \sum_{m_1, m_2} |m_1, m_2\rangle \langle m_1, m_2 | j, m\rangle \quad , \quad (\text{B.10}) \end{aligned}$$

where we suppressed the j_i 's on the right hand side since they are already fixed.

In general this procedure is done via fixing one particular j , choosing the maximal $m(j)$, since there is only one state corresponding to this, and then applying $J_- = J_{1-} \oplus J_{2-}$ with $J_{\pm} |j, m\rangle = \sqrt{(j \mp m)(j \pm m + 1)} |j, m \pm 1\rangle$ onto the respective side.

Before we proceed in this way, we should choose a convention of the basis in the product state. We are looking for a basis of the group $SU(2) \otimes SU(2)$. Above we constructed bases for $SU(2)$ starting from their doublets. One convenient choice, which follows this path, is to choose the outcome of the outer product of the two doublets. In general this will be 2×2 -matrices. In the space of hermitian 2×2 -matrices the Pauli-matrices together with the $\mathbf{1}$ form a basis. We want to express the outer product in this basis, e.g. a diquark made of two up quarks corresponds to

$$|uu\rangle = \begin{pmatrix} 1 \\ 0 \end{pmatrix} \otimes \begin{pmatrix} 1 \\ 0 \end{pmatrix} = \begin{pmatrix} 1 & 0 \\ 0 & 0 \end{pmatrix} = \frac{1}{2} (\mathbf{1} + \sigma_3) \quad . \quad (\text{B.11})$$

Now we can go back to the bracket notation and perform the calculation of the Clebsch-Gordan coefficients. For the isovector diquark we start with the $|u u\rangle$ -state, apply $T_-^{2\otimes 2} = \tau_- \oplus \tau_-$ and bring the coefficients on the right side, such that we get

$$s^+ = |u u\rangle = \frac{1}{2}(\mathbf{1} + \sigma_3) \quad (\text{B.12a})$$

$$s^0 = \frac{1}{\sqrt{2}}(|u d\rangle + |d u\rangle) = \frac{1}{\sqrt{2}}\sigma_1 \quad (\text{B.12b})$$

$$s^- = |d d\rangle = \frac{1}{2}(\mathbf{1} - \sigma_3) \quad . \quad (\text{B.12c})$$

In calculations of Clebsch-Gordan coefficients it is always more involved to change the multiplet. In our case this would lead too far. We just argue, that a singlet state is always anti-symmetric. Therefore we write the basis for the isoscalar diquark as

$$s^s = \frac{1}{\sqrt{2}}(|u d\rangle - |d u\rangle) = \frac{1}{\sqrt{2}}i\sigma_2 \quad . \quad (\text{B.12d})$$

To find the singlet representation one could also just argue that, in the space of hermitian 2×2 matrices there is only one matrix left that is orthonormal on the other three.

The same procedure can now be applied for the mesons. The state in the isovector triplet with maximal isospin-3 component is the $|u \bar{d}\rangle$ state. If we apply now $T_-^{2\otimes 2} = \tau_- \oplus \bar{\tau}_-$ we get additional minus signs. Again expanding in the basis of Pauli-Matrices and $\mathbf{1}$ yields

$$r^+ = |u \bar{d}\rangle = \frac{1}{2}(\sigma_1 + i\sigma_2) \quad (\text{B.13a})$$

$$r^0 = \frac{1}{\sqrt{2}}(|d \bar{d}\rangle - |u \bar{u}\rangle) = -\frac{1}{\sqrt{2}}\sigma_3 \quad (\text{B.13b})$$

$$r^- = -|d \bar{u}\rangle = -\frac{1}{2}(\sigma_1 - i\sigma_2) \quad (\text{B.13c})$$

$$r^s = \frac{1}{\sqrt{2}}(|d \bar{d}\rangle + |u \bar{u}\rangle) = \frac{1}{\sqrt{2}}\mathbf{1} \quad (\text{B.13d})$$

There is some arbitrariness in the choice of the minus signs here (one could also start with $|d \bar{u}\rangle$ and then apply J_+ which leads to a all over minus sign), because the basis elements are only normalized to $\text{tr}_f \{r^i \dagger r^j\} = \delta^{ij}$. When performing calculations one usually implies conditions onto the observables, and the signs are adjusted then.

B.1.3 Color-singlet representation of $SU(3) \otimes SU(3)$

As in the flavor case, also in color space quarks transform according to the fundamental representation. Thus for the quarks we can write down the basis

$$r = (1, 0, 0) \quad g = (0, 1, 0) \quad b = (0, 0, 1) \quad , \quad (\text{B.14})$$

	$\tau_+^{(12)}$	$\tau_-^{(12)}$	$\tau_+^{(13)}$	$\tau_-^{(13)}$	$\tau_+^{(23)}$	$\tau_-^{(23)}$
r	0	g	0	b	0	0
g	r	0	0	0	0	b
b	0	0	r	0	g	0
	$\bar{\tau}_+^{(12)}$	$\bar{\tau}_-^{(12)}$	$\bar{\tau}_+^{(13)}$	$\bar{\tau}_-^{(13)}$	$\bar{\tau}_+^{(23)}$	$\bar{\tau}_-^{(23)}$
\bar{r}	0	$-\bar{g}$	0	$-\bar{b}$	0	0
\bar{g}	$-\bar{r}$	0	0	0	0	$-\bar{b}$
\bar{b}	0	0	$-\bar{r}$	0	$-\bar{g}$	0

Table B.1: Transformation properties of the basis (B.14) and (B.17) under the ladder operators (B.19).

where the generators of the group can be expressed in terms of the Gell-Mann matrices

$$\begin{aligned}
\lambda_1 &= \begin{pmatrix} 0 & 1 & 0 \\ 1 & 0 & 0 \\ 0 & 0 & 0 \end{pmatrix} & \lambda_2 &= \begin{pmatrix} 0 & -i & 0 \\ i & 0 & 0 \\ 0 & 0 & 0 \end{pmatrix} & \lambda_3 &= \begin{pmatrix} 1 & 0 & 0 \\ 0 & -1 & 0 \\ 0 & 0 & 0 \end{pmatrix} \\
\lambda_4 &= \begin{pmatrix} 0 & 0 & 1 \\ 0 & 0 & 0 \\ 1 & 0 & 0 \end{pmatrix} & \lambda_5 &= \begin{pmatrix} 0 & 0 & -i \\ 0 & 0 & 0 \\ i & 0 & 0 \end{pmatrix} & \lambda_6 &= \begin{pmatrix} 0 & 0 & 0 \\ 0 & 0 & 1 \\ 0 & 1 & 0 \end{pmatrix} \\
\lambda_7 &= \begin{pmatrix} 0 & 0 & 0 \\ 0 & 0 & -i \\ 0 & i & 0 \end{pmatrix} & \lambda_8 &= \frac{1}{\sqrt{3}} \begin{pmatrix} 1 & 0 & 0 \\ 0 & 1 & 0 \\ 0 & 0 & -2 \end{pmatrix}
\end{aligned} \tag{B.15}$$

as

$$\tau_i = \frac{\lambda_i}{2} . \tag{B.16}$$

Anti-quark as well as diquarks transform according to the complex conjugate fundamental representation $\bar{\mathbf{3}}$ with the basis

$$\bar{r} = (1, 0, 0) \quad \bar{g} = (0, 1, 0) \quad \bar{b} = (0, 0, 1) . \tag{B.17}$$

Parallel to the flavor $SU(2)$ case and Eq. (B.6) the generators of this representation can be expressed in terms of the λ_i by

$$\bar{\tau}_i = -\frac{\lambda_i^*}{2} . \tag{B.18}$$

The construction of the $SU(3)$ multiplets is some more involved and a detailed treatment of the $SU(3)$ -flavor multiplets can be found in [44]. In the color case one very important simplification occur: hadrons are color singlets. Thus, from the product $\mathbf{3} \otimes \bar{\mathbf{3}} = \mathbf{1} \oplus \mathbf{8}$, for our purpose, we only need to construct the anti-symmetric singlet-1-state.

Therefore, as for the $SU(2)$ -flavor case, we can build ladder operators out of the λ_i 's and find out the transformation behavior of the basis under these ladder operators. The transformation laws under the ladder operators defined by

$$\begin{aligned}
\tau_{\pm}^{(12)} &= \tau_1 \pm i \tau_2 & \bar{\tau}_{\pm}^{(12)} &= \bar{\tau}_1 \mp i \bar{\tau}_2 \\
\tau_{\pm}^{(13)} &= \tau_4 \pm i \tau_5 & \bar{\tau}_{\pm}^{(13)} &= \bar{\tau}_4 \mp i \bar{\tau}_5 \\
\tau_{\pm}^{(23)} &= \tau_6 \pm i \tau_7 & \bar{\tau}_{\pm}^{(23)} &= \bar{\tau}_6 \mp i \bar{\tau}_7 \quad ,
\end{aligned}
\tag{B.19}$$

can be found in Tab. B.1.

Inspired by Eq. (B.13d) we can write down the color-singlet representation

$$\mathbf{c}^s = \frac{1}{\sqrt{3}}(|r \bar{r}\rangle + |g \bar{g}\rangle + |b \bar{b}\rangle) = \frac{1}{\sqrt{3}} \mathbf{1}_c \quad , \tag{B.20}$$

where $\mathbf{1}_c$ is the unity matrix in the space of complex 3×3 -matrices. The anti-symmetry of this singlet state can be shown by means of the transformation properties Tabular B.1. In terms of two arbitrary color quantum numbers a, b this state can be expressed by the Kronecker delta $\frac{1}{\sqrt{3}} \delta_{a\bar{b}}$.

B.2 Kinematics in the triangle diagram

In this appendix kinematical issues of the triangle diagram shall be presented in some detail. At first we will write down the most general kinematical set up and the special choices of the parameters used corresponding to the particular cases. In all cases we want to assume the participating external particles to be on-shell and conservation of total momentum being valid.

B.2.1 General considerations

The general kinematics of a Bethe-Salpeter amplitude with incoming total momentum P and relative momentum q , outgoing quark-momentum q_+ and outgoing anti-quark momentum (or incoming quark momentum) q_- , see also Figure B.1(a), reads

$$\begin{aligned}
P &= q_+ - q_- & q_+ &= q + \eta P \\
q &= \bar{\eta} q_+ + \eta q_- & q_- &= q - \bar{\eta} P
\end{aligned}
\tag{B.21}$$

where $\eta + \bar{\eta} = 1$ are momentum partitioning parameters, to distribute the total momentum onto the two constituents. One fixes these parameters prior to solving the Bethe-Salpeter equation. Thus, in our calculations they appear as fixed values, depending on the Bethe-Salpeter amplitudes under investigation.

In the triangle diagram we have three Bethe-Salpeter amplitudes, thus three total momenta. For these general considerations we want to assume all of them as incoming. Working on the physical state space the momentum conservation is valid, which yields in this conventions

$$P_1 + P_2 + P_3 = 0 \quad , \tag{B.23}$$

and leaves us two independent external momenta.

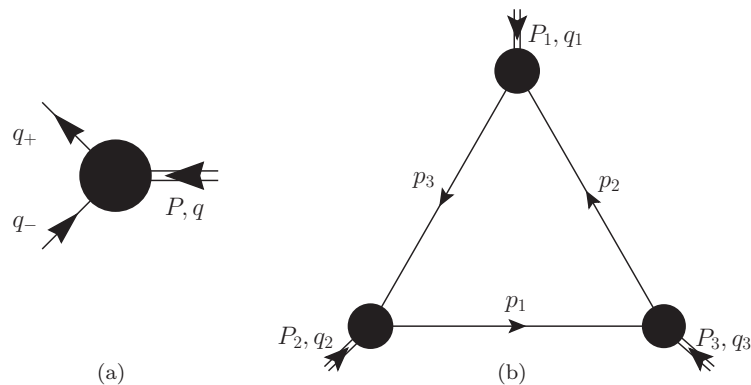


Figure B.1: Kinematics of a Bethe-Salpeter amplitude (a) and in the triangle diagram (b).

Implementing the kinematics of the Bethe-Salpeter amplitudes above into the triangle diagram, see also Figure B.1(b), we get for quark momenta expressed at the respective Bethe-Salpeter amplitudes:

$$BSA\ 1 : \quad p_2 = q_1 - \bar{\eta}_1 P_1 \quad p_3 = q_1 + \eta_1 P_1 \quad (B.24a)$$

$$BSA\ 2 : \quad p_3 = q_2 - \bar{\eta}_2 P_2 \quad p_1 = q_2 + \eta_2 P_2 \quad (B.24b)$$

$$BSA\ 3 : \quad p_1 = q_3 - \bar{\eta}_3 P_3 \quad p_2 = q_3 + \eta_3 P_3 \quad . \quad (B.24c)$$

Now, we can set the respective quark momenta to be equal and find relations among momenta of different Bethe-Salpeter amplitudes

$$p_2 : \quad q_1 - \bar{\eta}_1 P_1 = q_3 + \eta_3 P_3 \quad \longrightarrow \quad q_3 = q_1 - \eta_3 P_3 - \bar{\eta}_1 P_1 \quad (B.25a)$$

$$p_3 : \quad q_2 - \bar{\eta}_2 P_2 = q_1 + \eta_1 P_1 \quad \longrightarrow \quad q_2 = q_1 + \eta_1 P_1 + \bar{\eta}_2 P_2 \quad (B.25b)$$

$$p_1 : \quad q_3 - \bar{\eta}_3 P_3 = q_2 + \eta_2 P_2 \quad \longrightarrow \quad 0 = P_1 + P_2 + P_3 \quad , \quad (B.25c)$$

where the third line gives the conservation of total momentum if one inserts the relations for q_2 and q_3 . This can be used as a cross-check.

Now we have written down the most general kinematics for the triangle diagram, Figure B.1(b). In practical calculations one needs to choose a certain inertial frame, like the rest frame of the decaying particle, or the Breit frame in electromagnetic form factor calculations, which means to fix the external momenta. Also one has to choose a momentum of integration $k = (k_1, k_2, k_3, k_4)$, $k \cdot k = k^2$, see further Equation (B.69). The result of the calculations should be independent of the choice of the frame and momentum of integration, but it is favorable to choose this parameter in a for the practical calculations convenient manner.

B.2.2 Breit frame

When not describing transitions, in calculations of electromagnetic form factors one often uses the so called Breit frame, where the momentum transferred by the photon becomes purely spacelike. In this setup one identifies the Bethe-Salpeter amplitude 3 in Figure B.1(b) with the incoming boundstate of mass

M , $P_3 := P_i$, $q_3 := q_i$ and the Bethe-Salpeter amplitude 2 with the outgoing boundstate with the same mass, $P_2 := -P_f$, $q_2 := -q_f$. At spot 1, one inserts the constituent-photon vertex $\Gamma_\mu(P_1 := P_\gamma, q_1 := q_\gamma)$, with the incoming photon momentum $Q = P_\gamma$. The kinematics is chosen as such that incoming and outgoing bound states share the momentum transfer symmetrically,

$$P_i = \begin{pmatrix} 0 \\ 0 \\ -\kappa \\ i\sqrt{M^2 + \kappa^2} \end{pmatrix} \quad P_f = \begin{pmatrix} 0 \\ 0 \\ \kappa \\ i\sqrt{M^2 + \kappa^2} \end{pmatrix} . \quad (\text{B.26})$$

One free external momentum is now identified with the photon momentum, the other is an average momentum of the two bound-state momenta, the so called Breit momentum,

$$Q := P_\gamma = P_f - P_i = \begin{pmatrix} 0 \\ 0 \\ 2\kappa \\ 0 \end{pmatrix} \quad P := \frac{1}{2}(P_f + P_i) = \begin{pmatrix} 0 \\ 0 \\ 0 \\ i\sqrt{M^2 + \kappa^2} \end{pmatrix} , \quad (\text{B.27})$$

which has the advantage that the photon momentum Q is only spacelike, thus real, and the Breit momentum P becomes only timelike, thus imaginary. If we invert these equations we get

$$P_i = P - \frac{Q}{2} \quad P_f = P + \frac{Q}{2} . \quad (\text{B.28})$$

The constituent-photon vertex is symmetric, thus a simple choice will be $\eta_\gamma = \frac{1}{2}$. For an elastic form factor, the initial and final state will be the same bound state, thus the momentum partitioning parameter will not change and we have in the following $\eta_i = \eta_f := \eta$.

Now, rephrasing the first two equations of (B.25), and expressing them in the two external momenta yields

$$q_i = q_\gamma - \eta P - \frac{\bar{\eta}}{2} Q \quad (\text{B.29a})$$

$$q_f = q_\gamma - \eta P + \frac{\bar{\eta}}{2} Q . \quad (\text{B.29b})$$

The aim is now to push all imaginary parts into the constituent-photon vertex, leaving the relative momenta of the Bethe-Salpeter amplitudes real. This can be done via defining the momentum of integration as

$$\mathbf{k} = q_\gamma - \eta P \quad (\text{B.30})$$

and one ends up with

$$q_i = \mathbf{k} - \frac{\bar{\eta}}{2} Q \quad (\text{B.31a})$$

$$q_f = \mathbf{k} + \frac{\bar{\eta}}{2} Q \quad (\text{B.31b})$$

$$q_\gamma = \mathbf{k} + \eta P , \quad (\text{B.31c})$$

and their squares

$$q_i^2 = k^2 + \bar{\eta}^2 \kappa^2 - 2\bar{\eta} \kappa k_3 \quad (\text{B.32a})$$

$$q_f^2 = k^2 + \bar{\eta}^2 \kappa^2 + 2\bar{\eta} \kappa k_3 \quad (\text{B.32b})$$

$$q_\gamma^2 = k^2 - \eta^2 \left(M^2 + \frac{\kappa}{2} \right) + i 2\eta \sqrt{M^2 + \kappa^2} k_4 \quad , \quad (\text{B.32c})$$

where the two relative momenta, and thus also their squares, of the Bethe-Salpeter amplitudes are now purely real, and thus no continuation of the Chebyshev moments into the complex plane is needed. All the complex parts are transferred to the constituent-photon vertex.

Finally for the constituent momenta we get

$$p_1 = k - \bar{\eta} P \quad (\text{B.33a})$$

$$p_2 = k + \eta P - \frac{Q}{2} \quad (\text{B.33b})$$

$$p_3 = k + \eta P + \frac{Q}{2} \quad , \quad (\text{B.33c})$$

thus all propagators have to be evaluated in some region in the complex plane.

B.2.3 $\rho \rightarrow \pi\pi$

One can interpret the kinematics of the $\rho \rightarrow \pi\pi$ transition either as a Breit frame calculation, where the photon gets exchanged with the ρ -meson, or as the kinematics, where one chooses the decaying particle to be at rest. In the end both interpretations will lead to the same kinematics.

At first we want to identify the ρ -meson with spot 1 in Figure B.1(b), $P_1 := P_\rho$, $q_1 := q_\rho$, which shall be at rest, and the two outgoing Pions with spots 2 and 3, $P_{2,3} := -P_{\pi_2,\pi_3}$, $q_{2,3} := -q_{\pi_2,\pi_3}$, with both pions fly in different directions, but with the same amount of momentum κ , which is defined via momentum conservation in the four-component

$$P_\rho = \begin{pmatrix} 0 \\ 0 \\ 0 \\ i M_\rho \end{pmatrix} \quad P_{\pi_2} = \begin{pmatrix} 0 \\ 0 \\ \kappa \\ i \sqrt{M_\pi^2 + \kappa^2} \end{pmatrix} \quad P_{\pi_3} = \begin{pmatrix} 0 \\ 0 \\ -\kappa \\ i \sqrt{M_\pi^2 + \kappa^2} \end{pmatrix} . \quad (\text{B.34})$$

Here we choose the first free external momentum to be the ρ -meson momentum, and the second free external momentum as the relative momentum between the two outgoing pions. With

$$P = P_\rho = \begin{pmatrix} 0 \\ 0 \\ 0 \\ i M_\rho \end{pmatrix} \quad Q = \frac{1}{2} (P_{\pi_2} - P_{\pi_3}) = \begin{pmatrix} 0 \\ 0 \\ \kappa \\ 0 \end{pmatrix} \quad (\text{B.35})$$

we get exactly the same structure as for the Breit frame, Equations (B.27), if one takes into account the conservation of external momenta $M_\rho = 2\sqrt{M_\pi^2 + \kappa^2}$. The inverse of Equations (B.35) are

$$P_{\pi_2} = \frac{1}{2} P + Q \quad P_{\pi_3} = \frac{1}{2} P - Q \quad . \quad (\text{B.36})$$

The difference to the Breit Frame is, that we do not want to push all the complex parts into the ρ -Bethe-Salpeter amplitude, since this would imply to analytically continue its Chebyshev moments in a big region in the complex plane. Instead we push the imaginary part symmetrically onto both pion Bethe-Salpeter amplitudes. Additionally since we work in the isospin-symmetric limit and thus the quark and the anti-quark have the same mass, the momentum partitioning parameter is set to $\eta = \bar{\eta} = \frac{1}{2}$, which will yield further simplifications.

Recalling Equations (B.25) and (B.29), we get

$$-q_{\pi_3} = q_\rho - \frac{1}{2}Q - \frac{1}{4}P \quad (\text{B.37a})$$

$$-q_{\pi_2} = q_\rho - \frac{1}{2}Q + \frac{1}{4}P \quad . \quad (\text{B.37b})$$

One choice could be $k = q_\rho$, but to decrease the region in the complex plane, where the Bethe-Salpeter amplitudes have to be known, we choose

$$q_\rho = k + \frac{1}{2}Q \quad (\text{B.38a})$$

$$-q_{\pi_3} = k - \frac{1}{4}P \quad (\text{B.38b})$$

$$-q_{\pi_2} = k + \frac{1}{4}P \quad , \quad (\text{B.38c})$$

which have the squares

$$q_\rho^2 = k^2 + \frac{\kappa^2}{4} - \kappa k_3 \quad (\text{B.39a})$$

$$q_{\pi_3}^2 = k^2 - \frac{M_\rho^2}{16} - i \frac{M_\rho}{2} k_4 \quad (\text{B.39b})$$

$$q_{\pi_2}^2 = k^2 - \frac{M_\rho^2}{16} + i \frac{M_\rho}{2} k_4 \quad . \quad (\text{B.39c})$$

We see, that the ρ momentum is real and just shifted on the real axis, both pion Bethe-Salpeter amplitudes have to be known in the same region of the complex plane.

The quark momenta then become

$$p_1 = k + \frac{1}{2}Q \quad (\text{B.40a})$$

$$p_2 = k - \frac{1}{2}P - \frac{1}{2}Q \quad (\text{B.40b})$$

$$p_3 = k + \frac{1}{2}P - \frac{1}{2}Q \quad . \quad (\text{B.40c})$$

B.2.4 $\Delta \rightarrow N\pi$

The kinematics in the $\Delta N\pi$ -System is some more involved than the two cases above, since one has particles with three different masses and three different momentum partitioning parameters. We will set the Δ -baryon to be at rest $P_1 := P_\Delta$, $q_1 := q_\Delta$, $\eta_1 = \bar{\eta}_\Delta$, decaying into the outgoing Nucleon $P_2 := -P_N$, $q_2 := -q_N$, $\eta_2 = \bar{\eta}_N$, and pion $P_3 := -P_\pi$, $q_3 := -q_\pi$. Introducing a new

momentum partitioning parameter η_Q in the triangle, the external momenta are similar to the $\rho \rightarrow \pi\pi$ case,

$$P_\Delta = \begin{pmatrix} 0 \\ 0 \\ 0 \\ i M_\Delta \end{pmatrix} \quad P_N = \begin{pmatrix} 0 \\ 0 \\ \kappa \\ i \sqrt{M_N^2 + \kappa^2} \end{pmatrix} \quad P_\pi = \begin{pmatrix} 0 \\ 0 \\ -\kappa \\ i \sqrt{M_\pi^2 + \kappa^2} \end{pmatrix} \quad (\text{B.41})$$

and

$$P = P_\Delta = \begin{pmatrix} 0 \\ 0 \\ 0 \\ i M_\Delta \end{pmatrix} \quad Q = (\bar{\eta}_Q P_N - \eta_Q P_\pi) = \begin{pmatrix} 0 \\ 0 \\ \kappa \\ 0 \end{pmatrix}, \quad (\text{B.42})$$

with

$$\eta_Q = \frac{\sqrt{M_N^2 + \kappa^2}}{\sqrt{M_N^2 + \kappa^2} + \sqrt{M_\pi^2 + \kappa^2}} \quad \bar{\eta}_Q = \frac{\sqrt{M_\pi^2 + \kappa^2}}{\sqrt{M_N^2 + \kappa^2} + \sqrt{M_\pi^2 + \kappa^2}}. \quad (\text{B.43})$$

Again we could write down two independent momenta of the triangle, one of which is spacelike and one timelike. As above they give the nucleon and pion momenta:

$$P_N = Q + \eta_Q P \quad P_\pi = -Q + \bar{\eta}_Q P \quad . \quad (\text{B.44})$$

from which one can derive the relative momenta

$$-q_\pi = q_\Delta - \frac{1}{2} Q + \left(\frac{\bar{\eta}_Q}{2} - \eta_\Delta \right) P \quad (\text{B.45a})$$

$$-q_N = q_\Delta - \eta_N Q + (\bar{\eta}_\Delta - \eta_N \eta_Q) P \quad . \quad (\text{B.45b})$$

Now it is not possible to put all imaginary parts into one of the relative momenta, due to the different momentum partitioning parameters, which are due to the different masses of the participating particles. We choose the momentum of integration such that one minimizes the area in the complex plane, where the nucleon has to be evaluated:

$$q_\Delta = k + \eta_N Q \quad (\text{B.46a})$$

$$-q_N = k + (\bar{\eta}_\Delta - \eta_N \eta_Q) P \quad (\text{B.46b})$$

$$-q_\pi = k + \left(\eta_N - \frac{1}{2} \right) Q + \left(\frac{\eta_Q}{2} - \eta_\Delta \right) P \quad , \quad (\text{B.46c})$$

which reduce to Equations (B.38) in the case of $\eta_Q = \eta_N = \eta_\Delta = \frac{1}{2}$. Finally we end up with the relative momentum squares

$$q_\Delta^2 = k^2 + \eta_N^2 \kappa^2 - 2\eta_N \kappa k_3 \quad (\text{B.47a})$$

$$q_N^2 = k^2 - (\bar{\eta}_\Delta - \eta_N \eta_Q)^2 M_\Delta^2 + i 2 (\bar{\eta}_\Delta - \eta_N \eta_Q) M_\Delta k_4 \quad (\text{B.47b})$$

$$q_\pi^2 = k^2 + \left(\eta_N - \frac{1}{2} \right)^2 \kappa^2 - \left(\frac{\eta_Q}{2} - \eta_\Delta \right)^2 M_\Delta^2 \\ + 2 \left(\eta_N - \frac{1}{2} \right) \kappa k_3 + i 2 \left(\frac{\eta_Q}{2} - \eta_\Delta \right) M_\Delta k_4 \quad , \quad (\text{B.47c})$$

and the quark momenta

$$p_1 = k + (1 - \eta_\Delta - \eta_Q) P - Q \quad (\text{B.48a})$$

$$p_2 = k - \eta_N Q - \eta_\Delta P \quad (\text{B.48b})$$

$$p_3 = k - \eta_N Q + \bar{\eta}_\Delta P \quad (\text{B.48c})$$

B.3 The quark propagator in the complex plane

Performing calculations in Euclidean spacetime has the disadvantage of introducing complex variables. In our calculations this leads to the fact that we need to know the quark propagator for complex p^2 -values. To self-consistently solve the quark-DSE in the complex p^2 -plane the idea is to solve the DSE on the real p^2 -axis first, then shift the momentum of integration from the quark to the gluon momentum, such that the gluon dressing function $\mathcal{G}(q^2)$ only has to be evaluated at real arguments. Then the quark momentum becomes complex and one has to solve (3.12) on a complex grid. Using Cauchy's formula it is sufficient to solve the equation not on the whole grid, but on a contour, that surrounds the required area [71]. In coupled BSE/DSE calculations, it is advantageous to solve the quark DSE on a parabola combined with fits to the real axis solution at large momentum-squared and then uses a numerically reliable representation of the Cauchy formula

$$f(z) \approx \frac{\sum_j \frac{w_j f(z_j)}{z_j - z}}{\sum_j \frac{w_j}{z_j - z}} \quad f'(z) \approx \frac{\sum_j \frac{w_j f(z_j)}{(z_j - z)^2} - f(z) \sum_j \frac{w_j}{(z_j - z)^2}}{\sum_j \frac{w_j}{z_j - z}} \quad (\text{B.49})$$

which is especially suitable for Bethe-Salpeter equation studies of heavy quarkonium systems and excited states [72]. For our calculations we use such a representation of the quark propagator dressing functions.

B.4 Taylor expansion

Throughout this thesis we used Bethe-Salpeter amplitudes that were solved numerically, thus they, or to be more specific their Chebyshev moments, were only known on a finite grid on the real q^2 -axis. This grid was not the same for all of the amplitudes and also not equidistant. To know the amplitudes on any point on the positive real q^2 -axis and also in the complex plane, we performed a Taylor-expansion from the nearest grid point.

$$f(q^2) \approx f(q_i^2) + \frac{f'(q_i^2)}{1!} (q^2 - q_i^2) + \frac{f''(q_i^2)}{2!} (q^2 - q_i^2)^2 + \dots \\ \dots + \frac{f^{(n)}(q_i^2)}{n!} (q^2 - q_i^2)^n \quad (\text{B.50})$$

To perform such an expansion up to n -th order one needs to know the values of the derivatives up to n -th order in the point q_i^2 . Several possibilities exist to obtain approximations for these derivatives, e.g., performing a Padé approximation and taking the derivatives of the approximation function or performing a spline fit up to n -th order. Throughout this thesis we calculated our derivatives

via the method of *divided differences*, which we will explain in the following. For a more detailed treatment and mathematical proofs we refer to [73].

To begin with, we assume to know a function f which is continuous and differentiable up to $(n+1)$ -th order, only on a finite set of grid points $\{x_0, x_1, x_2, \dots, x_n\}$. The aim is now to know the function on the entire axis.

Therefore we define the divided differences

$$\langle x_i \rangle = f(x_i) \quad (\text{B.51a})$$

$$\langle x_0, x_1 \rangle = \frac{\langle x_0 \rangle - \langle x_1 \rangle}{x_0 - x_1} \quad (\text{B.51b})$$

$$\langle x_0, x_1, x_2 \rangle = \frac{\langle x_0, x_1 \rangle - \langle x_1, x_2 \rangle}{x_0 - x_2} \quad (\text{B.51c})$$

$$\vdots \quad \quad \quad \vdots$$

$$\langle x_0, x_1, x_2, \dots, x_n \rangle = \frac{\langle x_0, x_1, \dots, x_{n-1} \rangle - \langle x_1, x_2, \dots, x_n \rangle}{x_0 - x_n}, \quad (\text{B.51d})$$

with which we can express the function f as

$$\begin{aligned} f(x) = & \langle x_i \rangle + \langle x_0, x_1 \rangle (x - x_0) + \langle x_0, x_1, x_2 \rangle (x - x_0)(x - x_1) \\ & + \langle x_0, x_1, x_2, \dots, x_n \rangle (x - x_0)(x - x_1) \dots (x - x_{n-1}) + R_n(x), \end{aligned} \quad (\text{B.52})$$

where $R_n(x)$ is the remainder term. This is the so called *Newton interpolation formula*, which represents a generalization of the Taylor formula. In fact it turns out that one can express the remainder term as

$$R_n(x) = \frac{(x - x_0)(x - x_1) \dots (x - x_n)}{(n + 1)!} f^{(n+1)}(\xi), \quad (\text{B.53})$$

with ξ being a point in the interval containing the whole set $\{x, x_0, \dots, x_n\}$. For simplicity we want to assume from now on $x_0 = \min\{x_0, \dots, x_n\}$ and $x_n = \max\{x_0, \dots, x_n\}$. Since Equation (B.53) is true for any order $k \leq n$, we find for any such k

$$\frac{f^{(k)}(\xi_k)}{k!} = \langle x_0, x_1, x_2, \dots, x_k \rangle, \quad \xi_k \in [x_0, x_k]. \quad (\text{B.54})$$

Expressed the other way round we found that for the divided difference of order k of a function f on the gridpoints $\{x_0, \dots, x_k\}$, there exists at least one point $\xi \in [x_0, x_k]$ with Equation (B.54) being valid. In fact Equation (B.54) will lead us to an approximation for the derivatives at the grid points x_i . For even k we approximate the derivatives by:

$$\frac{f^{(k)}(x_i)}{k!} \approx \langle x_{i-k/2}, \dots, x_i, \dots, x_{i+k/2} \rangle, \quad \text{for } k \text{ even.} \quad (\text{B.55a})$$

For odd k Equation (B.54) is not symmetric. Therefore we symmetrize between the forward and backward difference

$$\begin{aligned} \frac{f^{(k)}(x_i)}{k!} \approx & \frac{1}{2} \left(\langle x_{i-(k+1)/2}, \dots, x_i, \dots, x_{i+(k-1)/2} \rangle \right. \\ & \left. + \langle x_{i-(k-1)/2}, \dots, x_i, \dots, x_{i+(k+1)/2} \rangle \right), \quad \text{for } k \text{ odd.} \end{aligned} \quad (\text{B.55b})$$

The only caveat with this definitions (B.55) is that they are not well defined for points x_j with $j < \frac{k}{2}$ and $j > n - \frac{k}{2}$. Since in practical calculations the order of the Taylor expansion k will be much smaller than the number of grid points $k \ll n$, these problems will only occur at border terms. In our calculations we replaced the not defined derivatives with the nearest well-defined derivatives

for $k = 1, 2$:

$$f^{(k)}(x_0) := f^{(k)}(x_1) \qquad f^{(k)}(x_n) := f^{(k)}(x_{n-1}) \qquad (\text{B.56a})$$

for $k = 3, 4$:

$$f^{(k)}(x_0) = f^{(k)}(x_1) := f^{(k)}(x_2) \quad f^{(k)}(x_n) = f^{(k)}(x_{n-1}) := f^{(k)}(x_{n-2}). \qquad (\text{B.56b})$$

A side-effect of this method is, that one reduces oscillation effects in the boarder range that can occur when performing approximation on functions on a finite set of grid points.

Thus, now we found an approximation for the derivatives for any of the grid points x_i and we can rewrite Equation (B.50)

$$f(q^2) \approx f(q_i^2) + \frac{\langle q_{i-1}^2, q_i^2 \rangle + \langle q_i^2, q_{i+1}^2 \rangle}{2} (q^2 - q_i^2) + \langle q_{i-1}^2, q_i^2, q_{i+1}^2 \rangle (q^2 - q_i^2)^2 + \dots \qquad (\text{B.57})$$

This formula is now valid for any q^2 in the complex plane, as long as one is not in a neighborhood of poles and branch cuts.

In our calculations of the triangle diagram we performed Taylor expansions up to fourth order.

B.5 Euclidean spacetime

In this appendix I want to collect the main issues, when performing calculations in four dimensional Euclidean space instead of $3 + 1$ dimensional Minkowski spacetime.

Conventions and translation rules

The defining difference between 4D-Euclidean space and $(3 + 1)$ D Minkowski spacetime is the metric $g^{\mu\nu}$. While for the Euclidean space it is just the Kronecker Delta $g^{\mu\nu} = \delta_{\mu\nu}$, in Minkowski spacetime it becomes the flat Minkowski metric $g^{\mu\nu} = \eta^{\mu\nu}$ with $\eta^{\mu\nu} = \text{diag}\{1, -1, -1, -1\}$.

A general vector in Minkowski spacetime reads

$$a_\mu^M = \begin{pmatrix} a_0 \\ \vec{a} \end{pmatrix} \qquad (\text{B.58})$$

$$(a^M)^2 = a_\mu^M a_\nu^M \eta^{\mu\nu} = a_0^2 - \vec{a}^2 = a_0^2 - a_i^2 \quad , \qquad (\text{B.59})$$

where i runs from 1 to 3. In Euclidean space the Minkowski vector (B.58) is

represented by the vector

$$a_\mu^E = \begin{pmatrix} \vec{a} \\ i a_0 \end{pmatrix} \quad (\text{B.60})$$

$$(a^E)^2 = a_\mu^E a_\nu^E \delta^{\mu\nu} = a_i^2 - a_0^2 \quad . \quad (\text{B.61})$$

If one compares (B.59) and (B.61) one finds:

$$(a^E)^2 = - (a^M)^2 \quad . \quad (\text{B.62})$$

Gamma-algebra

The defining equation for the Clifford algebra in Euclidean space,

$$\{\gamma_\mu^E, \gamma_\nu^E\} = 2\delta_{\mu\nu} \quad , \quad (\text{B.63})$$

is satisfied if

$$\gamma_i^E = -i\gamma_i^M \quad (\text{B.64})$$

$$\gamma_4^E = \gamma_0^M \quad , \quad (\text{B.65})$$

where the γ_μ^M are the Dirac Gamma-Matrices in Minkowski spacetime which satisfy the Clifford Algebra $\{\gamma_\mu^M, \gamma_\nu^M\} = 2\eta_{\mu\nu}$.

As in the Minkowski case one can define a Matrix γ_5 that commutes with all other Gamma matrices as

$$\gamma_5^E = -\gamma_1^E \gamma_2^E \gamma_3^E \gamma_4^E \quad . \quad (\text{B.66})$$

The γ -matrices become expressed by means of the Pauli-Matrices (B.3) and in standart representation they read

$$\gamma_i^E = \begin{pmatrix} 0 & -i\sigma_i \\ i\sigma_i & 0 \end{pmatrix} \quad \gamma_4^E = \begin{pmatrix} \mathbf{1} & 0 \\ 0 & -\mathbf{1} \end{pmatrix} \quad \gamma_5^E = \begin{pmatrix} 0 & \mathbf{1} \\ \mathbf{1} & 0 \end{pmatrix} \quad , \quad (\text{B.67})$$

and the slash product becomes

$$\not{a}^E = a_\mu^E \gamma_\mu^E = a_i^E \gamma_i^E + a_4^E \gamma_4^E = -i a_i^M \gamma_i^M + i a_0^M \gamma_0^M = i \not{a}^M \quad . \quad (\text{B.68})$$

Integral measure

A general four vector in Euclidean space can be expressed in spherical coordinates as

$$\mathbf{k} = \begin{pmatrix} k_1 \\ k_2 \\ k_3 \\ k_4 \end{pmatrix} = \sqrt{k^2} \begin{pmatrix} \sin \psi \sin \theta \sin \varphi \\ \sin \psi \sin \theta \cos \varphi \\ \sin \psi \cos \theta \\ \cos \psi \end{pmatrix} = \sqrt{k^2} \begin{pmatrix} \sqrt{1-z^2} \sqrt{1-y^2} \sin \varphi \\ \sqrt{1-z^2} \sqrt{1-y^2} \cos \varphi \\ \sqrt{1-z^2} y \\ z \end{pmatrix} \quad , \quad (\text{B.69})$$

with $k^2 = |\mathbf{k}|^2$. This parameterization gives the following integral measure in momentum space

$$\int d^4k = \frac{1}{(2\pi)^4} \int_0^\infty dk^2 \frac{k^2}{2} \int_{-1}^1 dz \sqrt{1-z^2} \int_{-1}^1 dy \int_{-\pi}^\pi d\varphi \quad . \quad (\text{B.70})$$

Bibliography

- [1] M. GELL-MANN. “A schematic model of Baryons and Mesons.” *Physical Letters*, 8;3: 2. 1964
- [2] G. ZWEIG. “An SU(3) model for strong interaction symmetry and its breaking I.” *CERN preprint*, pp. TH-401. CERN-TH-401. 1964
- [3] G. ZWEIG. “An SU(3) model for strong interaction symmetry and its breaking II.” *CERN preprint*, pp. TH-412. CERN-TH-412. 1964
- [4] D. JARECKE, P. MARIS and P. C. TANDY. “Strong decays of light vector mesons.” *Phys. Rev. C*, 67: 035202. 2003
- [5] D. W. JARECKE. “Properties of mesons from Bethe-Salpeter amplitudes.” Ph.D. thesis, Kent State University. Advisor: Tandy, Peter C. 2005
- [6] M. E. PESKIN and D. V. SCHROEDER. *An Introduction to Quantum Field Theory* (Westview Press, 1995)
- [7] L. H. RYDER. *Quantum field theory*. second edn. (Cambridge University Press, 1996)
- [8] F. J. DYSON. “The Radiation Theories of Tomonaga, Schwinger, and Feynman.” *Phys. Rev.*, 75: 486. 1949
- [9] F. J. DYSON. “The S Matrix in Quantum Electrodynamics.” *Phys. Rev.*, 75: 1736. 1949
- [10] J. SCHWINGER. “On the Green Functions of Quantized Fields II.” *PNAS*, 37: 455. 1951
- [11] J. SCHWINGER. “On the Green Functions of Quantized Fields I.” *PNAS*, 37: 452. 1951
- [12] R. ALKOFER and L. VON SMEKAL. “The infrared behavior of QCD Green’s functions: Confinement, dynamical symmetry breaking, and hadrons as relativistic bound states.” *Phys. Rept.*, 353: 281. 2001
- [13] R. J. RIVERS. *Path Integral methods in quantum field theory* (Cambridge University Press, 1987)
- [14] R. ALKOFER, M. Q. HUBER and K. SCHWENZER. “Infrared Behavior of Three-Point Functions in Landau Gauge Yang-Mills Theory.” *Eur. Phys. J.*, C62: 761. 2009

- [15] M. Q. HUBER, R. ALKOFRER and S. P. SORELLA. “Infrared analysis of Dyson-Schwinger equations taking into account the Gribov horizon in Landau gauge.” *Phys. Rev.*, D81: 065003. 2010
- [16] R. ALKOFRER, M. Q. HUBER and K. SCHWENZER. “Algorithmic derivation of Dyson-Schwinger Equations.” *Comput. Phys. Commun.*, 180: 965. 2009
- [17] N. NAKANISHI. “A general survey of the theory of the Bethe-Salpeter equation.” *Supplement of the Progress of Theoretical Physics*, 43: 1. 1969
- [18] E. E. SALPETER and H. A. BETHE. “A Relativistic Equation for Bound-State Problems.” *Phys. Rev.*, 84: 1232. 1951
- [19] M. GELL-MANN and F. LOW. “Bound States in Quantum Field Theory.” *Phys. Rev.*, 84: 350. 1951
- [20] G. EICHMANN. “Hadron properties from QCD bound-state equations.” Ph.D. thesis, Institut für Physik, Karl Franzens Universität Graz. 2009
- [21] P. MARIS and P. C. TANDY. “Bethe-Salpeter study of vector meson masses and decay constants.” *Phys. Rev. C*, 60: 055214. 1999
- [22] P. MARIS and P. C. TANDY. “ π , K^+ , and K electromagnetic form factors.” *Phys. Rev. C*, 62: 055204. 2000
- [23] M. S. BHAGWAT and P. MARIS. “Vector meson form factors and their quark-mass dependence.” *Phys. Rev. C*, 77: 025203. 2008
- [24] P. MARIS and P. TANDY. “QCD modeling of hadron physics.” *Nuclear Physics B - Proceedings Supplements*, 161: 136 . Proceedings of the Cairns Topical Workshop on Light-Cone QCD and Nonperturbative Hadron Physics. 2006
- [25] R. ALKOFRER, A. HOLL, M. KLOKER, A. KRASSNIGG and C. D. ROBERTS. “On nucleon electromagnetic form factors.” *Few Body Syst.*, 37: 1. 2005
- [26] G. EICHMANN, A. KRASSNIGG, M. SCHWINZERL and R. ALKOFRER. “A covariant view on the nucleons’ quark core.” *Annals Phys.*, 323: 2505. 2008
- [27] D. NICMORUS, G. EICHMANN and R. ALKOFRER. “Delta and Omega electromagnetic form factors in a Dyson-Schwinger/Bethe-Salpeter approach.” ArXiv: 1008.3184. 2010
- [28] C. D. ROBERTS. “Electromagnetic pion form-factor and neutral pion decay width.” *Nucl. Phys.*, A605: 475. 1996
- [29] P. MARIS, C. D. ROBERTS, S. M. SCHMIDT and P. C. TANDY. “T-dependence of pseudoscalar and scalar correlations.” *Phys. Rev.*, C63: 025202. 2001
- [30] P. MARIS and P. C. TANDY. “Electromagnetic transition form factors of light mesons.” *Phys. Rev.*, C65: 045211. 2002
- [31] H. J. MUNCZEK and A. M. NEMIROVSKY. “Ground-state qqbar mass spectrum in quantum chromodynamics.” *Phys. Rev. D*, 28: 181. 1983

- [32] P. MARIS and C. D. ROBERTS. “ π^- and K -meson Bethe-Salpeter amplitudes.” *Phys. Rev. C*, 56: 3369. 1997
- [33] H. J. MUNCZEK and P. JAIN. “Relativistic pseudoscalar q anti- q bound states: Results on Bethe-Salpeter wave functions and decay constants.” *Phys. Rev.*, D46: 438. 1992
- [34] R. ALKOFER, P. WATSON and H. WEIGEL. “Mesons in a Poincare covariant Bethe-Salpeter approach.” *Phys. Rev. D*, 65: 094026. 2002
- [35] S. PRELOVSEK ET AL. “Lattice study of light scalar tetraquarks with $I=0,2,1/2,3/2$: are sigma and kappa tetraquarks?” *Phys. Rev. D*, 82: 094507. 2010
- [36] M. BLANK and A. KRASSNIGG. “Matrix algorithms for solving (in)homogeneous bound state equations.” ArXiv: 1009.1535. 2010
- [37] M. S. BHAGWAT, M. A. PICHOWSKY and P. C. TANDY. “Confinement phenomenology in the Bethe-Salpeter equation.” *Phys. Rev. D*, 67: 054019. 2003
- [38] C. H. LLEWELLYN-SMITH. “A relativistic formulation for the quark model for mesons.” *Ann. Phys.*, 53: 521. 1969
- [39] A. KRASSNIGG. “Survey of $J = 0, 1$ mesons in a Bethe-Salpeter approach.” *Phys. Rev. D*, 80: 114010. 2009
- [40] A. KRASSNIGG and M. BLANK. “A covariant study of tensor mesons.” ArXiv: 1011.6650. 2010
- [41] G. EICHMANN. “The Analytic Structure of the Quark Propagator in the Covariant Faddeev Equation of the Nucleon.” Master’s thesis, Institut für Physik, Karl Franzens Universität Graz. 2006
- [42] P. MARIS. “Effective masses of diquarks.” *Few Body Syst.*, 32: 41. 2002
- [43] P. MARIS. “Electromagnetic properties of diquarks.” *Few Body Syst.*, 35: 117. 2004
- [44] W. GREINER and B. MÜLLER. Quantum Mechanics - Symmetries. 2nd edn. (Springer Verlag, 1994)
- [45] D. NICMORUS, G. EICHMANN, A. KRASSNIGG and R. ALKOFER. “Delta-baryon mass in a covariant Faddeev approach.” *Phys. Rev. D*, 80: 054028. 2009
- [46] R. RICKEN, M. KOLL, D. MERTEN and B. C. METSCH. “Strong two-body decays of light mesons.” *Eur. Phys. J.*, A18: 667. 2003
- [47] S. GODFREY and N. ISGUR. “Mesons in a Relativized Quark Model with Chromodynamics.” *Phys. Rev.*, D32: 189. 1985
- [48] R. KOKOSKI and N. ISGUR. “Meson decays by flux-tube breaking.” *Phys. Rev. D*, 35: 907. 1987

- [49] R. P. FEYNMAN, M. KISLINGER and F. RAVNDAL. “Current Matrix Elements from a Relativistic Quark Model.” *Phys. Rev. D*, 3: 2706. 1971
- [50] S. AOKI, M. FUKUGITA, K.-I. ISHIKAWA, N. ISHIZUKA, K. KANAYA, Y. KURAMASHI, Y. NAMEKAWA, M. OKAWA, K. SASAKI, A. UKAWA and T. C. YOSHIÉ. “Lattice QCD calculation of the ρ meson decay width.” *Phys. Rev. D*, 76: 094506. 2007
- [51] M. GOCKELER ET AL. “Extracting the rho resonance from lattice QCD simulations at small quark masses.” *PoS, LATTICE2008*: 136. 2008
- [52] X. FENG, K. JANSEN and D. B. E. RENNER. “Scattering from finite size methods in lattice QCD.” *PoS, LATTICE2009*: 109. 2009
- [53] X. FENG, K. JANSEN and D. B. E. RENNER. “Resonance Parameters of the rho-Meson from Lattice QCD.” ArXiv: 1011.5288. 2010
- [54] S. AOKI and OTHERS (PACS-CS COLLABORATION). “Calculation of ρ meson decay width from the PACS-CS configurations.” ArXiv: 1011.1063. 2010
- [55] J. FRISON and OTHERS (BMW COLLABORATION). “Rho decay width from the lattice.” ArXiv: 1011.3413. 2010
- [56] C. HANHART, J. R. PELAEZ and G. RIOS. “Quark mass dependence of the rho and sigma from dispersion relations and Chiral Perturbation Theory.” *Phys. Rev. Lett.*, 100: 152001. 2008
- [57] J. NEBREDA and J. R. PELÁEZ. “Strange and nonstrange quark mass dependence of elastic light resonances from SU(3) unitarized chiral perturbation theory to one loop.” *Phys. Rev. D*, 81: 054035. 2010
- [58] T. MELDE, W. PLESSAS and B. SENGL. “Quark-model identification of baryon ground and resonant states.” *Phys. Rev. D*, 77: 114002. 2008
- [59] T. MELDE, L. CANTON and W. PLESSAS. “Structure of meson-baryon interaction vertices.” *Phys. Rev. Lett.*, 102: 132002. 2009
- [60] T. R. HEMMERT, B. R. HOLSTEIN and J. KAMBOR. “Chiral Lagrangians and Delta(1232) interactions: Formalism.” *J. Phys.*, G24: 1831. 1998
- [61] Z.-G. WANG. “Strong decay $\Delta^{++} \rightarrow p\pi$ with light-cone QCD sum rules.” *Eur. Phys. J.*, C57: 711. 2008
- [62] T. M. ALIEV, K. AZIZI and M. SAVCI. “The strong coupling constants of pseudoscalar mesons with decuplet–octet baryons in QCD.” *Nucl. Phys.*, A847: 101. 2010
- [63] C. ALEXANDROU, G. KOUTSOU, J. W. NEGELE, Y. PROESTOS and A. TSAPALIS. “Nucleon to Delta transition form factors with $N_F = 2 + 1$ domain wall fermions.” ArXiv: 1011.3233. 2010
- [64] P. MARIS, C. D. ROBERTS and P. C. TANDY. “Pion mass and decay constant.” *Physics Letters B*, 420: 267 . 1998

- [65] K. NAKAMURA and OTHERS (PARTICLE DATA GROUP). “Review of particle physics.” *J. Phys.*, G37: 075021. 2010
- [66] G. EICHMANN, R. ALKOFRER, A. KRASSNIGG and D. NICMORUS. “Nucleon mass from a covariant three-quark Faddeev equation.” 2009
- [67] R. ALKOFRER, C. S. FISCHER, F. J. LLANES-ESTRADA and K. SCHWENZER. “The quark-gluon vertex in Landau gauge QCD: Its role in dynamical chiral symmetry breaking and quark confinement.” *Annals Phys.*, 324: 106. 2009
- [68] Y. NAMBU and G. JONA-LASINIO. “Dynamical Model of Elementary Particles Based on an Analogy with Superconductivity. I.” *Phys. Rev.*, 122: 345. 1961
- [69] W.-K. TUNG. Group theory in physics (World Scientific, 1985)
- [70] J. SAKURAI. Modern Quantum Mechanics (Addison-Wesley Publishing, 1994)
- [71] C. S. FISCHER, P. WATSON and W. CASSING. “Probing unquenching effects in the gluon polarization in light mesons.” *Phys. Rev. D*, 72: 094025. 2005
- [72] A. KRASSNIGG. “Excited mesons in a Bethe-Salpeter approach.” *PoS, CONFINEMENT8*: 075. 2008
- [73] A. GELFOND. Differenzenrechnung (VEB Deutscher Verlag der Wissenschaften, 1958)

Acknowledgement

At first I want to thank my advisor, Andreas Krassnigg, for introducing me into the field of DSE/BSE calculations and providing me the meson Bethe-Salpeter Amplitudes and quark propagators. You left me enough freedom to follow my ideas, but still brought me back on the right track when I was lost.

I want to thank my office neighbour Martina Blank for the coffee and chatting breaks and sharing her knowledge and deep insights into BSE/DSE calculations with me and creating a really good atmosphere in our office. Thanks to You I could oversee several bad moments this year!

I also really want to thank Gernot Eichman for always patiently answering my questions and blowing away the haze when I could not see anything anymore. You provided me the baryon Bethe-Salpeter amplitudes, quark and diquark propagators and even your source code(!).

I also want to thank Reinhard Alkofer for introducing me into his group.

Among all the colleagues I was happy to meet during the time of my studies in Graz and Dresden, here I want to thank two, who were quite important for the realization of this thesis, Regina Kleinhappel for our endless coffee sessions and the sympathy and motivation in the good and bad times in this last 18 months, and Tina Herbst for the Peskin-Schroeder meetings, which gave me an amount of new insights into the topic of quantum field theories, which I could also use for this thesis.

Even a physicist has some free time he can spend with non-physicist (even though there was not much the last one and a half year). Here I want to thank my friends. Eventhough you really wondered in how many ways one can calculate a 1, and why I don't just write down the result if I know it, but have to calculate it, you always gave me a warm place to come to and brought me back on the road of reality, when I was lost in this physics world. While you are included in the last sentences anyway I especially want to thank my flatmates (with partners :)) for all the time we spend together. I really love to share this time with you.

Last but not least, I'm mostly indebted to my parents, who supported me all the way. For parents its not easy to let their kids go, but you alwas made it possible for me (and my brothers) to study whatever I wanted, wherever I wanted and find my way. I can't thank you enough!

I acknowledge financial support of the Paul-Urban-Stipendienstiftung and the FWF under Project Nr. 20496-N16 which gave me the opportunity to present some results of this thesis already on different conferences and workshops.